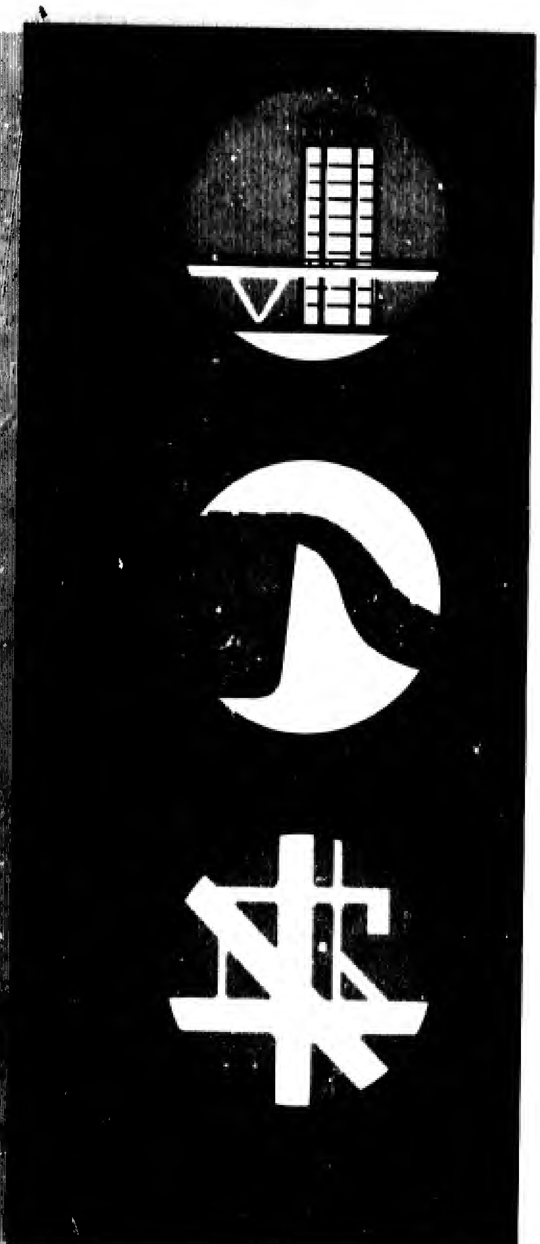

AD 687293

November 1968

Technical Report

# EXISTING STRUCTURES EVALUATION
## Part I: Walls

Prepared for:

OFFICE OF CIVIL DEFENSE
OFFICE OF THE SECRETARY OF THE ARMY
WASHINGTON, D.C. 20310

STANFORD
RESEARCH
INSTITUTE

MENLO PARK
CALIFORNIA

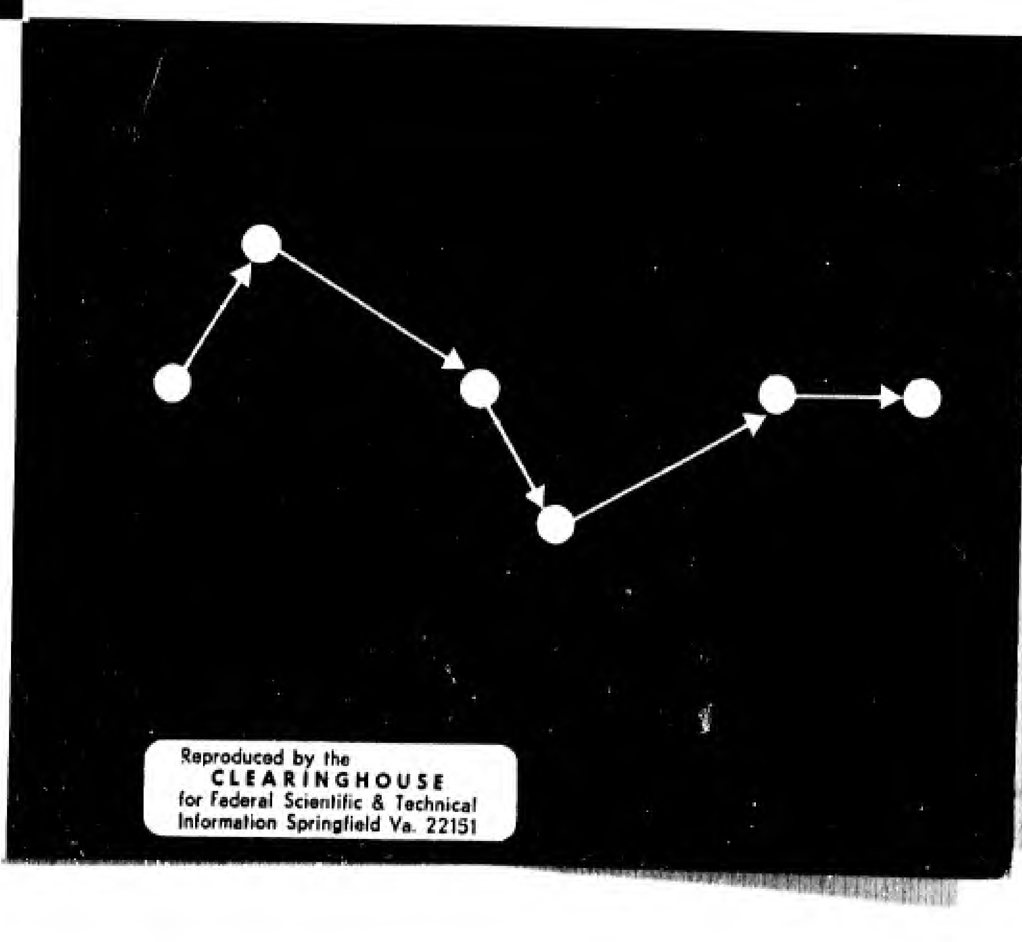

Technical Report

# SUMMARY OF EXISTING STRUCTURES EVALUATION Part I: Walls

November 1968

Contract No.
OCD-DAHC20-67-C-0136

OCD Work Unit
No. 1126C

Prepared for:

OFFICE OF CIVIL DEFENSE
OFFICE OF THE SECRETARY OF THE ARMY
WASHINGTON, D.C. 20310

STANFORD
RESEARCH
INSTITUTE

MENLO PARK
CALIFORNIA

By:

C. K. Wiehle
J. L. Bockholt
Public Works Systems

OCD Review Notice

This report has been reviewed in the Office of Civil Defense and approved for publication. Approval does not signify that the contents necessarily reflect the views and policies of the Office of Civil Defense.

Technical Report

# SUMMARY OF EXISTING STRUCTURES EVALUATION Part I: Walls

November 1968

Contract No.
OCD-DAHC20-67-C-0136

OCD Work Unit
No. 1126C

Prepared for:

OFFICE OF CIVIL DEFENSE
OFFICE OF THE SECRETARY OF THE ARMY
WASHINGTON, D.C. 20310

STANFORD
RESEARCH
INSTITUTE

SRI

MENLO PARK
CALIFORNIA

By:

C. K. Wiehle
J. L. Bockholt
Public Works Systems

## SUMMARY


### Introduction

The objective of the overall program was to develop an evaluation procedure applicable to existing NFSS-type structures for determining the blast protection afforded and the estimated cost of structure modifications to improve the blast protection. The approach adopted for the evaluation of existing structures was to formulate a procedure for examining the response of a structure over a range of incident overpressure levels to determine the pressure at which failure of the various components occurs. Such a procedure would consist of (1) a method for determining the air blast loading on the structure and structural elements, (2) a method for determining the structural response, and (3) a method to establish the failure criterion for each structural member of interest. A general outline of the procedure is presented in Figure S-1.

### Exterior Walls

The initial effort was directed primarily toward the development of a method to determine the response of exterior walls to nuclear blast. The method provides the "failure criteria input data" for exterior walls for the overall evaluation procedure shown on Figure 1.

Prediction of the collapse of exterior walls required the development of a resistance function for each wall type of interest and the establishment of failure, or collapse, criteria. Because of the difference in response, it was necessary to consider three types of exterior walls. These were unreinforced concrete or masonry unit walls without

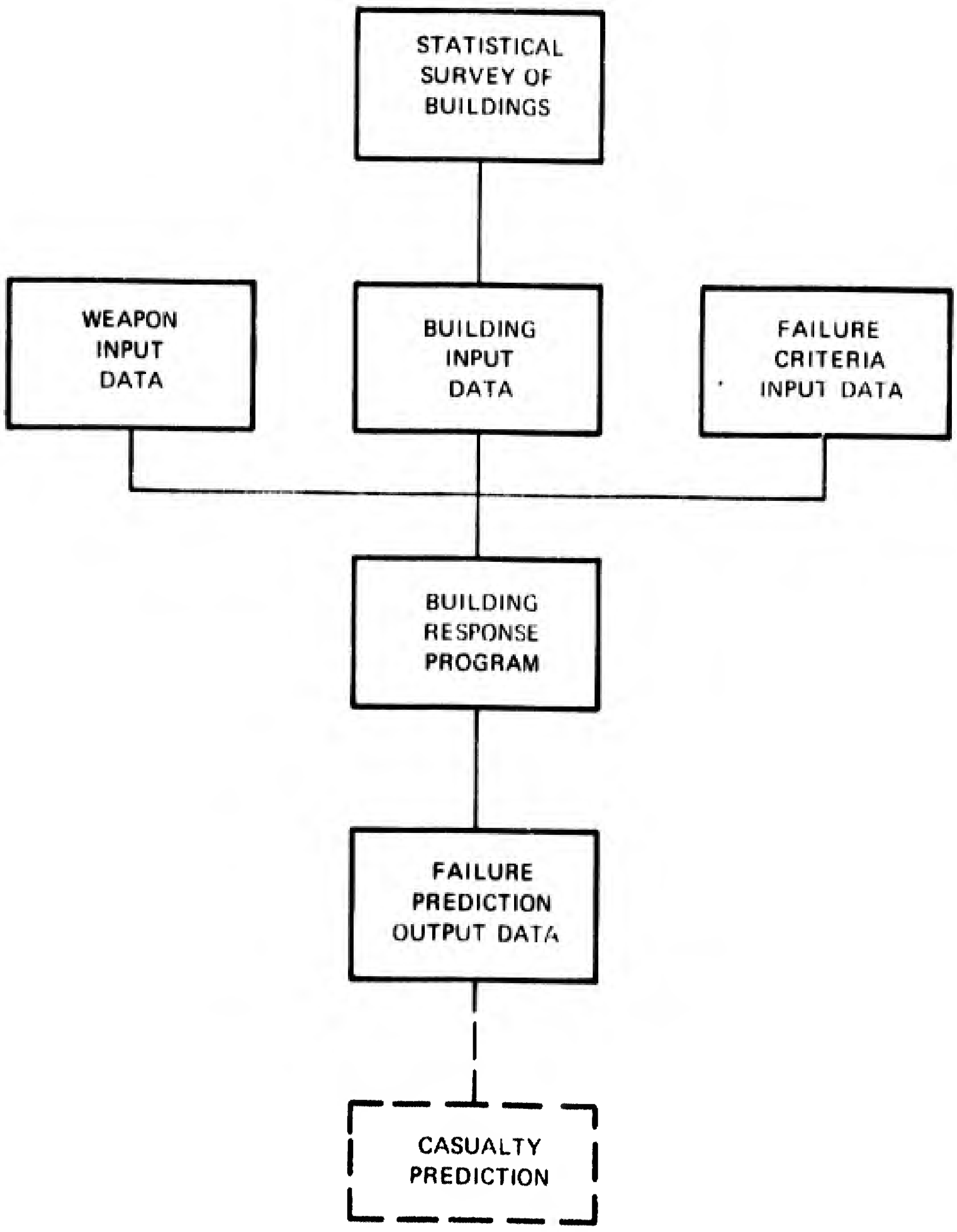


FIG. S-1 FLOW DIAGRAM FOR THE EXISTING STRUCTURES EVALUATION PROCEDURE arching, reinforced concrete walls, and unreinforced concrete or masonry unit walls with arching. For this initial study, it was assumed that the primary wall response was a one-way structural action between horizontal supports and that the wall was loaded by a uniform lateral load. Illustrations of the resistance functions for the three types of walls are shown on Figures S-2, S-3, and S-4.

In general, the failure criterion adopted for the unreinforced concrete or masonry unit walls, both with and without arching, was based on the instability of the wall due to excessive deflection. For the reinforced concrete walls, the failure criterion was based on the wall instability and on the elongation of the reinforcing steel. For the purpose of the evaluation of exterior wall elements in this study, failure implies collapse or disintegration of the wall. Furthermore, incipient collapse is defined as that point in the response where the wall can be considered as on the threshold of collapse.

Since wall reactions are an important input to the overall response of the supporting structure, a method is included in the analysis for determining the time-dependent wall reactions.

This report on exterior walls is a report on the progress of establishing a procedure for the evaluation of structures subjected to nuclear blast; thus it covers a phase of the overall effort.

## Discussion

### Background

To determine the dynamic response of the walls treated in this study, a computer program was developed utilizing the Newmark $\beta$ Method to analyze numerically the walls having the resistance functions previously mentioned. Transformation factors were used to reduce the wall, which is in reality a distributed mass system, to an equivalent single-degree-of-freedom

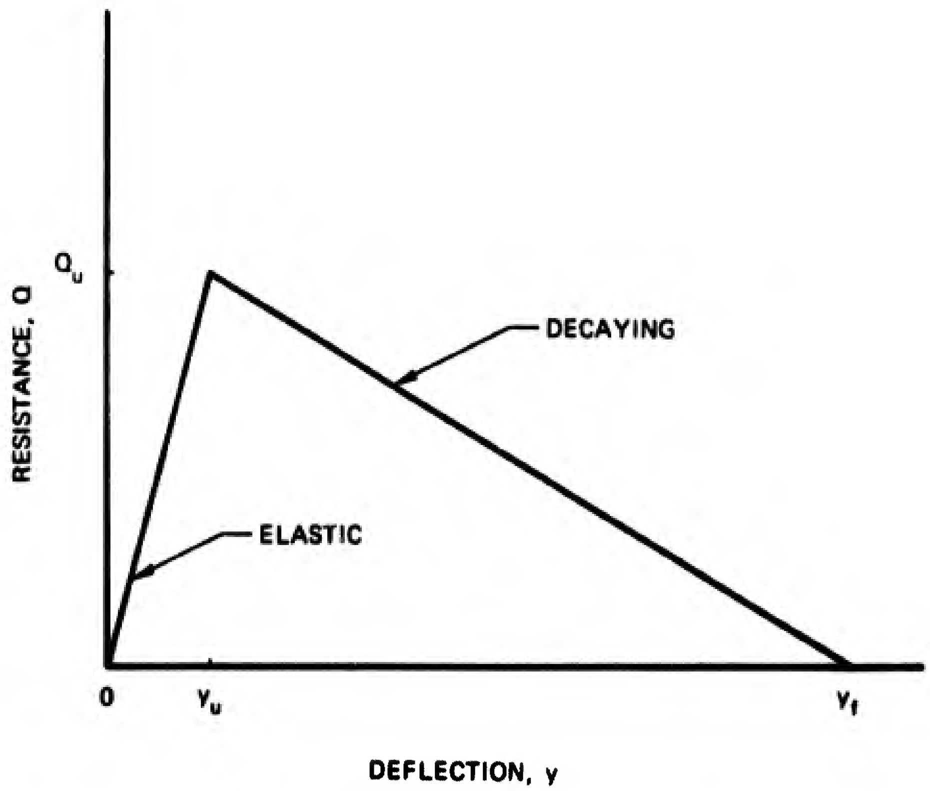


FIG. S-2 ILLUSTRATION OF RESISTANCE FUNCTION FOR A SIMPLY SUPPORTED UNREINFORCED CONCRETE OR MASONRY UNIT WALL WITHOUT ARCHING

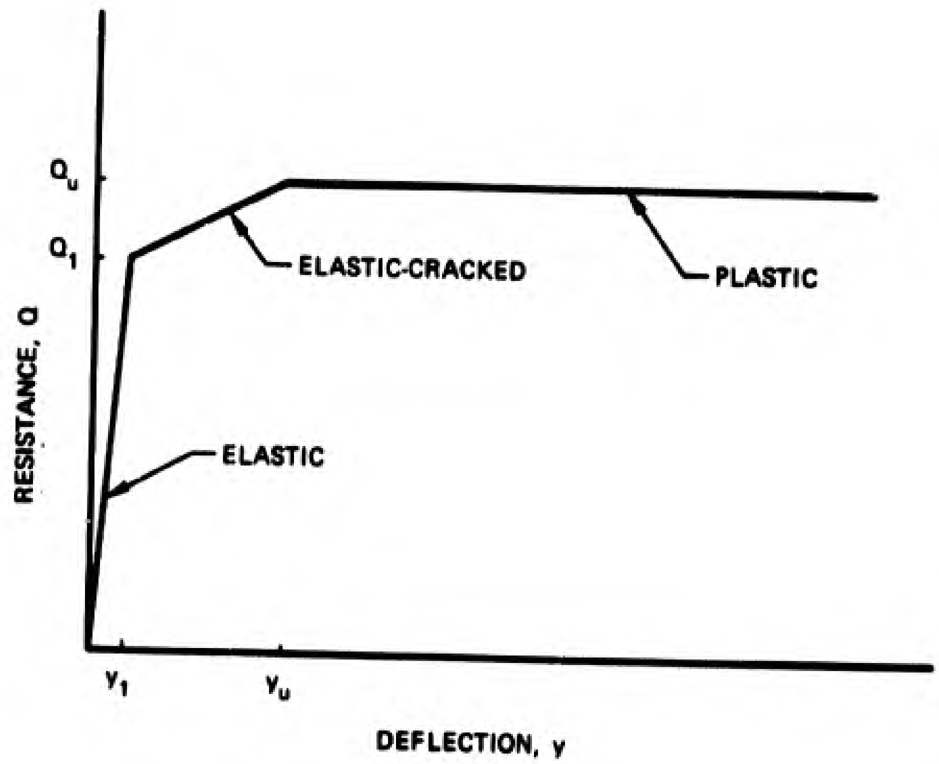


FIG. S-3 ILLUSTRATION OF RESISTANCE FUNCTION FOR A SIMPLY SUPPORTED REINFORCED CONCRETE WALL

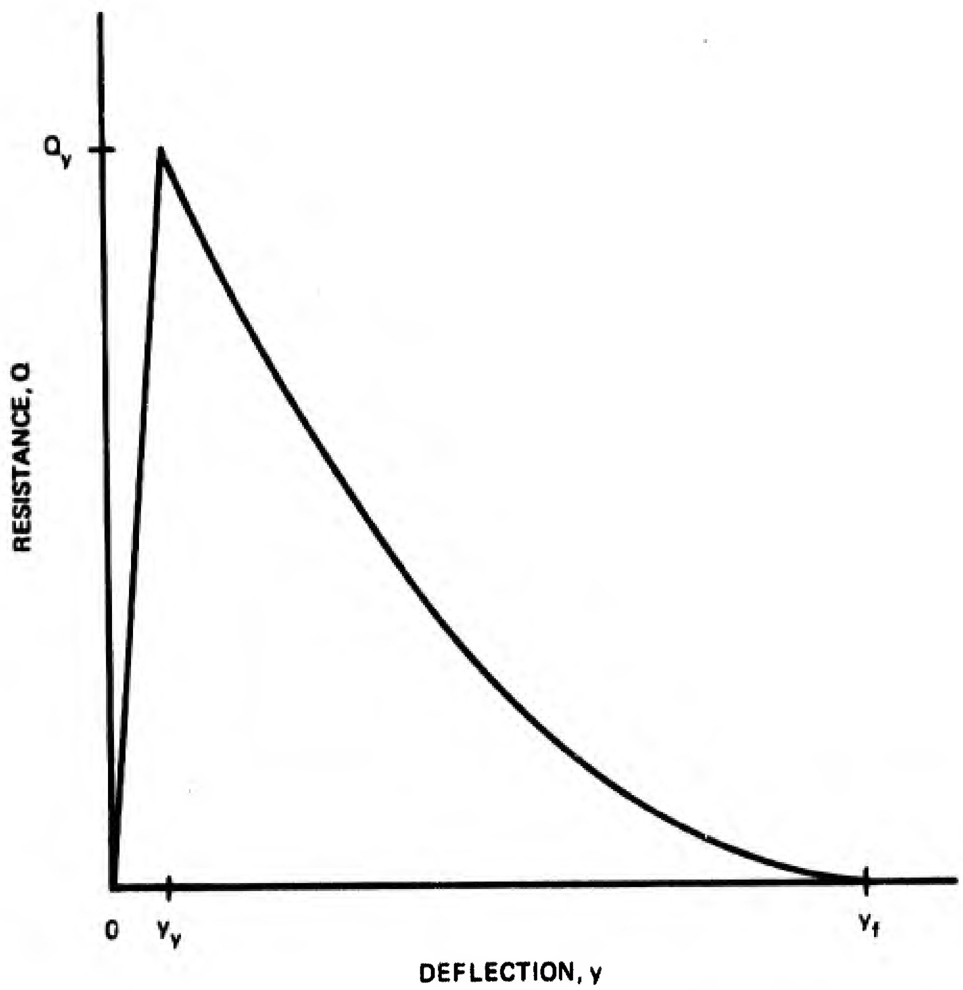


FIG. S-4 ILLUSTRATION OF RESISTANCE FUNCTION FOR AN UNREINFORCED CONCRETE OR MASONRY UNIT WALL WITH ARCHING system. The input data required in the program consist of the wall and load properties, with the resulting output being a complete time-history of the response of the wall to failure, including reactions and midspan displacement, velocity, and acceleration. The time-history may be determined for a wall subjected to a given loading, or the magnitude of the load causing incipient collapse may be found for various load types.

## Findings

During the preparation of the computer programs for the three types of exterior wall models treated, it was possible to analyze the response of selected walls up to collapse for various dynamic load conditions. The information from these computer runs permitted a comparison to be made between the limited experimental data on dynamically loaded walls and the mathematical models developed. Unfortunately, because of the paucity of experimental information on the collapse of laterally loaded walls, only a partial verification of the analytical procedure was possible. As experimental data becomes available, it is anticipated that additional analyses will be performed, and, if necessary, that the evaluation procedures will be modified or supplemented.

Since only limited experimental data were available, specific wall elements were selected to investigate the sensitivity of the predicted incipient collapse pressure over a range of various parameters. The parameters examined included the type and duration of the lateral load function, the vertical load in the plane of the wall, and the wall properties appropriate to each of the three types of walls. A brief summary of the findings of the parametric study follows.

For the range of parameters considered, it was found for all three types of walls that the modulus of elasticity and unit weight of the wall material had a minor effect on the incipient collapse pressure. Also, it was found that the ultimate concrete compressive strength of reinforced concrete walls had little effect on the collapse pressure.

Factors that have only limited influence on the incipient collapse pressure for unreinforced concrete or masonry unit walls without arching include the modulus of rupture, height, and thickness of the wall. However, the effect of the last two parameters is greater for walls with arching. Also, for reinforced concrete walls, the vertical load in the plane of the wall has only limited effect on the collapse pressure.

The limited parametric study showed that factors that generally have a considerable influence on the incipient collapse pressure of a wall include the weapon yield, clearing time, and load duration. In addition, other factors that are important in determining the incipient collapse pressure are the vertical load in the plane of unreinforced walls without arching, the percent tension steel in reinforced concrete walls, and the ultimate compressive strength and support stiffness for walls with arching.

An examination of the reaction-time history for an unreinforced masonry wall showed that the area under the reaction-time curve, or impulse, increased with increasing load magnitude. This indicates that the assumption that exterior walls can be treated as frangible elements for determining the reactive forces, or input load to the structural frame, is incorrect for most of the walls in NFSS-type structures.

## Recommendations

Because of the lack of sufficient experimental data, the analytical results from this study could not be compared with a wide variety of actual situations. Even though the parametric study summarized above indicated the importance of a number of factors on the incipient collapse pressure of exterior walls, the validity of the procedures could not be established adequately to permit conclusions to be made. Therefore, in addition to continuing the analytical effort, it became apparent during the investigation that supplementary information was needed in related areas such as those discussed in the following recommendations:

- It is recommended that static and dynamic tests of typical exterior walls be conducted to permit an examination of the validity of the mathematical models presented in this report or to establish the basis for additional or substitute procedures. The specific areas of interest for which experimental information is needed include the resistance function for various types of walls, the effect of two-way wall action, the effect of shear and connections on wall failure, the reaction of walls through the collapse phase, and the effect of support stiffness for walls with arching. In addition, information should be obtained on the collapse mechanism of walls to establish the primary collapse mode and to determine a realistic failure criterion for each wall type. The tests should provide information on the collapse mechanism at various pressure levels above that of incipient collapse, and the test parameters should include various support conditions and vertical inplane wall loads. Instrumentation should provide data on the loading, deflection, velocity, and reactive force throughout the total range of wall response.

- Because of the importance of the net pressure for predicting the collapse of wall elements, it is recommended that air blast studies be made to establish more definitive load-time prediction techniques than are now available. Such studies should include at least two factors. First, the conventional air blast load schemes provide the average load-time relationship on the exterior surface of various geometric shapes. These schemes, although generally satisfactory for design purposes, are inadequate for describing the external load-time function needed to predict the collapse of various wall elements in a large multistory building. Therefore, a rational method is needed for determining the load-time function at any point of interest on the surface of a structure. Second, the net load on a wall with openings is influenced by the back face loading, which depends on the wave propagation into the room and the subsequent pressure build-up due to room-filling. At the present time, techniques are available for predicting the average interior pressure build-up during the room-filling phase for limited geometries and for the lower overpressure levels. These methods should be extended to include other geometries of interest and the higher overpressures. In addition, techniques should be developed for estimating the loading on the interior wall surfaces as a result of the wave front propagation into the room.

Technical Report

# EXISTING STRUCTURES EVALUATION
# PART I: WALLS

November 1968

SRI Project No. MU 6300-020

Contract No.
OCD-DAHC20-67-C-0136
OCD Work Unit
No. 1126C

Prepared for:

Office of Civil Defense
Office of the Secretary of the Army
Washington, D.C. 20310


By:

C. K. Wiehle

J. L. Bockholt

Public Works Systems

STANFORD
RESEARCH
INSTITUTE

MENLO PARK
CALIFORNIA

## FOREWORD

This report is one of a series covering research of a continuing nature under a project for blast resistance evaluation of existing structures in the National Fallout Shelter Survey (NFSS) inventory of the U.S. Office of Civil Defense (OCD).

The objective is to develop an evaluation method for estimating blast resistance and the cost of structure modifications to improve blast protection.

The evaluation method differs from vulnerability analysis techniques by carrying along significant statistical yardsticks (e.g., on strengths of materials) in the calculations sufficient to meet the needs of shelter operations research or war-gaming. It differs from protective design/analysis by aiming at a 50% probability basis, rather than the 90%-99% probability basis intended in design/analysis methods.

The results expected of the evaluation method will provide inputs for systems analyses related to performance of structures and effects on shelterees. For the latter purpose, the evaluation method results will include data on fragments and their sizes, masses, accelerations, velocities, and displacements.

The approach used for the continuing research was to develop an evaluation method for each of several structural elements (e.g., window glass, walls, and slabs), including reaction load-time history, and then for structural frames.

The research includes applications to specific buildings, such as those selected in a statistically adequate sample of NFSS structures under another OCD project, thereby making possible various extrapolations to the overall NFSS structures picture.

ABSTRACT

The objective of this investigation was to develop an evaluation procedure applicable to existing NFSS-type structures for determining the blast protection afforded and the cost of structure modifications to improve the blast protection. The approach adopted was to formulate a procedure that would permit examining the response of a structure over a range of incident overpressure levels to determine the pressure at which failure of the various elements occurs. Because of the scope of the overall evaluation program, the initial phase was primarily concerned with the response of the exterior walls.

The initial effort included the development of analytical procedures and computer programs to predict the collapse of three types of blast loaded exterior wall elements. The wall types considered were unreinforced concrete or masonry unit walls without arching, reinforced concrete walls, and unreinforced concrete or masonry unit walls with arching. To determine the sensitivity of the collapse pressure of exterior walls to various factors, a parametric study was conducted of the response of selected wall elements subjected to arbitrary dynamic loads. In addition, the analytical predictions were compared with the limited laboratory and nuclear field test data.

CONTENTS

CONTENTS (continued)

CONTENTS (concluded)

ILLUSTRATIONS

ILLUSTRATIONS

ILLUSTRATIONS

ILLUSTRATIONS

# I INTRODUCTION

Under contract to the Office of Civil Defense, Stanford Research Institute is conducting an investigation of the evaluation of existing structures subjected to nuclear air blast. The objective of the overall program is to develop an evaluation procedure applicable to existing NFSS-type structures for determining the blast protection afforded and the estimated cost of structure modifications to improve the blast protection. The purpose of the initial phase of the work presented in this report was to develop an evaluation procedure for the response of exterior walls to blast loading.

## Background

The evaluation of existing structures is an exceedingly complex problem that includes many unknown aspects of both the nuclear air blast loading on, and the failure mechanisms of, structures. Past damage prediction schemes have generally been developed for physical vulnerability studies and have limited application to the examination of the behavior of an individual structure. Although comprehensive analytical studies and experimental data provided the basis for these methods, averaging and statistical techniques were employed to obtain the probability of a specified level of damage to a selected class of structures for various weapon yields and ranges.

Illustrations of these methods are presented in Ref. 1 where the type of structure and weapon yield can be used to enter a nomograph, graph, or table to obtain the range for severe or moderate damage. However, there are a number of limitations to such methods for damage prediction as applicable to the evaluation of structures. For instance, one limitation is inherent in the definition of the class of damage, i.e., severe damage in Ref. 1 is defined as "A degree of damage that precludes further use of the structure or object for its intended purpose without essentially complete reconstruction. For a structure or building, collapse is generally implied." This is a rather generalized description of damage that may have some significance for predicting the average damage to a large quantity of structures, but it is essentially meaningless when applied to an individual structure. For a detailed description of damage sufficient for predicting personnel casualties or shelter adequacy for resisting air blast, the methods provide only qualitative information. For instance, what is the meaning of a description of damage, such as severe building damage, when applied to predicting the damage of a shelter located within the building? Are such methods definitive enough to permit basing a recommendation for locating a shelter in one particular existing building rather than another if various overpressure levels were considered? Or, can the methods provide data on which to base a selection of which structure, from among many, would be the best to upgrade for providing blast resistant shelters?

The methods described in Ref. 1 were based on a detailed rational analysis of structure behavior that required specific input data. However, an important simplification that entered into the development of the charts and nomographs was the use of average input data in the analytical calculations. The results, therefore, may be good average predictions of damage for each building type, but the degree of accuracy for predicting the damage to individual components and structures at a specific location is not well-defined. Even if it is assumed that the definition of structural damage by these methods is pertinent to the problem of evaluating existing structures, the predictions would still be in error by an unknown amount for all buildings except those similar to the "averaged" building.

On the other hand, detailed methods have been developed for predicting the dynamic response of structures in the elastic and elasto-plastic range. However, there are also limitations to these methods for use in predicting structural collapse.* In general, the fundamental concept on which dynamic design procedures for protective structures have been developed is the elasto-plastic response of reinforced concrete or steel structures, where the ductility ratio is an important design parameter. Since definitive procedures have not been available for predicting failure, the ductility ratio has often been used as a criterion for determining the failure of a member or building. However, while the ductility ratio may be adequate for design, its use may not be appropriate for failure prediction. For example, the experimental results in Ref. 2 indicate that the ultimate failure, or collapse, of two-way reinforced concrete flat slabs resulted from tensile membrane action. Therefore, what is the relationship of this type of slab failure to a failure criterion based on slab deflection (ductility), which is in turn based on flexural action? Also, even if such methods could be used to evaluate the performance of each member of a building, there may be practical limitations to the analysis of all buildings in an entire city. This is primarily because of the problem of gathering specific input data from individual structures before an analysis could be performed. For instance, the computer program in Ref. 3 requires specific input data on the building and elements, such as the number of floors and bays, damping coefficient, bay and column widths, moment of inertia, and modulus of elasticity, as well as the loading data. It would appear that the difficulty of a large scale data gathering operation for predicting the damage throughout a city would limit the use of such methods to any large extent. However, it is felt that this particular

---

* A discussion of the definition of failure, as used in this report, is given in Section III.

problem could be overcome by conducting a statistical survey of a representative sampling of buildings in a city of interest in a manner similar to the NFSS structure sampling presented in Ref. 4.

As an example of the use of the survey data, consider Volume IV of Ref. 4.* For that study, it was found necessary to survey 55 structures in Albuquerque to obtain a statistical significant sample representative of the NFSS building types. This sample consisted of four single frame building types and four combination frame types. Of the 55 structures in the 8 types, 19 buildings were categorized as concrete beam and girder, 18 as load bearing wall, and 10 as a combination of load bearing wall and concrete beam and girder. The remaining eight buildings were distributed one or two each in the remaining five categories. One approach for the use of this type of information in an evaluation procedure could be to select--from among the three larger groups--a number of buildings (such as five) that were representative of the group and to analyze these typical or average structures in detail. The results would, therefore, be an average for the group. However, it is possible that because of the large difference in structures, it may be preferable to analyze all 55 structures in the 8 groups. In either event, if the sampling method for selecting the 55 structures is valid, the results from a relatively few structures would be indicative of the majority of structures throughout the city.

A second possible approach would be to use the building data to conduct a variation-of-parameter study. For the study noted above, the data for the various types of structures would indicate the range of parameters representative of the buildings in each category. It would not be necessary to analyze each structure in detail for each parameter. Instead, the

---

* It should be noted that the data in the referenced RTI reports are not in the appropriate form for an evaluation study as discussed herein.

most common values for each parameter would be determined and used in the analysis. For instance, it is indicated in Volume IV of Ref. 4 that the thickness of the exterior walls of the first floor of the 55 buildings in Albuquerque range from 1 to 30 in. thick. However, two thicknesses (8 and 12 in.) represent 54 percent of all walls, and five thicknesses (4, 8, 10, 12, and 18 in.) represent 75 percent of the walls. Therefore, to obtain a representative performance it would not be necessary to examine a building for each of the 13 exterior wall thicknesses, rather only two to five thicknesses would need to be examined.

## Approach

### Structure Evaluation

It would be desirable if a structure evaluation procedure were available that could be applied to the following types of OCD problems:

- Casualty and injury predictions
- Debris prediction
- Damage assessment
- Selection of existing structures that provide the best protection
- Selection of existing structures that have a potential for modification for upgrading to provide blast shelters

Unfortunately, at the present time there is no procedure or combination of procedures that can be used to satisfy the above requirements. Therefore, a procedure is needed that is sufficiently flexible to provide the detail necessary to assess individual structure damage, and yet not require an analysis of every structure in an entire city. One possible method, which appears practical for the evaluation of structures, is the development of a computer program, similar to those in Refs. 3 and 5, for predicting the damage to structures and structural elements in sufficient detail to satisfy the types of problems mentioned above. For instance, the output data from an examination of various types of structures for a city could be used to assist in the selection of the types of structures best suited for providing modest blast protection without modification. Alternatively, the output data, to whatever level of detail required, could be used as input data for the analysis of casualties and injuries for various attack assumptions.

The overall approach adopted in this study for the evaluation of existing structures to resist nuclear air blast has been the formulation of a procedure for examining the response of a structure over a range of incident overpressure levels to determine the pressure at which collapse of the various elements occurred. A selected structure would be examined to determine the minimum incident overpressure at which initial damage occurred. This would usually be the pressure required to cause failure of the window glass. The building would then be examined at successive higher increments of incident overpressure (say 1/4 or 1/2 psi) to determine the sequence of element or frame failure. As noted in Ref. 6, this process would be continued until a complete description of structural failure was obtained over the overpressure range of interest.

Because of the complexity of both the air blast loading and the structural response calculations, the evaluation procedure would employ a computer to perform the numerical computations. The program would be designed with sufficient flexibility to permit subsequent modification as more complete information became available from current studies by various organizations.* Basically, the procedure would consist of (1) a

---

* In particular, the investigations concerned with air blast entering rooms at Ballistics Research Laboratories, with the ultimate strength of slabs at Waterways Experiment Station, with the failure of wall panels at URS Corporation, and with the behavior and failure of frames at University of Ill'nois.

method for determining the air blast loading on the structure and structural elements, (2) a method for determining the structural response, and (3) a method to establish the failure criterion for each structural member of interest. A general outline of the procedure is presented in Figure 1. An iterative process would be employed whereby the structural response could be examined for various levels of incident overpressure and compared with a failure criterion to predict the overpressure level at which failure of each member would occur. As mentioned previously, the pertinent building data would be obtained by a statistical survey of a city or area to limit the damage calculations to a manageable quantity.

Wall Element Evaluation

The effort covered in this report was directed primarily toward the development of an evaluation procedure to determine the response of exterior walls to nuclear air blast. The method provides the "failure criteria input data" for exterior walls for the overall evaluation procedure shown on Figure 1. The approach for this phase was to use established analytical procedures wherever possible, and existing experimental information. As noted in the body of the report, to predict adequately the response of wall elements up to collapse failure, it was necessary to modify and adapt current procedures for specific use in this report. However, simplified analytical models were used for wall elements to prevent the overall evaluation procedure of a structure from becoming unwieldly due to excessive computational effort.

The procedure adopted in this study was to establish the resistance function for each wall element of interest by considering the approximate response mode and by assuming that the wall was subjected to a uniformly distributed static load. The member was then transformed into an equivalent single-degree-of-freedom dynamic system by the use of transformation factors for the load, resistance, and mass, as noted in Ref. 7. The equation of motion was then solved on a computer using the numerical integration procedure outlined in Ref. 8.

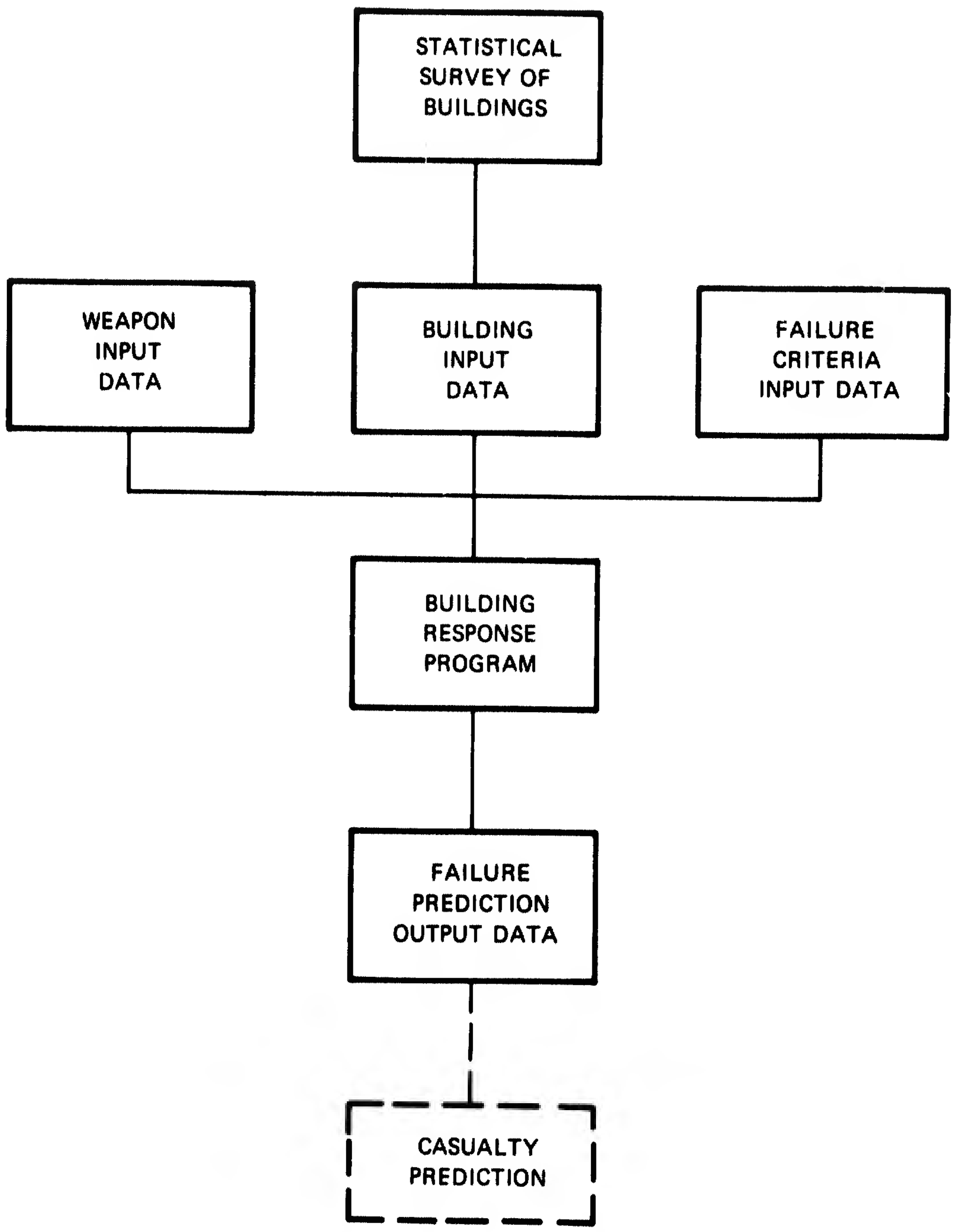


FIG. 1 FLOW DIAGRAM FOR THE EXISTING STRUCTURES EVALUATION PROCEDURE

## Report Limitations

It should be emphasized that this report on exterior walls is a report on the progress of establishing a procedure for the evaluation of structures subjected to nuclear blast; thus, it covers only a phase of the overall effort. Also, at the present time, the available information is insufficient for establishing definitive evaluation procedures for predicting the collapse of all types of walls of interest. However, current analytical and experimental studies of wall and slab response should provide additional information in the future. At that time, it is anticipated that the procedures presented herein, including the computer programs, will be upgraded or modified accordingly. In addition, the computer programs developed for each wall type are not necessarily in their final stage of development. First, even though the programs were used for parametric studies, the evaluation of the programs for adaptability to a wide range of realistic wall elements is incomplete. Also, it is expected that some changes will be required when the wall element programs are integrated into the overall structure evaluation program.

## Report Organization

Section II contains a discussion of the pressure-time load functions used in the evaluation of wall elements, and the resistance functions for walls are presented in Section III. The method used to determine the reactive force of dynamically loaded wall elements on the supporting structure is given in Section IV. A discussion of the correlation of the wall response models with the limited available experimental data, together with a variation-of-parameter study, is contained in Section V. Section VI contains a summary and recommendations for further study.

The equations necessary to determine the ultimate strength of reinforced concrete members are summarized in Appendix A, and Appendix B contains a short discussion of the failure of reinforced concrete members based on concrete crushing. Three current methods for calculating the arching in unreinforced masonry walls are summarized in Appendix C, and a discussion of the computer progra s developed to predict the collapse of walls is included in Appendix D.

Following the appendixes, a list of the references and the nomenclature used throughout the report are presented.

Acknowledgments

The authors gratefully acknowledge the assistance and guidance of James F. Halsey of Stanford Research Institute and Norbert E. Landdeck of the Office of Civil Defense during the conduct of this program. In addition, acknowledgments are due Professor M. A. Sozen of the University of Illinois for his information concerning the response and failure of lightly reinforced concrete members.

## II AIR BLAST LOADING

### Introduction

An important factor in the evaluation of existing structures subjected to nuclear air blast is the determination of the pressure-time function on each structural element of interest. This is a complex problem, since, even before the blast wave interacts with the structure, it is influenced by many factors, such as weapon yield and location, weather conditions, terrain, surface type, and blast shielding. Even if it were assumed that the free-field, pressure-time relationship were known for a blast wave incident on the side of a building, the determination of the loading function on a wall element is difficult because of the interaction processes. The primary difficulty arises because the structural element responds to the differential or net loading, which requires a knowledge of the loading on both the front and back surfaces.

The complexity of the problem can be demonstrated by considering the loading on an exterior wall panel of a building with window openings. Determination of a load description sufficient for analyzing the wall response requires the front face loading, which includes the wave reflection and clearing processes on the building, and the back face loading, which includes the wave diffraction, reflection, and filling processes in the room. Unfortunately, no definitive technique exists for obtaining an accurate load-time history for such a wall with reasonable reliability. As discussed in Ref. 6., conventional air blast load prediction methods are often inadequate for the determination of damage to multistory buildings in city complexes. It was also noted in the referenced document that current air blast loading techniques were developed primarily for design purposes. Furthermore, the use of such methods can lead to large errors in damage prediction if consideration is not given to the original assumptions used in developing the method. Therefore, it should be emphasized that for the evaluation of actual structures, consideration should be given to establishing more realistic blast load schemes than are now available.

## Air Blast Loading Schemes

Although nuclear air blast, as such, was not included as a part of this study, it is obviously important for realistic prediction of wall collapse for actual structures. However, for this initial study, the determination of a precise load-time function was not necessary to establish prediction methods for the collapse of exterior walls. Instead, several load-time functions were selected for use in the comparisons of wall response discussed in Section V. From the standpoint of the wall models developed in Section III, the four types of air blast load functions presented in the following subsections were felt to be adequate to demonstrate the relative wall behavior and to study parametric variations, even though the net wall loading was not included directly. The load cases used are not exhaustive, but the computer programs developed in this project are arranged to accept any load function desired.

### Loading Case No. 1

The first case selected was the conventional load scheme for the interaction of an air blast wave at normal incidence with the front face of a closed rectangular structure in Ref. 1. As noted in Figure 2, after reflection, a linear decay to the stagnation pressure is assumed. Since the walls were considered as solid panels in the analysis, back face loadings are not included. Also, since the primary purpose of this initial study was to predict wall collapse, negative phase loading was not included.

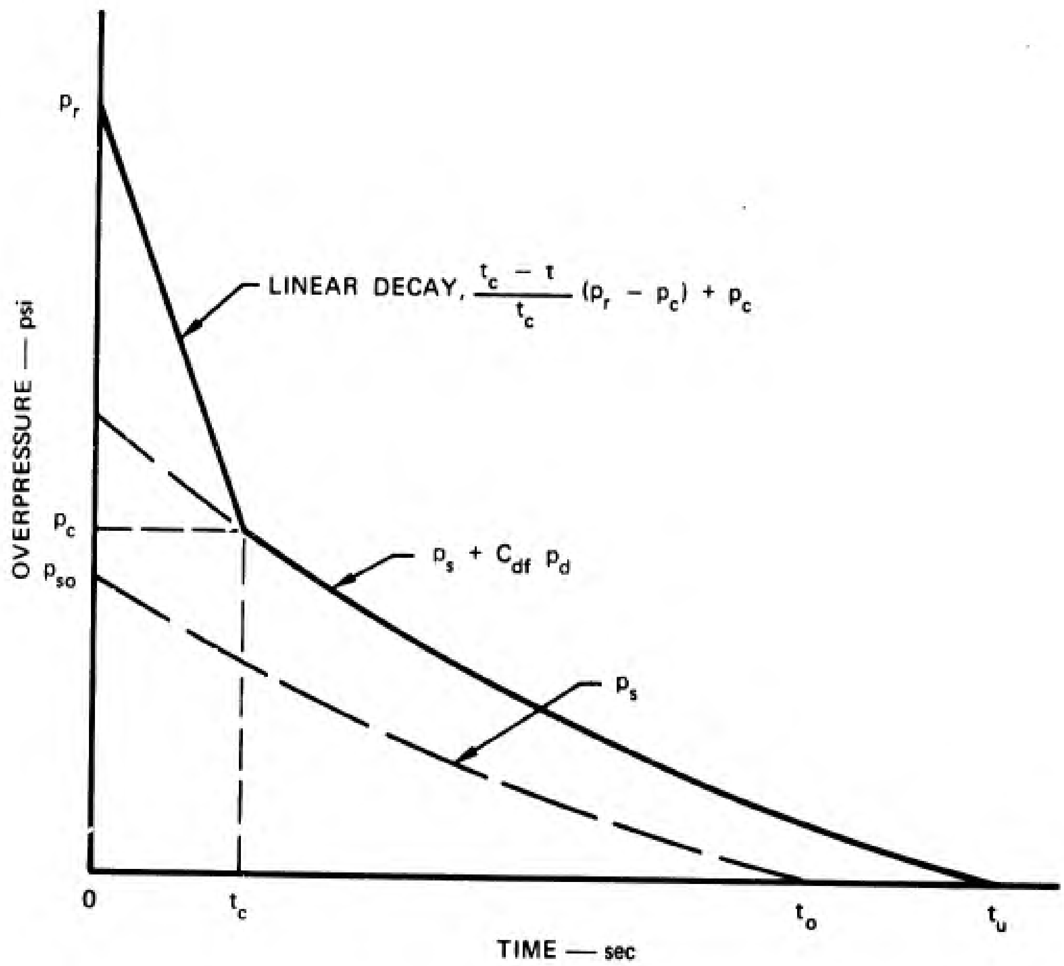


FIG. 2 FRONT FACE AIR BLAST LOADING
LOADING CASE NO. 1

The equations used to describe the load-time function for analyzing the wall response for Loading Case No. 1 are as follows:*

Input - $p_{so}$, W, $P_o$, $c_o$, S

$$p_r = 2\, p_{so} \left( \frac{7\, P_o + 4\, p_{so}}{7\, P_o + p_{so}} \right) \tag{1}$$

$$p_{do} = \frac{5}{2} \left( \frac{p_{so}^{\;2}}{7\, P_o + p_{so}} \right) \tag{2}$$

$$p_s = p_{so} \left( 1 - \frac{t}{t_o} \right) e^{-t/t_o} \tag{3}$$

$$p_d = p_{do} \left( 1 - \frac{t}{t_u} \right)^2 e^{-2t/t_u} \tag{4}$$

$$U = c_o \left( 1 + \frac{6\, p_{so}}{7\, P_o} \right)^{1/2} \tag{5}$$

$$t_c = \frac{3S}{U} \tag{6}$$

$$p_c = p_s + C_{df}\, p_d \quad (\text{at time} = t_c) \tag{7}$$

$$t_o = \frac{W^{1/3}}{(2.2399 + 0.1886\, p_{so})} \quad (\text{from Ref. 9}) \tag{8}$$

For the various loading phases shown in Figure 2:

$$p(t) = \frac{t_c - t}{t_c} (p_r - p_c) + p_c \qquad 0 \le t \le t_c \tag{9}$$

---

* The nomenclature used in this report is presented in the last section; only exceptions are defined in the text.

$$p(t) = p_s + C_{df}\, p_d \qquad t_c \le t \le t_o \qquad (10)$$

$$p(t) = 0 \qquad t \ge t_o \qquad (11)$$

Assumptions are:

$$t_u = t_o$$

$$C_{df} = 1.0$$

Loading Cases Nos. 2 and 3

As noted on Figures 3 and 4, Loading Cases Nos. 2 and 3 are for a triangular and a rectangular load pulse, respectively. These two loading schemes were selected since they represent the simplified wave forms used in many instances for the design of structures to resist nuclear blast forces (e.g., Refs. 7 and 10). The equations for the two cases, which can include a finite rise-time for the initial wave front, are as follows:

Triangular Load. See Figure 3:

Input - $p_m$, $t_o$, $t_r$

$$p(t) = p_m \left(\frac{t}{t_r}\right) \qquad 0 \le t \le t_r \qquad (12)$$

$$p(t) = p_m \left(\frac{t-t_r}{t_o-t_r}\right) \qquad t_r \le t \le t_o \qquad (13)$$

$$p(t) = 0 \qquad t \ge t_o \qquad (11)$$

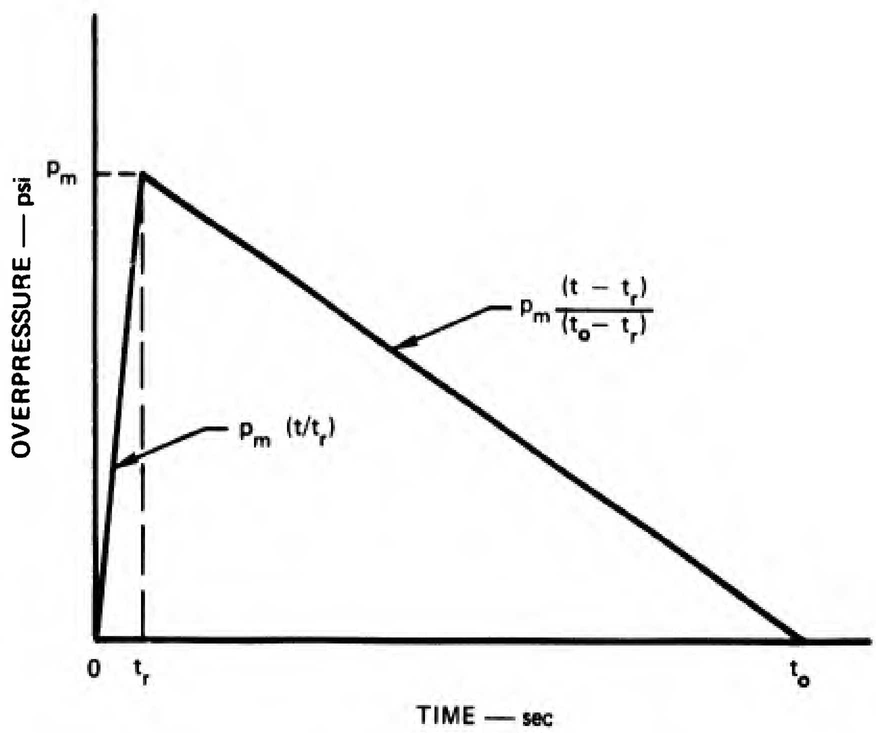


FIG. 3 FRONT FACE AIR BLAST LOADING
LOADING CASE NO. 2

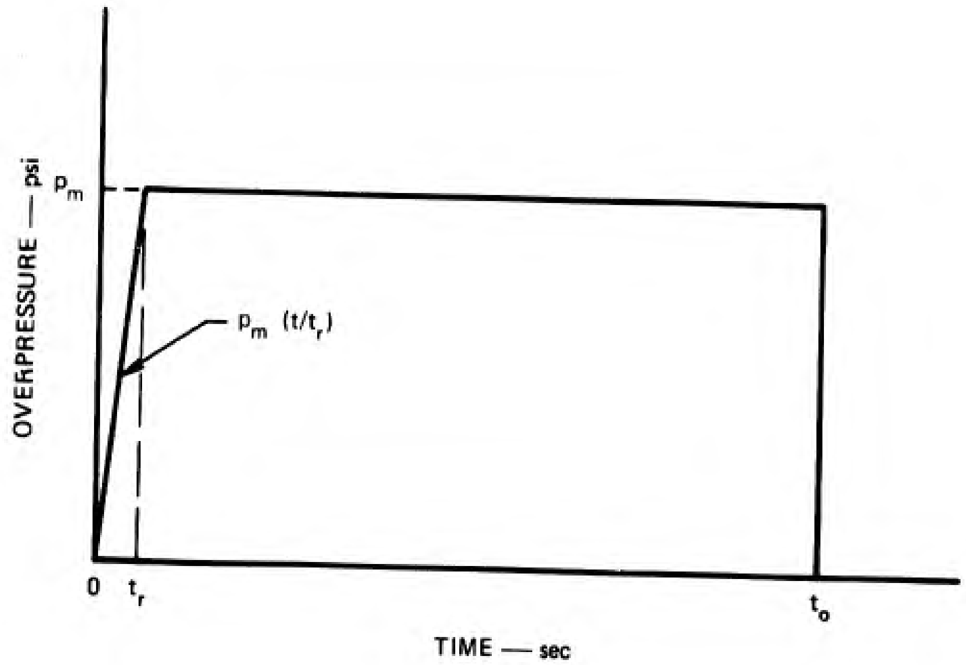


FIG. 4 FRONT FACE AIR BLAST LOADING
LOADING CASE NO. 3

Rectangular Load. See Figure 4:

Input - $p_m$, $t_o$, $t_r$

$$p(t) = p_m \left(\frac{t}{t_r}\right) \qquad 0 \le t \le t_r \qquad (12)$$

$$p(t) = p_m \qquad t_r \le t \le t_o \qquad (14)$$

$$p(t) = 0 \qquad t \ge t_o \qquad (11)$$

Loading Case No. 4

The fourth air blast loading case was selected primarily to permit comparisons to be made of the mathematical models developed in this study with the experimental results from the URS Shock Tunnel Facility (Ref. 11). As shown on Figure 5, the load function consists of a step pulse, with or without a rise time, to a uniform pressure followed by a linear decay to zero pressure. The equations used to describe Loading Case No. 4 are:

Input - $p_m$, $t_1$, $t_o$, $t_r$

$$p(t) = p_m \left(\frac{t}{t_r}\right) \qquad 0 \le t \le t_r \qquad (12)$$

$$p(t) = p_m \qquad t_r \le t \le t_1 \qquad (14)$$

$$p(t) = p_m \left(\frac{t-t_1}{t_o-t_1}\right) \qquad t_1 \le t \le t_o \qquad (15)$$

$$p(t) = 0 \qquad t \ge t_o \qquad (11)$$

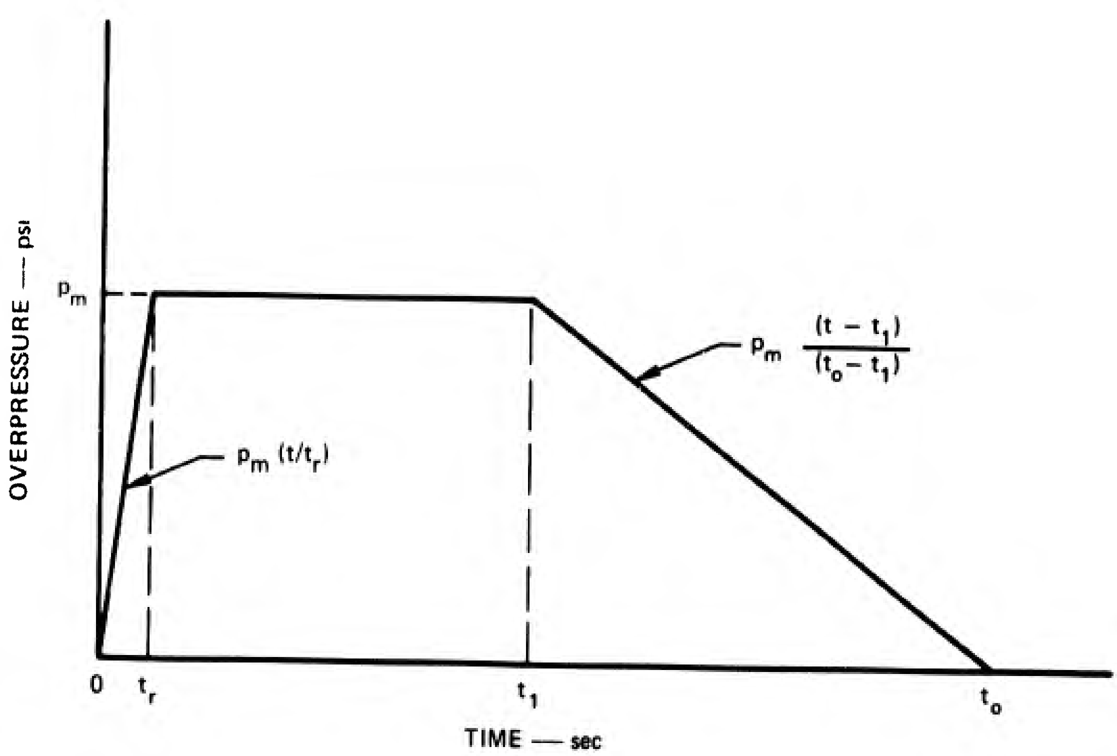


FIG. 5 FRONT FACE AIR BLAST LOADING
LOADING CASE NO. 4

BLANK PAGE

## III RESISTANCE FUNCTIONS

### Introduction

#### Development of Resistance Functions

The method adopted in this study to predict the behavior of exterior walls required the development of a resistance function for each wall element of interest. As a structural member deflects under the influence of an external load, an internal force develops that tends to restore the member to its equilibrium position. At a given deflection, the internal restoring force, or resistance, is defined as numerically equal to the static load required to produce the deflection (Ref. 7). Basic assumptions in the development of resistance functions are that the deflected shape of the member under dynamic load is identical to that under some static load and that the distribution of the restoring force and dynamic load is the same. The resistance function for walls can be idealized as elastic, elasto-plastic, plastic, strain hardening, and decaying or unstable, as noted on Figure 6 (Refs. 7 and 12).

Development of a resistance function for a specific wall element requires a knowledge of the mode of response and a criterion for determining the limiting or collapse deflection. Since the response of walls is also dependent on the type of wall construction, it was necessary to establish the three general types of walls for analysis purposes described earlier. In addition, since the shape of the resistance function is dependent on the support conditions, walls with simple supports, fixed supports, and fixed-hinged supports (propped-cantilever) are treated separately for each type of wall.

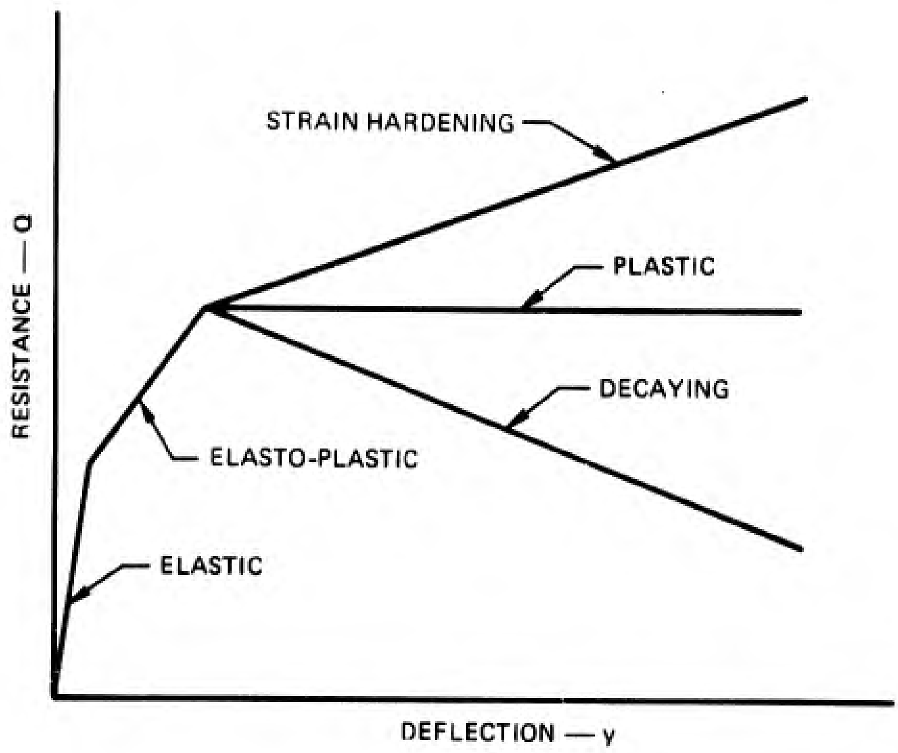


FIG. 6 RESISTANCE FUNCTION

The exterior walls of buildings are generally categorized as panel, curtain, and load-bearing. Panel walls can be defined as nonload bearing walls that are supported by the structural framework of the building at each floor level (Ref. 13). In general, such walls are designed for wind pressure only, although as noted in Ref. 14, in actual buildings, panel walls can act as diaphragms or shear walls in resisting deformations of the structure, especially for large blast forces. Curtain walls are self-supporting exterior walls that are independent of the frame, although they are usually laterally anchored to the frame at each floor level. Except for their own dead weight, curtain walls are also nonload bearing. On the other hand, the exterior walls make up the main structural member of a load bearing wall building. As such, load-bearing walls support primary building loads in addition to their own dead weight.

To establish the resistance functions for the exterior walls evaluated in this program, it was assumed that the primary structural response was a one-way structural action between horizontal supports, such as between two successive floor slabs, as shown on Figure 7. Although an exterior load-bearing or curtain wall is generally supported by intermediate vertical pilasters or interior walls, the one-way action assumption was believed justified in the initial study because it appeared reasonable for many wall configurations, since after the bending failure of a nonreinforced wall supported on four sides (which occurs at very small deflections), the primary resistance to collapse of the wall is provided by the vertical dead load of the building. Also, for vertical supports spaced greater than about twice the vertical span, the side supports do not significantly affect the wall resistance. However, recent unpublished blast loading rests by URS Corporation (Ref.15) on simply supported brick wall panels, with a width-to-height ratio of 1.5, indicated a significant increase in the resistance of walls supported on all four sides compared with walls supported on the top and bottom edges only.

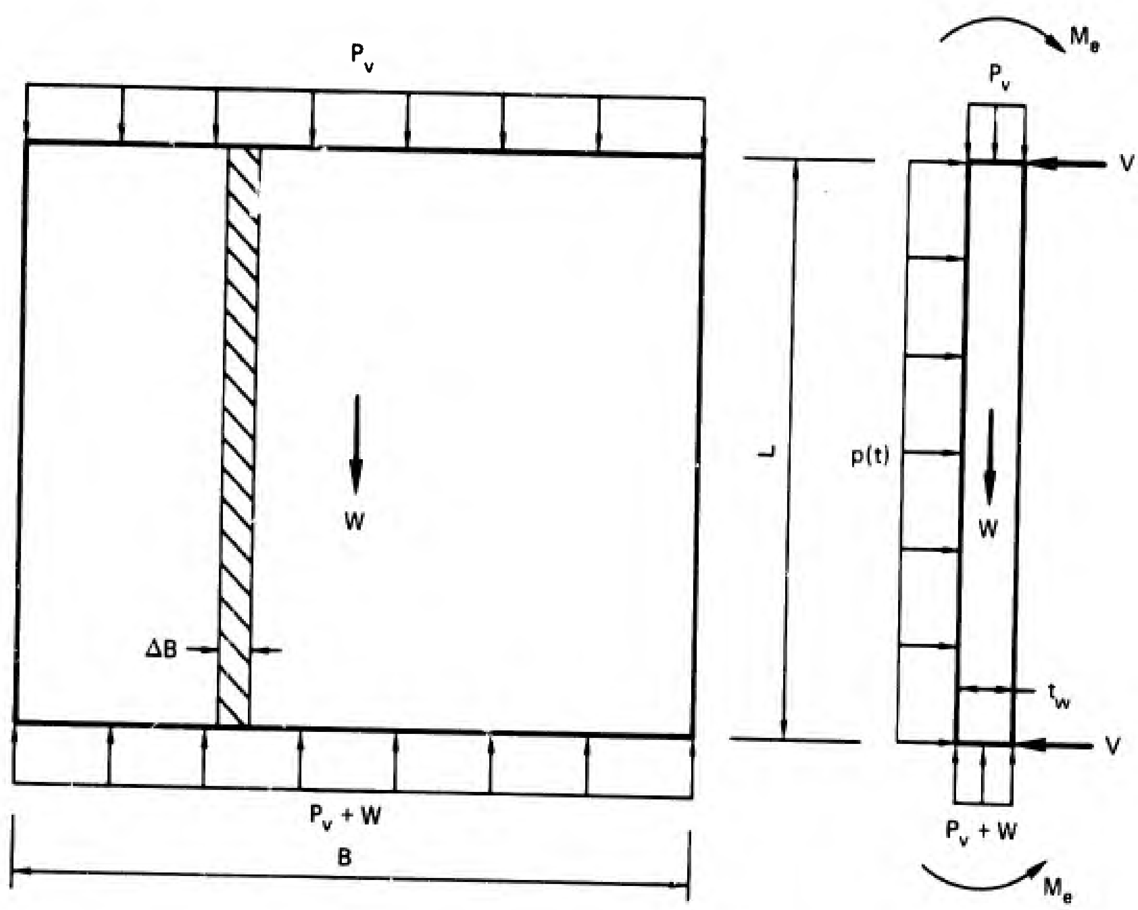


FIG. 7 WALL ELEMENT ASSUMED FOR ANALYSIS

It is apparent from these limited tests on 8 ft high by 12 ft wide wall panels that the two-way action may be quite important for walls of usual dimensions. Although the effect of vertical load was not included in the tests, the tests indicated that it may be desirable to include provisions for the resistance of two-way wall action at a later time in the procedures herein.

To evaluate unreinforced concrete or masonry unit walls in existing buildings, two general categories were considered, i.e., walls with and without arching. Arching in walls results from the resistance of the supports to the outward movement in the plane of a wall that is deflecting as a result of a lateral load. Although arching may not influence the behavior of a majority of the types of wall construction of interest, it can be very important for some configurations. Therefore, arching was included in the evaluation procedures. The development of separate response models for walls with and without arching was necessary, since different basic assumptions are required for analysis purposes.

### Failure Criteria

In addition to the development of resistance functions, another problem associated with the evaluation of wall elements subjected to nuclear blast forces is the establishment of a criterion of failure or collapse. The term failure generally implies that the performance of a structure has failed to meet some minimum requirement. Therefore, since satisfactory performance may involve only the functional use of a building, failure could be defined for many conventional structure applications as merely excessive elastic deflection, without actually concerning the structural integrity directly.

On the other hand, nuclear blast resistant structures are generally designed to permit inelastic deformations to occur, and failure in such cases indicates considerably larger deformations than encountered in conventionally designed structures. Even so, the definition of failure may not include collapse. It may be excessive permanent deflection that prevents reuse of the building or element, or a structure may be considered to have failed if it will not sustain another loading cycle equivalent to the design load.

For the purposes of the evaluation of exterior wall element in this study, failure implies collapse or disintegration of the wall. Furthermore, incipient collapse is defined as that point in the response where the wall can be considered as on the threshold of collapse. The pressure at incipient collapse is therefore the load that is just sufficient in magnitude to cause a collapse of the wall--a load of slightly lesser magnitude would not result in collapse. Since the assumptions for failure vary for each type of wall element, the failure criteria used in this study are presented in each of the subsections for the three types of walls considered.

## Unreinforced Concrete or Masonry Unit Wall (Without Arching)

From the standpoint of structural response, panel, curtain, and load-bearing walls of unreinforced concrete or masonry unit construction are evaluated by a single mathematical model. However, to relate the model to actual building situations, it is necessary to include in the model provisions for various support conditions and magnitudes of vertical axial dead loads. For example, to determine the collapse of a panel wall, the wall would be evaluated as a simply supported member spanning successive floor levels. In addition to the blast loads, the wall would be subjected only to the dead weight of the wall between the floors. An exterior load-bearing wall would be analyzed with the same mathematical model, except that it would be analyzed as a segment of a wall that was continuous over the floor supports that provide lateral restraint. For this case, the vertical load would include both the building and wall loads above the wall segment under consideration.* Although the generic shape of the resistance function for the two walls would be similar, the magnitude of the resistance and, therefore, the predicted collapse pressure would not be the same even for walls constructed of the same materials.

### Resistance Function

In this investigation, the resistance function for unreinforced concrete or masonry unit walls, without arching, was assumed to be initially elastic followed by a decaying resistance. Under these conditions, the initial phase is controlled by the elastic bending strength, and an initial failure is assumed to occur in the wall when the extreme fiber stress reaches the modulus of rupture for concrete members or the tensile bond

---

* It should be mentioned that only the wall action was considered in this report. The overall response, such as overturning or sliding of a load-bearing wall building, will be considered in a subsequent study phase.

strength for brick or concrete masonry unit walls.† After the initial flexural failure, the wall resistance is provided by the geometry of the wall and the magnitude of the vertical axial forces in the plane of the wall. The inclusion of this equilibrium resistance mechanism provides a more rational basis for predicting the collapse load of a wall than is provided solely by the bending resistance function. It is apparent that the magnitude of the vertical load is a controlling factor in the behavior of a nonreinforced wall. For a static lateral load, a decaying resistance of the type assumed results in collapse when the bending capacity of the member is reached. However, for a load function that decays with time the resistance of the wall after the initial bending failure, even though of a decaying type, can be very important in determining the collapse pressure for the wall.

Simply Supported Wall. To develop the resistance function, as discussed above, for unreinforced concrete or masonry unit walls, an elemental width of wall subjected to a dynamic load is considered as indicated in Figure 7. During the initial elastic phase, the resistance of the wall shown in Figure 8 (a) is a function of the bending resistance of the wall and the vertical load. The maximum elastic resistance, $Q_1$, of a simply supported wall with a uniformly distributed load is developed when the moment at the center section is a maximum, or

$$M_c = \frac{Q_1 L}{8} \quad . \tag{16}$$

† Depending on the pattern in which the masonry units are laid and the support conditions, a modulus of rupture based on the beam strength of a masonry unit wall may be more appropriate than the tensile bond strength (Ref. 16). Although the method used to determine the magnitude of the stress value influences the predicted failure loading, it does not affect the development of the mathematical model.

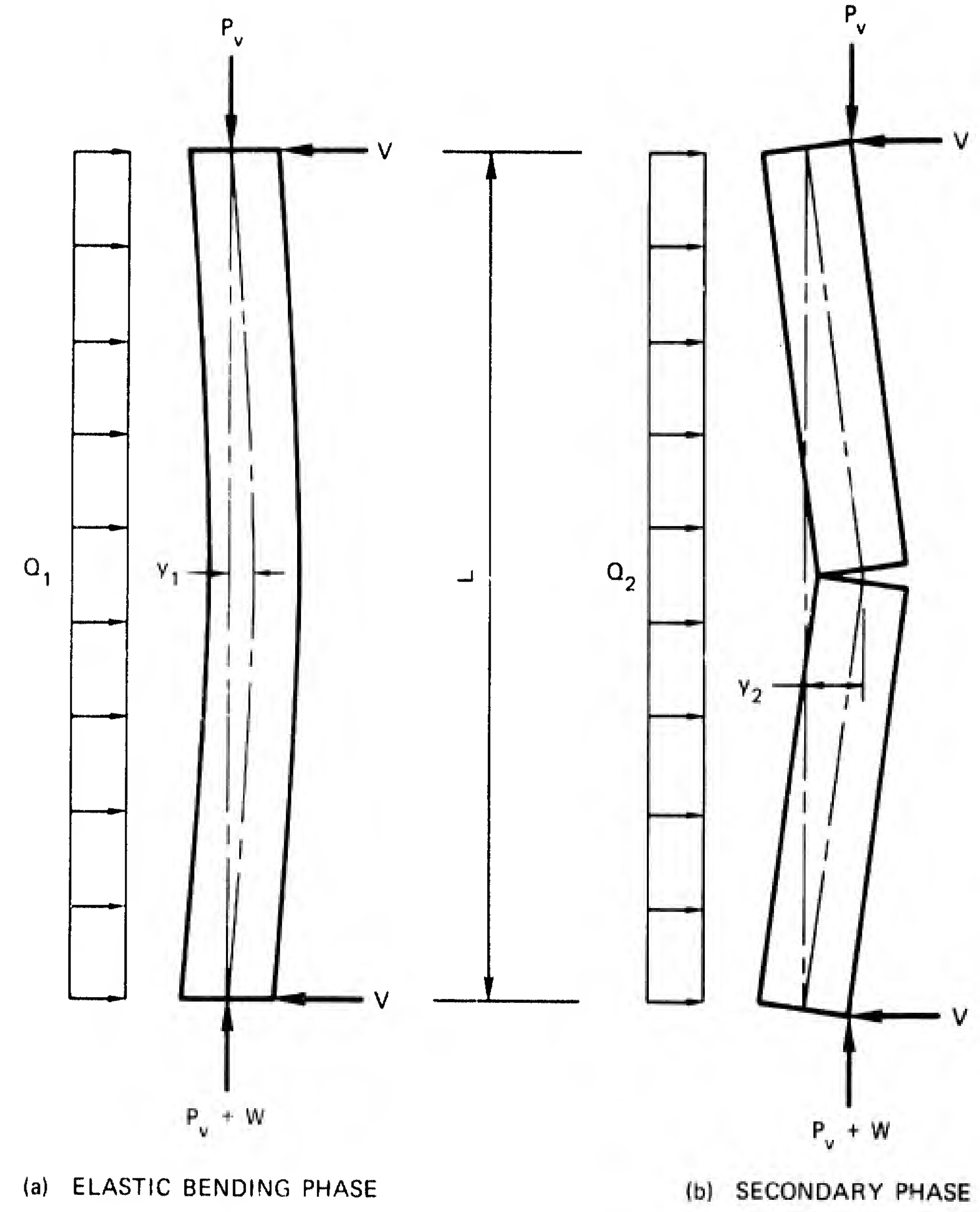


FIG. 8 ASSUMED MODEL FOR BEHAVIOR OF UNREINFORCED CONCRETE OR MASONRY UNIT WALL

If it is assumed that a linear relationship exists between the stress and strain across a section of the wall, the extreme fiber stress is equal to

$$f = \frac{Mc}{I} \pm \frac{P_v}{A} . \tag{17}$$

Substituting $M_c$ in the above equation, rearranging terms, and assuming that the tensile stress governs the wall failure, the maximum elastic resistance for a rectangular section is

$$Q_1 = \frac{4t_w}{3\ L}\left(f\ t_w + P_v\right) . \tag{18}$$

Depending on the type of wall construction, the value of f in Eq. 18 may be the modulus of rupture or the tensile bond strength.

The maximum deflection for the elastic phase is

$$y_1 = \frac{5\ Q_1\ L^3}{384EI_g} . \tag{19}$$

The above equations are not exact, since the effect of the eccentricity of the axial load, which results from the deflection of the wall under the lateral load, is neglected. However, for unreinforced walls of the type considered, the elastic deflections are small, and therefore, the increase in moment and deflection caused by the eccentricity are also small. For example, for a simply supported wall 8 in. thick and 8 ft in span, the errors in the moment and deflection given by the equations are approximately 3 percent. For the prediction of wall collapse, this percentage error is negligible.

Subsequent to the initial bending failure of the wall during the elastic phase, a crack is developed in the vicinity of the point of maximum moment, and the bending resistance of the wall reduces to zero. However, the wall does not necessarily collapse, since the axial force in the plane of the wall provides a restoring force, which results in a decaying type of resistance function. It is apparent that for a static or long duration dynamic lateral load a structural member with a decaying resistance function would collapse if the load equaled the maximum resistance. However, for situations where the clearing time of the reflected overpressure is relatively short, the influence of a decaying resistance function can be important for the prediction of the collapse pressure, even for long duration blast loads. It was found in this study that for most structures of interest the decaying resistance function should be included to yield realistic collapse pressures and times to collapse.

To develop the equation for the resistance during the secondary phase, it was assumed that the wall cracked along a horizontal section and that the two resulting wall segments rotated about the supports as rigid bodies, as shown on Figure 8 (b). Furthermore, for this phase, the small curvature of the wall developed in the elastic phase was neglected. The resistance in the secondary or decaying phase is related to the vertical axial load, the wall dead load, the wall dimensions, and the deflection. By taking moments about one of the supports, it can be shown that the maximum resistance during the decaying phase is equal to

$$Q_2 = \frac{4}{L} \left( t_w - y_2 \right) \left( 2 P_v + W \right) . \qquad (20)$$

As shown on Figure 9 this maximum resistance may be greater than, equal to, or less than the maximum elastic resistance.

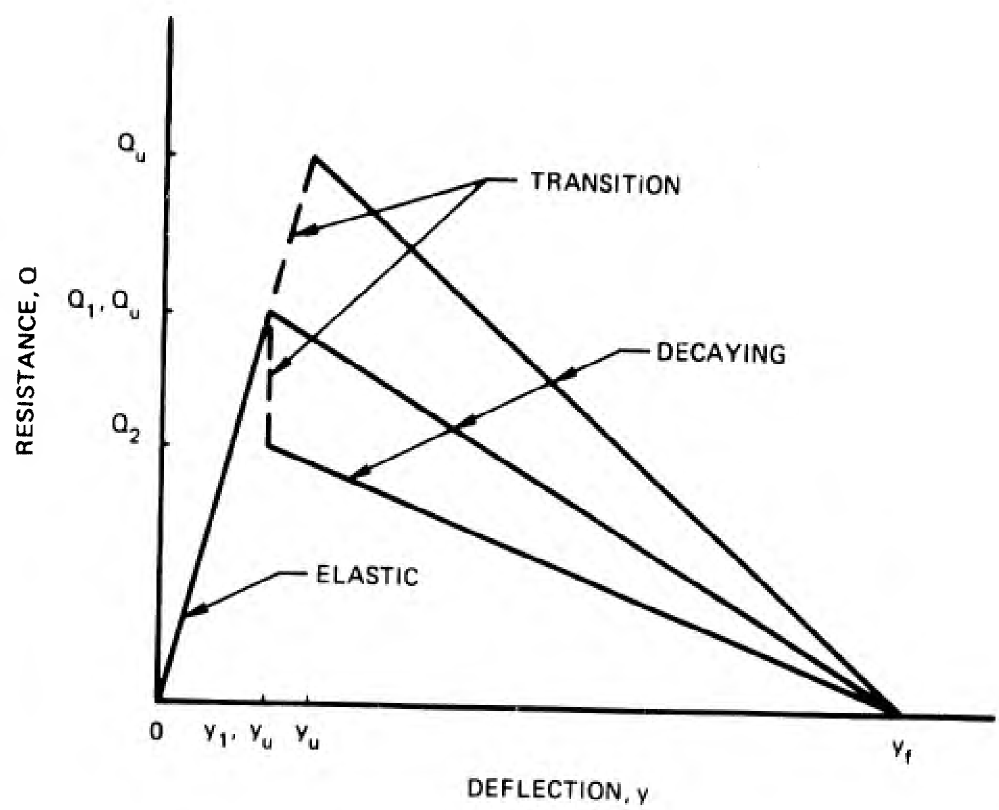


FIG. 9 RESISTANCE FUNCTION FOR A SIMPLY SUPPORTED UNREINFORCED CONCRETE OR MASONRY UNIT WALL WITHOUT ARCHING

Since the method of determining the resistance curves for the elastic and decaying phases generally results in a discontinuity, an assumption regarding the transition between the two phases was required. For the case where the maximum decaying phase resistance is greater than the maximum elastic phase resistance, the elastic resistance is assumed to increase linearly until it intersects the upper decaying resistance function, as shown by the dashed line on Figure 9. For the case where the maximum decaying phase resistance is less than the maximum elastic phase resistance, the resistance function is assumed to decrease to the lower decaying resistance function as shown on the figure. In an actual case, the resistance function would exhibit a smooth transition between the two phases, rather than as used in the mathematical model herein (the error in the assumed response is minor, however).

The assumption for the location of the vertical dead load, $P_v$, during the secondary phase affects both the maximum resistance and the deflection at which collapse is predicted. The actual location of the resultant of the vertical forces during the response of the wall depends on a number of factors, such as the point of application of the floor loads and the deflection of the wall, and is therefore indeterminate. In this study, it was assumed that before cracking of the wall the vertical dead load acted at the centroid of the wall section. After cracking, it was assumed that the vertical dead load acted in the plane of the inner wall surface. These assumptions, of course, neglect the distribution of the load over a finite area. This simplification was adopted, since, as the wall deflects, the center of the wall dead load also moves toward the inner wall surface. When the deflection of the wall is equal to the wall thickness, the center of the vertical force is in the vicinity of the inner wall surface.

Fixed-End Wall. As noted in the previous subsection, the resistance function for a simply supported, one-way unreinforced wall was bilinear, with an elastic and a decaying resistance phase. The resistance function for a uniformly loaded fixed-end wall is similar, expect that the maximum elastic resistance is developed when the moment at support is a maximum, or

$$M_e = \frac{Q_1 L}{12} \quad . \tag{21}$$

By substitution of Eq. 21 in Eq. 17, the maximum elastic resistance shown on Figure 9 is given by

$$Q_1 = \frac{2\ t_w}{L} \left( f\ t_w + P_v \right) \quad . \tag{22}$$

The maximum deflection for the elastic phase of a fixed-end wall is

$$y_1 = \frac{Q_1 L^3}{384 E I_g} \quad . \tag{23}$$

After cracking occurs at the fixed support, the bending resistance at the support is reduced to zero, and the wall responds as a simply supported wall. The resistance and deflection during this phase can be determined by Eqs. 18 and 19, respectively. However, since the maximum resistance for a simply supported element is only two-thirds that for a fixed-end element, the influence of this phase on the predicted wall collapse is not important. Therefore, the resistance for the secondary phase for a fixed-end wall is assumed to be identical to the decaying resistance determined by Eq. 20 for a simply supported wall.

Propped-Cantilever Wall. The shape of the resistance function for a wall fixed at one end and simply supported at the other end is identical to that for a fixed-end wall. The maximum elastic resistance for the propped cantilever is developed when the moment at the fixed support is maximum and is equal to Eq. 16 for a simply supported wall. The maximum elastic resistance is therefore given by Eq. 18.

The maximum deflection for the elastic phase occurs at a distance of 0.4215 L from the simply supported end and is equal to

$$y_1 = \frac{Q_1 L^3}{185EI_g} . \qquad (24)$$

For the reasons discussed in the previous subsection for fixed-end walls, the resistance for the secondary phase for a propped-cantilever wall is assumed to be identical to the decaying resistance function given by Eq. 20 for a simply supported wall.

Failure Criterion

In this study, the criterion for the collapse failure of the unreinforced concrete or masonry unit walls was the instability of the wall as a result of excessive deflection. For the wall model illustrated in Figure 8 (b) when the deflection, $y_f$, equals the wall thickness, $t_w$, the restoring force and therefore the resistance of the wall reduce to zero. When this occurs, the collapse of the wall is predicted, regardless of the magnitude of the applied lateral load.

## Reinforced Concrete Wall

The resistance function adopted for evaluation of reinforced concrete walls was essentially as outlined in Refs. 7 and 10. However, since the methods developed in the referenced documents are appropriate for conventional reinforced concrete members, certain modifications were necessary for application to lightly reinforced concrete walls herein. In general, reinforced concrete members subjected to flexure are categorized as overreinforced and underreinforced (e.g., Ref. 17). An overreinforced concrete member fails as a result of the crushing of the concrete, which reaches its ultimate strength before yielding of the reinforcing steel. Such a failure is associated with a sudden or brittle fracturing of the concrete and is avoided in design by the selection of appropriate safety factors for the permissible concrete stress and strain. An underreinforced concrete member in bending tends to fail by elongation of the tensile reinforcing steel. Such a member, when approaching its ultimate strength, exhibits a more or less gradual increase in deflection up to failure. Although an underreinforced concrete element may also ultimately collapse due to a fracture of the concrete, the warning of imminent failure is felt to be desirable for conventional structures, and is, in fact, assured by ultimate strength design procedures (Ref. 18). Underreinforcement is even more desirable for structures specifically designed for blast loading, since the members are usually designed to respond in the ductile range of the steel under the assumed blast load. In fact, Ref. 10 recommends a maximum of 2 percent reinforcing steel for flexural members to assure ductile behavior. This is generally less than would be obtained for static loads by ultimate strength design procedures, which are also based on the steel reaching its yield strength before a concrete failure (Ref. 18).

The above discussion is concerned with reinforced concrete members designed for flexure by a conventional procedure. However, in this study, the exterior walls of interest are not necessarily designed to resist bending forces, and reinforcement in the member may only be sufficient to meet a code requirement for temperature and shrinkage steel. The reinforcement steel ratio for such wall elements may be as little as 0.20 or 0.25 of 1 percent, which can be described as light reinforcement. Unfortunately, the behavior of lightly reinforced concrete members, under lateral loads sufficient to produce collapse failure, is not nearly so well-known as for conventionally reinforced members. Even so, there are several important differences in lightly reinforced members that are apparent from the limited data. First, the ultimate moment capacity of conventionally reinforced concrete members is generally much greater than the cracking moment, whereas for lightly reinforced members the ultimate and cracking moment capacity may be approximately the same. In fact, the modulus of rupture of the concrete in a lightly reinforced concrete member may result in a greater moment capacity than provided by the small steel area. Second, although a lightly reinforced member can be categorized as underreinforced, the mode of failure is significantly different than for conventional reinforced concrete. For a conventional, one-way reinforced concrete member in flexure, the tension steel elongates over a significant portion of the span length, as evidenced by numerous cracks in the tension surface of the concrete. The generic shape of the elastic curve for such members is similar before and after cracking of the concrete--even after the ultimate strength is exceeded, the deflected member exhibits a curvature for most of its span length (Ref. 19). On the other hand, lightly reinforced concrete members tend to form a single crack on reaching the ultimate concrete tensile strength in the vicinity of the maximum moment. Although such a member will exhibit an elastic behavior in the uncracked condition, after the modulus of rupture is exceeded, the deflection mode is primarily that of a rigid body rotation about the supports and the cracked section. Under these conditions, a plastic elongation of the reinforcing steel over a relatively small length at the cracked section would be anticipated. Although the actual load-deflection relationships of lightly reinforced concrete members is not well-documented, the rigid body rotation mode has been observed in experiments (Ref. 14).

Although the resistance of a lightly reinforced concrete member may or may not be reduced after cracking, the collapse of the wall can be accompanied by relatively large deflections as a result of the ductility of the steel. This is important for predicting collapse for time-dependent load-functions, especially where the clearing of the reflected overpressure can occur in times approximately equal to the natural period of vibration.

## Resistance Functions

In general, the resistance functions developed in this study for reinforced concrete walls exhibit an elastic phase, an elasto-plastic phase, and a purely plastic phase. The procedures used to obtain the function required the establishment of the maximum resistance and deflection for each phase. It was then assumed that a linear relationship existed between the maxima. The resistance functions for lightly reinforced concrete walls are presented in the following subsections for each of the three support conditions.

It was assumed in this program that the vertical dead load, if any, was applied to a wall element as an axial load in the plane of the wall, as shown on Figure 7. The effect of an initial eccentricity of the vertical load was not considered directly in determining either the wall deflection or resistance. However, if significant for a particular case, the eccentricity of the load can be included in calculating the ultimate moment capacity of the concrete wall section.

The solution of the resistance function equations for a specific wall element requires the determination of the ultimate moment capacity of the wall section. Therefore, the ultimate moment equations, which are based on conventional ultimate strength concepts, are presented in Appendix A for convenience.

Simply Supported Wall. For the purpose of this analysis, it was assumed that the internal resistance of a one-way, simply supported wall element is developed in two distinct phases, elastic and plastic. However, as mentioned previously for lightly reinforced concrete members, the uncracked section may provide a greater moment resistance than the cracked section. Therefore, to provide a more realistic resistance function, the elastic portion of the function is developed in two phases. This results in a trilinear elastic-plastic resistance function for simply supported walls, as illustrated in Figure 10, rather than the usually assumed bilinear relationship. This refinement was used, since relatively large errors in the initial resistance function would otherwise occur for the case where the resistance for the cracked wall is less than that for the uncracked wall, as noted by the dashed line in Figure 10.

To determine the resistance function for a specific lightly reinforced wall element, the maximum resistance in the initial elastic phase is assumed to be limited by the modulus of rupture of the concrete, and the maximum deflection for this phase is determined by using the elastic deflection equations and the moment of inertia for the uncracked section. After cracking of the concrete the maximum resistance in the secondary elastic phase is provided by the ultimate strength of the member, which is limited by the yielding of the reinforcing steel. The maximum deflection is calculated by the elastic deflection equation and the moment of inertia of the cracked section. For the determination of the moment of inertia, it is assumed that the section is uniformly cracked throughout

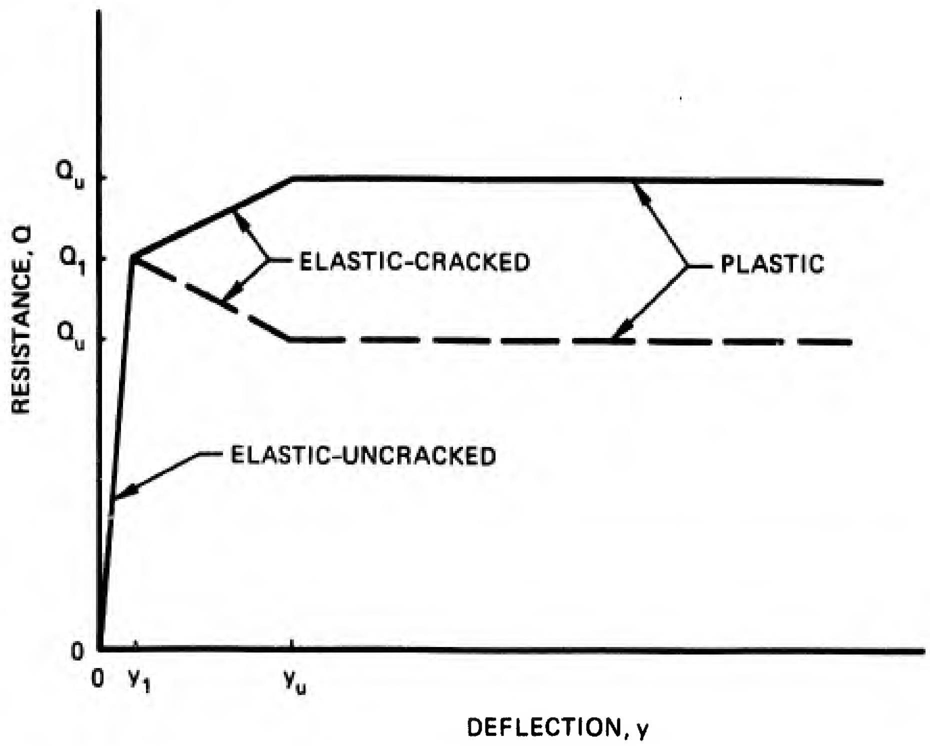


FIG. 10 RESISTANCE FUNCTION FOR A SIMPLY SUPPORTED REINFORCED CONCRETE WALL

its length. Although it is well-known that tensile cracking in reinforced concrete members under flexural loads is not uniformly distributed, the error in the magnitude of the deflection due to this assumption is not too important for the prediction of wall collapse. The resistance functions for walls with and without a vertical axial load are presented separately.

Wall Without Vertical Axial Load

The maximum resistance in the initial elastic phase for a simply supported wall with a uniformly distributed lateral load is developed when the center moment is a maximum just prior to cracking, and is given by Eq. 16,

$$M_c = \frac{Q_1 L}{8} \quad .$$

The modulus of rupture is given by the usual flexure formula,

$$f_r = \frac{Mc}{I_g} \quad . \tag{25}$$

Substituting $M_c$ in the above equation, the maximum resistance to the initial elastic phase, for a rectangular section, is given by

$$Q_1 = \frac{4 f_r t_w^2}{3 L} \quad . \tag{26}$$

The maximum deflection for the initial elastic phase is given by Eq. 19,

$$y_1 = \frac{5 Q_1 L^3}{384 EI_g} \quad .$$

After cracking of the concrete, the maximum resistance in the secondary elastic phase is equal to the ultimate resistance, $Q_u$, of the wall and is found by Eq. 16 by substituting the ultimate moment capacity of the center section, $M_{uc}$, for the center moment, $M_c$. The ultimate moment capacity of the cracked section is determined by the formulas presented in Appendix A.

The deflection, $y_u$, at the development of the ultimate resistance of the wall is found by Eq. 19 by substituting the ultimate resistance for $Q_1$ and by using the moment of inertia for the cracked concrete section.

<u>Wall With Vertical Axial Load</u>

From Ref. 20, the center moment for a simply supported wall element, with combined axial and uniformly distributed lateral load, can be determined by

$$M_c = \frac{QEI}{LP_v}\left(\sec \frac{L}{2}\sqrt{\frac{P_v}{EI}} - 1\right) .$$

For the initial elastic phase, the maximum resistance of a simply supported wall is developed when the center moment, $M_c$, in the above equation is a maximum just before cracking, and the moment of inertia is for an uncracked concrete section. By rearranging terms the resistance is

$$Q_1 = M_{mc} \frac{P_v L}{EI_g\left(\sec \frac{L}{2}\sqrt{\frac{P_v}{EI_g}} - 1\right)} . \qquad (27)$$

The maximum deflection for the initial elastic phase, from Ref. 20, is given by

$$y_1 = \frac{Q_1\ EI_g}{L\ P_v^2}\left(\sec \frac{L}{2}\sqrt{\frac{P_v}{EI_g}} - 1 - \frac{P_v\ L^2}{8EI_g}\right). \qquad (28)$$

After cracking of the concrete, the ultimate resistance, $Q_u$, is determined by substituting the ultimate moment capacity, $M_{uc}$, in

Eq. 27 for the center moment, $M_{mc}$. The ultimate deflection is given by Eq. 28 by substituting the ultimate resistance for $Q_1$ and by using the moment of inertia for the cracked concrete section.

Fixed End Wall. It was assumed in this analysis that the internal resistance for a one-way, fixed-end wall is developed in three distinct phases; elastic, elasto-plastic, and plastic. As noted for the resistance of simply supported walls, the elastic portion of the fixed-end wall resistance function is also developed in two phases; the initial elastic uncracked and the secondary elastic cracked phase. This results in a resistance function similar to that illustrated in Figure 11; the dashed line represents the case where the resistance for the cracked wall is less than that for the uncracked wall.

Wall Without Vertical Axial Load

The maximum resistance in the initial elastic phase for a fixed-end wall with a uniformly distributed lateral load is developed when the end moment is a maximum just before cracking and is given by

$$Q_1 = \frac{8}{L}\left(M_e + M_c\right) . \tag{29}$$

For a uniform wall thickness throughout the wall length

$$M_c = \frac{M_e}{2}$$

and the maximum resistance in the initial elastic phase becomes

$$Q_1 = \frac{12}{L} M_e . \tag{30}$$

For a linear relationship between the stress and strain across the section, the extreme fiber stress is given by Eq. 25, and the maximum

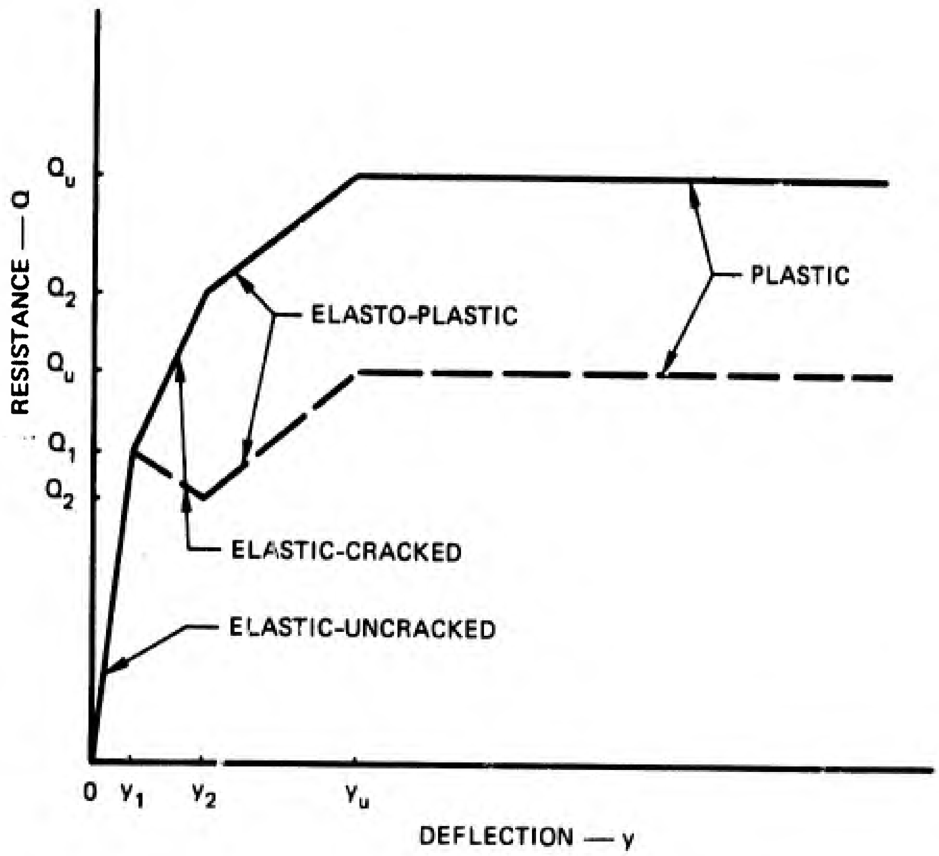


FIG. 11 RESISTANCE FUNCTION FOR A FIXED-END AND PROPPED-CANTILEVER REINFORCED CONCRETE WALL

resistance in the initial elastic phase for a rectangular section is given by

$$Q_1 = \frac{2 f_r t_w^2}{L} . \tag{31}$$

The maximum deflection for the initial elastic phase is given by Eq. 23

$$y_1 = \frac{Q_1 L^3}{384EI_g} .$$

Since the resistance given by Eq. 31 is greater than the resistance provided by the uncracked center section, it was assumed in this study that when the section at the support reaches the cracking resistance, the center section also cracks. Therefore, after cracking of the concrete at both the support and center sections, the maximum resistance in the secondary elastic phase is developed when the ultimate moment capacity, $M_{ue}$, is reached at the support and is given by Eq. 29 by substituting $M_{ue}$ for $M_e$, or

$$Q_2 = \frac{8}{L} \left(M_{ue} + M_{c2}\right) .$$

Considering the more general case, where the ultimate moment capacity of the center section is greater than one-half that at the supports

$$M_{c2} = \frac{M_{ue}}{2} \tag{32}$$

Therefore, the maximum resistance in the elastic phase for the cracked section can be obtained by substituting the ultimate moment capacity at the end section in Eq. 30, or

$$Q_2 = \frac{12}{L} M_{ue} . \tag{33}$$

The maximum deflection for the secondary elastic phase is obtained by substituting the maximum elastic resistance, $Q_2$, and by using the moment of inertia for the cracked section in Eq. 23 or

$$y_2 = \frac{Q_2 L^3}{384EI_c} \tag{34}$$

After the development of the ultimate moment capacity at the supports of a fixed-end wall, the reinforcing steel is at its yield strength, and the wall enters the elasto-plastic phase as shown on Figure 11. As the wall continues to deflect, an additional internal resistance, $\Delta Q$, is developed as a result of the simply supported wall action between the yielding supports. The maximum elasto-plastic resistance is developed when the center section reaches its ultimate moment capacity, and the additional resistance developed is identical to Eq. 16.

$$\Delta M = \frac{\Delta QL}{8} \tag{35}$$

The additional moment capacity developed during the elasto-plastic phase is the difference between the moment, $M_{c2}$, developed in the cracked center section at the end of the elastic phase, and the ultimate moment capacity, $M_{uc}$, of the center section, or

$$\Delta M = M_{uc} - M_{c2} \quad .$$

By substituting Eq. 32 in the above, the additional elasto-plastic resistance is equal to

$$\Delta M = M_{uc} - \frac{M_{ue}}{2} \quad . \tag{36}$$

Setting Eq. 35 equal to Eq. 36 and rearranging terms, the additional resistance is

$$\Delta Q = \frac{8}{L}\left(M_{uc} - \frac{M_{ue}}{2}\right) . \tag{37}$$

With the development of the ultimate moment at the center section of a fixed-end wall, a mechanism is formed, and the ultimate or plastic bending resistance of the wall is reached. Since the ultimate resistance of the wall is the sum of the resistances developed during the elastic and elasto-plastic phases

$$Q_u = Q_2 + \Delta Q \tag{38}$$

or

$$Q_u = \frac{8}{L}\left(M_{ue} + M_{uc}\right) . \tag{39}$$

In a like manner, the maximum deflection at the development of the ultimate resistance of the wall is the sum of the maximum deflections in the elastic and elasto-plastic phases. Since the wall deflects as a simply-supported member during the elasto-plastic phase, the additional deflection is equal to that given by Eq. 19, or

$$\Delta y = \frac{5\ \Delta Q\ L^3}{384EI_c} , \tag{40}$$

and the deflection at the ultimate resistance is the sum of Eqs. 34 and 40,

$$y_u = y_2 + \Delta y \tag{41}$$

$$y_u = \frac{L^3}{384EI_c}\left(Q_2 + 5\ \Delta Q\right) \tag{42}$$

or, by substituting the maximum resistances developed during the elastic and elasto-plastic phases, the deflection at ultimate resistance becomes

$$y_u = \frac{L^2}{48EI_c}\left(5\,M_{uc} - M_{ue}\right) . \qquad (43)$$

<u>Wall With Vertical Axial Load</u>

From Ref. 20, the end moment for a fixed-end wall element with combined axial and uniformly distributed transverse load, such as shown in Figure 7, can be determined by,

$$M_e = \frac{Q\,EI_g}{L\,P_v}\left(1 - \frac{\frac{L}{2}\sqrt{\frac{P_v}{EI_g}}}{\tan \frac{L}{2}\sqrt{\frac{P_v}{EI_g}}}\right) .$$

For the initial elastic phase, the maximum internal resistance of a fixed-end wall is developed when the end moment, $M_e$, in the above equation is a maximum just before cracking, and the moment of inertia is for an uncracked concrete section. By rearranging terms, the resistance is

$$Q_1 = M_{me}\,\frac{P_v L}{EI_g}\left(\frac{\tan \frac{L}{2}\sqrt{\frac{P_v}{EI_g}}}{\tan \frac{L}{2}\sqrt{\frac{P_v}{EI_g}} - \frac{L}{2}\sqrt{\frac{P_v}{EI_g}}}\right) . \qquad (44)$$

The maximum deflection for the initial elastic phase from Ref. 20 is given by

$$y_1 = Q_1 \frac{EI_g}{P_v L^2} \left[ - \left( 1 - \frac{\frac{L}{2}\sqrt{\frac{P_v}{EI_g}}}{\tan \frac{L}{2}\sqrt{\frac{P_v}{EI_g}}} \right) \left( \frac{1-\cos \frac{L}{2}\sqrt{\frac{P_v}{EI_g}}}{\cos \frac{L}{2}\sqrt{\frac{P_v}{EI_g}}} \right) \right.$$

$$\left. + \sec \frac{L}{2}\sqrt{\frac{P_v}{EI_g}} - \frac{P_v L^2}{8EI_g} - 1 \right] \quad . \qquad (45)$$

After cracking of the concrete at both the end and center sections, the maximum resistance in the secondary elastic phase is developed when the ultimate moment capacity is reached at the end support. This resistance can be obtained from Eq. 44 by substituting the ultimate moment capacity at the end section and the moment of inertia for the cracked concrete section and is equal to

$$Q_2 = M_{ue} \frac{P_v L}{EI_c} \left( \frac{\tan \frac{L}{2}\sqrt{\frac{P_v}{EI_c}}}{\tan \frac{L}{2}\sqrt{\frac{P_v}{EI_c}} - \frac{L}{2}\sqrt{\frac{P_v}{EI_c}}} \right) . \qquad (46)$$

The maximum deflection for the secondary elastic phase is obtained by substituting the maximum elastic resistance and moment of inertia for the cracked section into Eq. 45, or

$$y_2 = Q_2 \frac{EI_c}{P_v L^2} \left[ - \left( 1 - \frac{\frac{L}{2}\sqrt{\frac{P_v}{EI_c}}}{\tan \frac{L}{2}\sqrt{\frac{P_v}{EI_c}}} \right) \left( \frac{1-\cos \frac{L}{2}\sqrt{\frac{P_v}{EI_c}}}{\cos \frac{L}{2}\sqrt{\frac{P_v}{EI_c}}} \right) \right.$$

$$\left. + \sec \frac{L}{2}\sqrt{\frac{P_v}{EI_c}} - \frac{P_v L^2}{8EI_c} - 1 \right] . \qquad (47)$$

The above equations include the deflections and moments resulting from both the uniformly distributed lateral load and the vertical axial load.

As the deflection of the wall is increased above the maximum elastic deflection, the wall resistance enters the elasto-plastic phase, as shown on Figure 11, and an additional internal resistance, $\Delta Q$, is developed as a result of the simply supported wall action. The maximum elasto-plastic resistance is developed when the center section reaches its ultimate moment capacity, and the additional moment resistance is identical to Eq. 27,

$$\Delta M = \frac{\Delta Q \; EI_c}{L \; P_v} \left( \sec \frac{L}{2}\sqrt{\frac{P_v}{EI_c}} - 1 \right) . \qquad (48)$$

Since the additional moment capacity developed during the elasto-plastic phase is the difference between the moment, $M_{c2}$, developed in the cracked center section at the end of the elastic phase and the ultimate moment capacity, $M_{uc}$, of the center section

$$\Delta M = M_{uc} - M_{c2} \quad . \qquad (49)$$

Since the center moment at the end of the elastic phase is equal to

$$M_{c2} = M_{ue}\left(\frac{\frac{L}{2}\sqrt{\frac{P_v}{EI_c}} - \sin\frac{L}{2}\sqrt{\frac{P_v}{EI_c}}}{\sin\frac{L}{2}\sqrt{\frac{P_v}{EI_c}} - \frac{L}{2}\sqrt{\frac{P_v}{EI_c}}\cos\frac{L}{2}\sqrt{\frac{P_v}{EI_c}}}\right) \tag{50}$$

it can be shown by the substitution of Eqs. 47 and 48 into Eq. 45 that the additional resistance developed during the elasto-plastic phase is equal to

$$\Delta Q = \frac{P_v L}{EI_c\left(\sec\frac{L}{2}\sqrt{\frac{P_v}{EI_c}} - 1\right)}\left[M_{uc} - M_{ue}\frac{\frac{L}{2}\sqrt{\frac{P_v}{EI_c}} - \sin\frac{L}{2}\sqrt{\frac{P_v}{EI_c}}}{\sin\frac{L}{2}\sqrt{\frac{P_v}{EI_c}} - \frac{L}{2}\sqrt{\frac{P_v}{EI_c}}\cos\frac{L}{2}\sqrt{\frac{P_v}{EI_c}}}\right] \tag{51}$$

Since, from Eq. 38

$$Q_u = Q_2 + \Delta Q,$$

the ultimate resistance is

$$Q_u = \frac{P_v L}{EI_c}\left[\frac{M_{ue}}{1 - \cos\frac{L}{2}\sqrt{\frac{P_v}{EI_c}}} + \frac{M_{uc}}{\sec\frac{L}{2}\sqrt{\frac{P_v}{EI_c}} - 1}\right]. \tag{52}$$

In a like manner, the maximum deflection at the development of the ultimate resistance of the wall is the sum of the maximum deflections in the elastic and elasto-plastic phases. Since the wall deflects as a simply supported member during the elasto-plastic phase, the additional deflection is equal to that given by Eq. 28, or

$$\Delta y = \frac{\Delta Q \; EI_c}{L \; P_v^2} \left( \sec \frac{L}{2} \sqrt{\frac{P_v}{EI_c}} - 1 - \frac{P_v L^2}{8EI_c} \right) . \qquad (53)$$

The center deflection of the wall at the development of the ultimate resistance of the wall is equal to the sum of the deflections in the elastic and elasto-plastic phases, given by Eqs. 47 and 53, respectively, and is given by Eq. 41.

Propped-Cantilever Wall. The internal resistance of a propped-cantilever wall, i.e., fixed at one end and simply supported at the other, is of the same generic shape as that shown on Figure 11 for the fixed-end wall. Since the development of the resistance function for a propped cantilever is similar to that for a fixed-end wall, the equations for determining the resistance function for the propped cantilever will be presented in abbreviated form. (See the previous subsection on Fixed-End Wall for an explanation of the various phases for the resistance.)

### Wall Without Vertical Axial Load

The maximum resistance in the initial elastic phase for a propped-cantilever wall with a uniformly distributed lateral load is developed when the moment at the fixed end is a maximum just before cracking of the concrete, and is identical to Eq. 16

$$Q_1 = \frac{8 \; M_{me}}{L} . \qquad (54)$$

The maximum deflection for the initial elastic phase is given by Eq. 24

$$y_1 = \frac{Q_1 L^3}{185EI_g} .$$

For the secondary elastic phase after cracking of the fixed end, the maximum resistance and deflection are similar to Eqs. 16 and 24, respectively, and are given by

$$Q_2 = \frac{8\ M_{ue}}{L} \tag{55}$$

and

$$y_2 = \frac{Q_2\ L^3}{185EI_c} . \tag{56}$$

The maximum elasto-plastic resistance is developed when the center section reaches its ultimate moment capacity, and the additional resistance developed is

$$\Delta Q = \frac{4}{L}\left(2\ M_{uc} - M_{ue}\right) . \tag{57}$$

With the development of the ultimate moment at the center section of a propped-cantilever wall, the ultimate resistance developed is

$$Q_u = \frac{4}{L}\left(2\ M_{uc} + M_{ue}\right) . \tag{58}$$

The above equation is not exact, although it will be used to determine the maximum resistance for a propped-cantilever wall in this study. To calculate the exact maximum resistance, it is necessary to locate the point of maximum positive moment in the member. For a wall fixed on both ends, it is apparent by inspection that this maximum occurs at the center for both the elastic and elasto-plastic phases. Therefore, by superposition of the maximum moments at the center for both phases, the maximum resistance can be determined. On the other hand, for a propped cantilever, a maximum moment during the initial elastic phase occurs at a distance of 0.375 L from the propped end. Since the maximum moment for the simply supported or secondary phase is at the center, the point of maximum moment is not obvious. By a consideration of the elastic curves for the elastic and elasto-plastic phases, it can be shown that the maximum moment for determining the ultimate resistance of a wall with constant cross section occurs at a distance of 0.4142 L from the propped end. Furthermore, the ultimate resistance corresponding to the actual maximum moment is only about 3 percent less than the value given by Eq. 55, and is therefore negligible.

The additional deflection of a propped-cantilever wall during the elasto-plastic phase is given by

$$\Delta y = \frac{5\ L^2}{96EI_c}\left(2\ M_{uc} - M_{ue}\right) , \tag{59}$$

and the deflection at the development of the ultimate resistance of the wall is the sum of Eqs. 56 and 59, or

$$y_u = \frac{L^2}{96EI_c}\left(10\ M_{uc} - M_{ue}\right) . \tag{60}$$

As previously mentioned for the ultimate resistance given by Eq. 58, the deflection given by the above equation is not exact. Since the maximum deflection, at the development of the ultimate resistance of a propped-cantilever wall with a constant cross section, occurs at a distance of 0.4573 L from the propped end, the deflection given by Eq. 60 is in error by no more than about 4 percent.

## Wall With Vertical Axial Load

The maximum resistance in the initial elastic phase for a propped-cantilever wall with combined axial and uniformly distributed transverse load is developed when the moment at the fixed-end is a maximum just before cracking of the concrete. The maximum elastic resistance can be determined from Ref. 20 and is equal to

$$Q_1 = M_{me} \sqrt{\frac{P_v}{EI_g}} \left[ \frac{\tan L \sqrt{\frac{P_v}{EI_g}} - L \sqrt{\frac{P_v}{EI_g}}}{\left(\tan L \sqrt{\frac{P_v}{EI_g}}\right)\left(\tan \frac{L}{2} \sqrt{\frac{P_v}{EI_g}} - \frac{L}{2} \sqrt{\frac{P_v}{EI_g}}\right)} \right] . \quad (61)$$

The maximum deflection for the initial elastic phase is given by

$$y_1 = \frac{M_{me}}{2 P_v} \left(1 - \sec \frac{L}{2} \sqrt{\frac{P_v}{EI_g}}\right)$$

$$+ \frac{Q_1 \; EI_g}{P_v^2 \; L} \left(\sec \frac{L}{2} \sqrt{\frac{P_v}{EI_g}} - 1 - \frac{L^2 \; P_v}{8EI_g}\right) \quad (62)$$

For the secondary elastic phase after cracking of the fixed end, the maximum resistance and deflection are given by

$$Q_2 = M_{ue} \sqrt{\frac{P_v}{EI_c}} \left[ \frac{\tan L \sqrt{\frac{P_v}{EI_c}} - L \sqrt{\frac{P_v}{EI_c}}}{\left(\tan L \sqrt{\frac{P_v}{EI_c}}\right)\left(\tan \frac{L}{2} \sqrt{\frac{P_v}{EI_c}} - \frac{L}{2} \sqrt{\frac{P_v}{EI_c}}\right)} \right] \quad (63)$$

and

$$y_2 = \frac{M_{ue}}{2\,P_v}\left(1 - \sec\frac{L}{2}\sqrt{\frac{P_v}{EI_c}}\right)$$

$$+ \frac{Q_2\,EI_c}{P_v^2\,L}\left(\sec\frac{L}{2}\sqrt{\frac{P_v}{EI_c}} - 1 - \frac{L^2\,P_v}{8EI_c}\right) . \quad (64)$$

The maximum elasto-plastic resistance is developed when the center section reaches its ultimate moment capacity, and the additional resistance developed is

$$\Delta Q = \left(M_{uc} - M_{c2}\right)\frac{P_v L}{EI_c\left(\sec\frac{L}{2}\sqrt{\frac{P_v}{EI_c}} - 1\right)} \quad (65)$$

where

$$M_{c2} = \frac{Q_2 EI_c}{P_v L}\left(\sec\frac{L}{2}\sqrt{\frac{P_v}{EI_c}} - 1\right) - \frac{M_{ue}}{2}\left(\sec\frac{L}{2}\sqrt{\frac{P_v}{EI_c}}\right) . \quad (66)$$

With the development of the ultimate moment at the center section of a propped-cantilever wall, the ultimate resistance of the wall is developed and is equal to the sum of Eqs. 63 and 65, which is equal to Eq. 38.

The additional deflection of a propped-cantilever wall during the elasto-plastic phase is given by

$$\Delta y = \frac{\left(M_{uc} - M_{c2}\right)}{P_v}\left[1 - \frac{P_v L^2}{8EI_c\left(\sec\frac{L}{2}\sqrt{\frac{P_v}{EI_c}} - 1\right)}\right] \quad (67)$$

and the deflection at the development of the ultimate resistance of the wall is the sum of Eqs. 64 and 67, and is given by Eq. 41.

Failure Criterion

Unfortunately there is very little information available on which to base a failure or collapse criterion for reinforced concrete walls. In general, conventional reinforced concrete members are designed with an approximate balance between the strength of the concrete and the reinforcing steel. For such members, ultimate strength design concepts are based on the development of the ultimate strain in the concrete simultaneously with the yielding of the reinforcing steel. Although in actual practice, there are certain modifications to these concepts, such as limiting the maximum concrete strain or percent steel, the design yields a balance between the development of the working stresses in the concrete and steel. For conventional concrete members, there is an impressive body of experimental data available concerning such characteristics as load-deflection, end shear, diagonal tension, ductility, and combined axial and flexural loading. Usually the tests have been conducted to check a design theory or to assist in developing a concept for establishing a design theory. Although many tests were taken to "failure," a design criterion for failure can be significantly different from actual collapse of the member. Therefore, even for conventional types of reinforced concrete members, there is very little experimental data on their complete collapse.

For lightly reinforced concrete members there is even less collapse information available. For many of the concrete walls of interest in this study, the wall was not designed to resist a specific lateral load. The reinforcing steel is usually the result of a code requirement for a minimum steel ratio of 0.20 or 0.25 percent. Consequently, the wall may be so lightly reinforced that its structural action is not similar to that of a conventional reinforced concrete member. For instance, the moment capacity of a reinforced concrete beam is generally much greater than that of an identical plain concrete beam. However, for a lightly reinforced beam, it is possible that the moment capacity of the uncracked section is greater than that of the cracked section.

In addition, the deflected mode of a lightly reinforced concrete member after cracking may be considerably different than that for a conventional reinforced member. As mentioned previously, the yielding of the steel in a conventional member under uniform flexural loading involves a considerable portion of the length of the member, whereas the steel in a lightly reinforced member yields over a small length in the vicinity of the maximum moment.

Because of the unknowns, it has been necessary rather arbitrarily to establish the collapse criterion for lightly reinforced concrete members in this study. However, the development of a more rational prediction method is an important consideration in the evaluation of structures for nuclear blast, since the collapse criterion adopted influences both the collapse prediction and the reactive load delivered to the structural framing during the time of collapse.

For this study, collapse of reinforced concrete walls is determined when one of the following criteria is satisfied:

1. Limiting steel strain criterion. It is assumed that after the initial cracking of the concrete at the section of maximum moment, the wall rotates around the support and the cracked section as two rigid bodies, as shown in Figure 12. The deflection at collapse is determined by assuming that the elongation of the yielding steel occurs over a length, $\ell$, sufficient to develop the ultimate tensile strength of the reinforcing steel in bond to the concrete

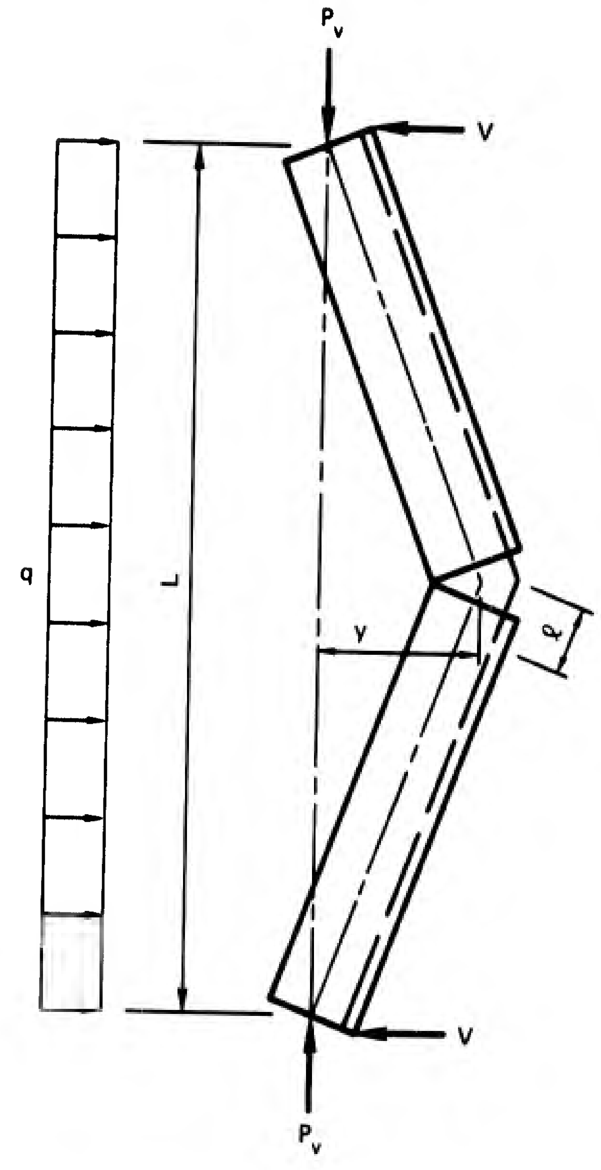


FIG. 12 MODE OF COLLAPSE FOR LIGHTLY REINFORCED CONCRETE MEMBERS

$$\ell = \frac{A_s f_u}{U'_u} \qquad (68)$$

and the ultimate center deflection at which collapse failure is predicted is equal to

$$y_f = \sqrt{(\ell \, \epsilon_{su})^2 + L \, \ell \, \epsilon_{su}} \quad . \qquad (69)$$

2. Instability criterion. As the deflection of the wall increases beyone the elastic phase, a deflection is reached where the external moment due to the vertical load is equal to the ultimate moment capacity of the wall, (from Figure 12), when

$$M_u = Py \quad . \qquad (70)$$

At this deflection, regardless of the magnitude of the lateral load, the wall becomes unstable and collapse is predicted.

3. Ductility criterion. The ductility ratio is defined as the ratio of the maximum deflection (usually the maximum permissible in design) to the yield deflection of a bending structural member. Since a ductility ratio for predicting collapse is sometimes estimated in the published data, the recommendation presented in Ref. 10 for reinforced concrete beams was adopted in this study for lightly reinforced concrete walls. Therefore, collapse of the wall is predicted when the ductility ratio is equal to,

$$\mu = \frac{0.10}{p} \qquad (71)$$

up to a maximum value of $\mu = 30$.

It may well be that other modes of collapse failure are more appropriate for lightly reinforced concrete wall members than those included above. For example, a failure criterion for panel walls could also be based on the shear or diagonal tension stress developed in the panel or on the strength of the wall-to-support connectors. For such a criterion, if the magnitude of the stress developed in any of the assumed modes exceeded the failure criterion at any time during the wall response, collapse would be predicted, regardless of the magnitude of the bending resistance of the wall. Although such collapse criteria were not included in the initial analysis, as better information becomes available, it will be used to modify or supplement the criteria used in this study.

Another possible failure criterion could be based on a secondary crushing of the concrete; although not used in this study, it is discussed in Appendix B. In addition, it is well-known that reinforced concrete members, when undergoing large bending deflections, are capable of developing tensile membrane forces in the reinforcement. Reference 21, in fact, includes an empirical factor for the catenary action for calculating the deflection of simply supported reinforced concrete slabs. Although tensile membrane action was not considered in the analysis procedure herein, it will be included in a subsequent report.

## Unreinforced Concrete or Masonry Unit Wall (With Arching)

Masonry walls--under conditions where they are constrained between essentially rigid supports--have been observed to have greater resistance to lateral loads than would be predicted by conventional bending analysis. This increased resistance results from the resistance of the supports to outward movement in the plane of the wall. It therefore seems logical--in cases where the supports are stiff enough to restrain sufficiently this in-plane movement--to compute the behavior of the panel on the basis of edge restraint, compressive strength, and geometry of deflection rather than from the flexural properties. This approach is the basis for the so-called arching action theory (Ref. 22).

### Development of the Resistance Function

The arching theory is based on the assumption that the resistance of the wall to lateral loads results entirely from compressive forces set up in the plane of the panel as a result of the tendency of the masonry material to crush at midspan and at the supports. Thus any bending resistance is disregarded by assuming that the masonry material has zero tensile strength. The error resulting from the fact that some tensile strength actually exists is believed to be minor and may thus be safely neglected for those cases where arching occurs. Because of the assumption of zero tensile strength, immediately upon application of the transverse load, cracks develop at the supports and midspan for fixed-end and propped-cantilever walls or at midspan only for simply supported walls. The behavior is thus independent of the type of support condition. During subsequent motion, each half-span is assumed to remain rigid and rotate about its support.

These two halves become wedged into the opening and compressive or arching forces develop at the supports and midspan. Because of these compressive forces, a force couple is developed that resists the rigid body rotation. The magnitude of the compressive forces, and thus the resisting couple, is dependent on the rigidity of the supports and the stress-strain properties of the wall material.

This behavior is similar to that assumed for the case of the unreinforced wall without arching after initial cracking has taken place, except that the axial force in the arching case is developed internally and is of a variable magnitude, whereas in the case without arching it is caused by external loads and is of a fixed magnitude.

The arching theory was initially developed using the assumption that the supports are considered to be rigid against outward movement of the wall (Ref. 22). The theory was later modified to include the case of a gap initially existing between the top of the wall and the support; however, it was still assumed that the support was rigid (Ref. 23). To include the case where the wall is supported by yielding supports at the top and bottom, the theory was modified still further in this report. This was done through use of an iterative procedure to determine the width of a variable gap at the top, which width depends on the magnitude of the arching force developed.

Rigid Supports. If the supports are considered to be rigid against outward movement of the wall the dimensions of the opening will remain a fixed value. It is assumed in this analysis that the rigid supports are at the top and bottom only, thus resulting in one-way arching in the vertical direction. The wall is also assumed to be of uniform cross section. Modification of the present theory would be required to apply the results obtained to walls supported on all four sides and to hollow unit masonry walls. The idealized wall is shown in a deformed position in Figure 13.

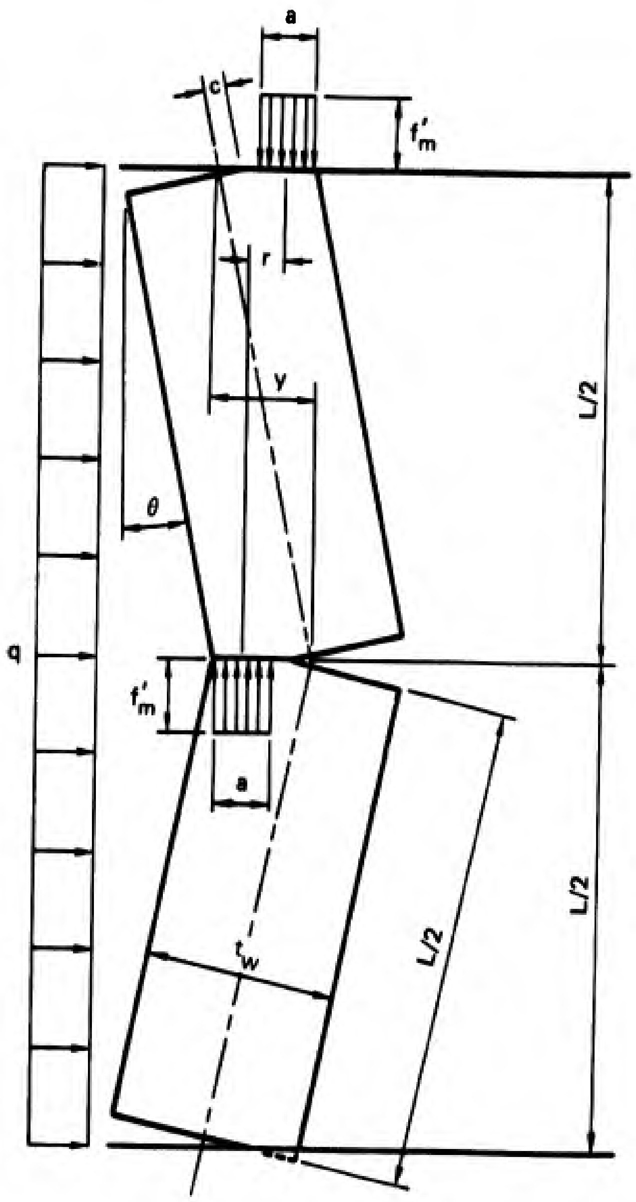


FIG. 13 ASSUMED ARCHING BEHAVIOR OF MASONRY WALL (Forces on Bottom Half Not Shown)

For equilibrium of forces in the vertical direction, the axial compressive forces and thus the width of the contact area and stress block must be the same at the ends and center. Because of the rigid body rotation, which assumes that each half of the span rotates about the first point in contact with the support, the contact area is seen in the figure to decrease with increasing center deflection. The axial stress can be determined from the stress-strain relationships of the masonry material. The strain along the contact area is a function of the center of deflection, which causes the fibers of the material to be shortened as the half-wall rotates. Various assumptions have been followed in previous developments in regard to the stress-strain relationship of the masonry material. These assumptions and the subsequent derivations are given in detail in Appendix C.

The assumption used here is a "linearized elastic-plastic" stress-strain relationship, presented originally in Ref. 23. This method is felt to be a simple, yet fairly accurate, representation of the actual situation. It was chosen for use over a method developed in Ref. 22, because although the latter method gives slightly more accurate results, it is much more complicated. The simpler method also serves as a basis of departure for the case of yielding supports, which is presented subsequently.

Essentially, this method assumes a linear relation between the mid-span deflection and the strain along the contact area up to a yield strain, $\epsilon_y$, that corresponds to the crushing stress, $f'_m$, of the material. This relationship is illustrated in Figure 14. The resisting moment is determined by assuming equivalent rectangular stress blocks to exist at the supports and center, as shown in Figure 13. The width "a" is chosen

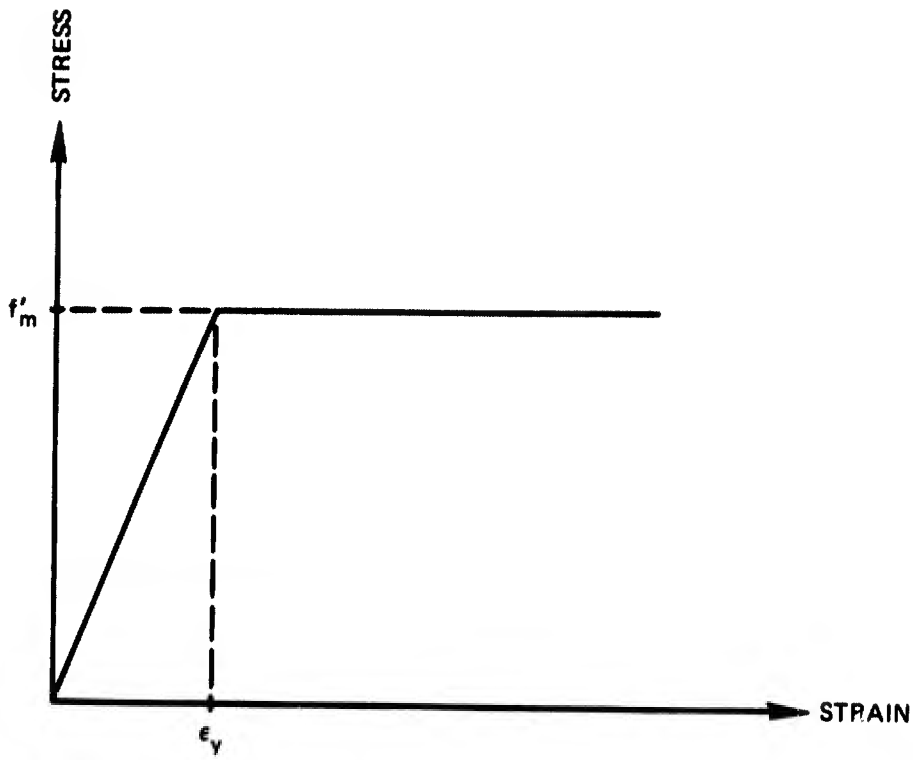


FIG. 14 ASSUMED STRESS-STRAIN RELATIONSHIP

so that the moment, $M_y$, is a maximum, thus resulting in

$$P_y = \frac{1}{2} f'_m (t_w - y_y) \tag{72}$$

and

$$M_y = \frac{1}{4} f'_m (t_w - y_y)^2 \tag{73}$$

where $y_y$ is the deflection corresponding to yield strain $\epsilon_y$ and is given by

$$y_y = \frac{t_w f'_m}{E_m} \times \frac{L_d}{L_d - L/2} \tag{74}$$

and

$$L_d = \sqrt{(L/2)^2 + t_w^2}\ . \tag{75}$$

The corresponding load resistance, $Q_y$, for a uniformly loaded wall is given by

$$Q_y = \frac{2 f'_m}{L} \times (t_w - y_y)^2 \tag{76}$$

The load resistance is considered to be linear between zero and $Q_y$ for midspan deflections less than $y_y$, while for deflections greater than $y_y$, the load resistance is equal to

$$Q = \frac{2 f'_m}{L} \times (t_w - y)^2 \qquad y > y_y \tag{77}$$

A typical resistance function for a masonry wall of this type is shown in Figure 15.

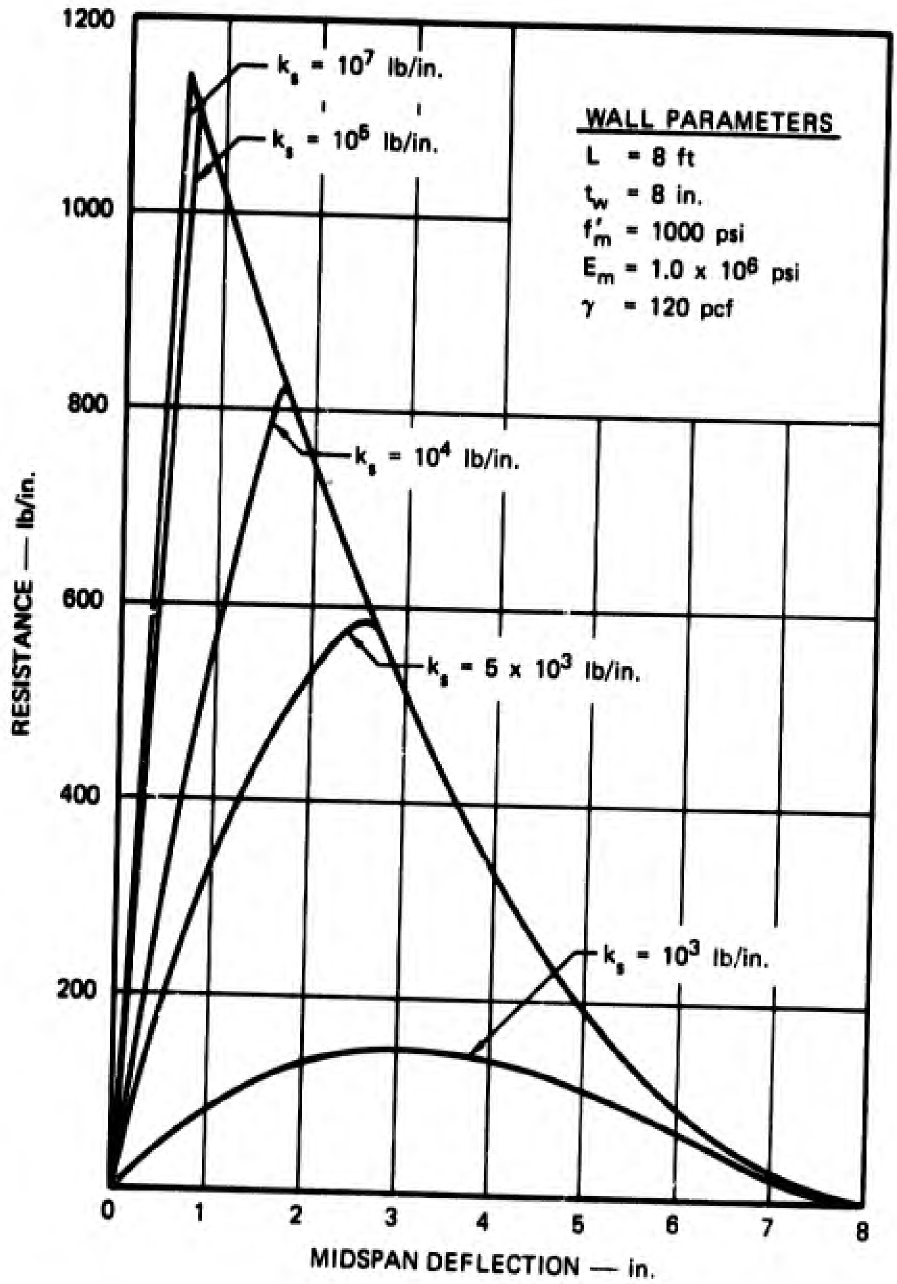


FIG. 15 RESISTANCE FUNCTIONS FOR SAMPLE UNREINFORCED WALL WITH ARCHING

Elastic Supports. For the case where the wall is supported by elastic supports at top and bottom, the resistance curve must be constructed in a different manner. The compressive force, and therefore the resisting moment, is now also dependent on the stiffness of the supports, $k_s$.

Instead of remaining rigid against in-plane movement, the supports will now yield outward as the walls compress against them. Again, considering one-way action, this outward movement is given by

$$\Delta x = P_v/k_s \tag{78}$$

where $P_v$ is the compressive force exerted by the wall on the support. This outward movement causes the compressive force $P_v$ to be reduced, in turn changing the previously determined value of $\Delta x$. The procedure thus becomes an iterative process to determine the values of $P_v$ and $\Delta x$ that correspond to each other. This procedure is given in greater detail in Appendix C. A typical resistance curve for a masonry wall of this type is also shown in Figure 15.

## Failure Criterion

The criterion for the collapse failure of the unreinforced masonry wall with arching is instability of the wall. This occurs when the deflection becomes large enough to cause the moment arm to go to zero. This results in the resisting moment vanishing and the wall collapsing. For the "linearized elastic-plastic" case, this occurs at a deflection equal to the thickness of the wall, $t_w$.

BLANK PAGE

## IV WALL REACTIONS

### Introduction

The response of a dynamically loaded element is affected by its own structural characteristics, as well as by those of the supporting structure; however, for the dynamic analysis of wall elements in this study, the usual assumption was made that the supports were nonresponding. Thus, the time-reactions of the wall on the supporting structure and the response of the structure due to the reactive loads were not considered directly in determining the collapse of the wall. However, in a subsequent phase of the existing structures evaluation project, the response of the building framework will be examined. Therefore, since wall reactions are inputs to the building response, it was appropriate to include a method for calculating the dynamic reactions in this study of wall elements.

### Dynamic Reactions

The method of calculating the dynamic reactions of dynamically loaded elements presented in Ref. 7 was also used in this program. A basic assumption in the method is that the time-dependent response of the various elements of a structure are so related that the interaction between elements does not appreciably affect the response of the individual elements. In effect, each element is analyzed as a separate single-degree-of-freedom system, rather than as a coupled infinite degree system. To determine the reaction-time function, therefore, it was assumed that the wall element supports are nonresponding and that the reaction so obtained can be used as the load applied to the supporting element.

The reaction of the equivalent single-degree-of-freedom system used to determine the wall response is equal to the spring resistance. However, the reactions of the actual wall are also a function of the distributed inertia. To account for these forces in the simplified method, it was assumed that the distribution of the inertia forces is proportional to the deflection at each point along the actual member, which is justified, since the acceleration at each point is proportional to its deflection. Since the deflected shape of the member under dynamic load was assumed to be equal to the deflected shape under static load, the assumed distribution of inertia forces does not account for the higher response modes. This assumption is probably of minor importance when predicting the reactions for a failing member.

The mathematical equations for the reactions presented in the following subsections are identical for the various types of walls considered in this study, since the equations are based on the deflected shape of the wall. However, the magnitude will be different, since the reactive force at any particular time depends on both the load and resistance functions. The reactions for walls with the three support conditions considered, are as follows.

Simply Supported Wall

The equation for the elastic deflection of a simply supported, one-way wall with a uniformly distributed lateral load is

$$y = \frac{qx}{24EI}(L^3 - 2Lx^2 + x^3). \tag{79}$$

Since it was assumed that the inertial forces are distributed in the same manner as the curve of the static deflection under the same distribution of the loading, the center of gravity of the inertia forces on one-half of the wall element shown in Figure 16 is

$$\bar{x} = \frac{\int_0^{L/2} xydx}{\int_0^{L/2} ydx} \tag{80}$$

which by substitution of Eq. 79 and integrating gives

$$\bar{x} = \frac{61}{192} L. \tag{81}$$

Since the forces on the wall element shown on Figure 16 are in dynamic equilibrium, the sum of the moments about the resultant of the inertia forces yields

$$V\left(\frac{61L}{192}\right) - M_c - \frac{1}{2} P\left(\frac{61L}{192} - \frac{L}{4}\right) = 0. \tag{82}$$

The deflection of the wall is small up to the point of flexural failure and the eccentricity of an axial dead load is negligible; therefore, the midspan moment, $M_c$, can be determined by

$$M_c = \frac{QL}{8} \tag{83}$$

which by substitution in Eq. 82 yields the reaction of a simply supported wall in the elastic phase

$$V = 0.393 Q + 0.107 P. \tag{84}$$

After the flexural failure of the wall in the elastic phase, both the resistance and deflection equations are altered as noted in the section on resistance functions. Since it was assumed that the motion of the wall after the initial flexural failure is in a rigid body rotational mode about the supports, there is a linear distribution of the inertia forces, as shown on the free-body diagram for one-half of the wall on

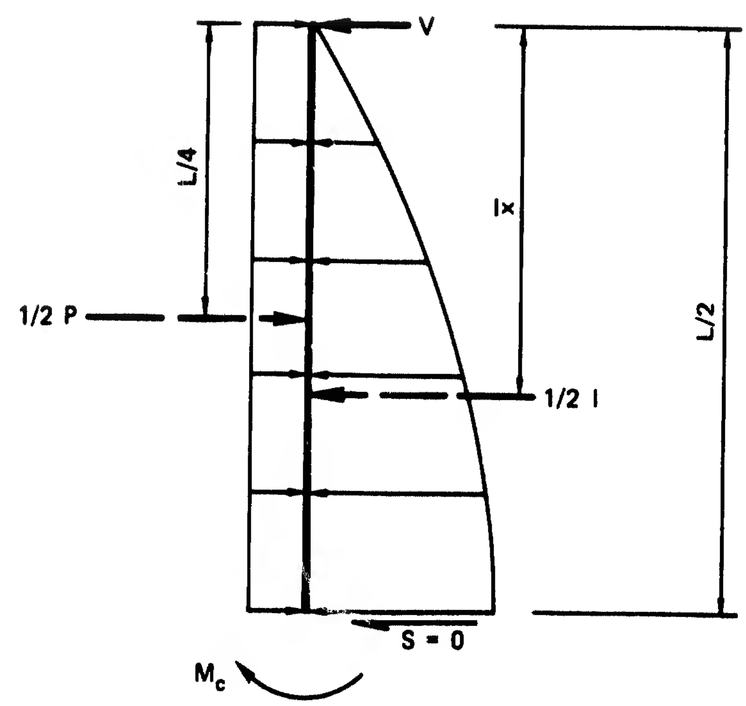


FIG. 16 DISTRIBUTION OF INERTIA FORCES ON ONE-HALF SIMPLY SUPPORTED WALL ELEMENT BEFORE FLEXURAL FAILURE

Figure 17. Since the centroid of the inertia forces is L/3 from the end, the sum of the moments about the inertia forces is

$$V \frac{L}{3} - \frac{1}{2} P \left( \frac{L}{3} - \frac{L}{4} \right) - M_r = 0 \tag{85}$$

which by substitution of Eq. 83 yields the reaction of a simply supported wall in the rotational phase

$$V = \frac{3}{8} Q + \frac{1}{8} P. \tag{86}$$

Since the duration of the blast loads of interest is generally much greater than the time to collapse of exterior wall elements, it is apparent from the above equations that the resistance may reduce to zero before the loading term. If this occurs, the wall reaction becomes solely a function of the loading. Therefore, it is conceivable that for many actual loading situations, the analysis would indicate that the reactive forces were sustained after the wall collapse was predicted. However, since there is no definitive method for determining the duration of the reaction under these conditions, it was assumed in this program that the reaction was reduced to zero at the time that the wall collapse was predicted.

Fixed-End Wall

The reaction for the elastic phase of a one-way, fixed-end wall with a uniformly distributed lateral load is determined in a manner similar to that in the previous subsection. For the wall element on Figure 18, it can be shown that the reaction during the elastic phase is equal to

$$V = 0.364 Q + 0.136 P \tag{87}$$

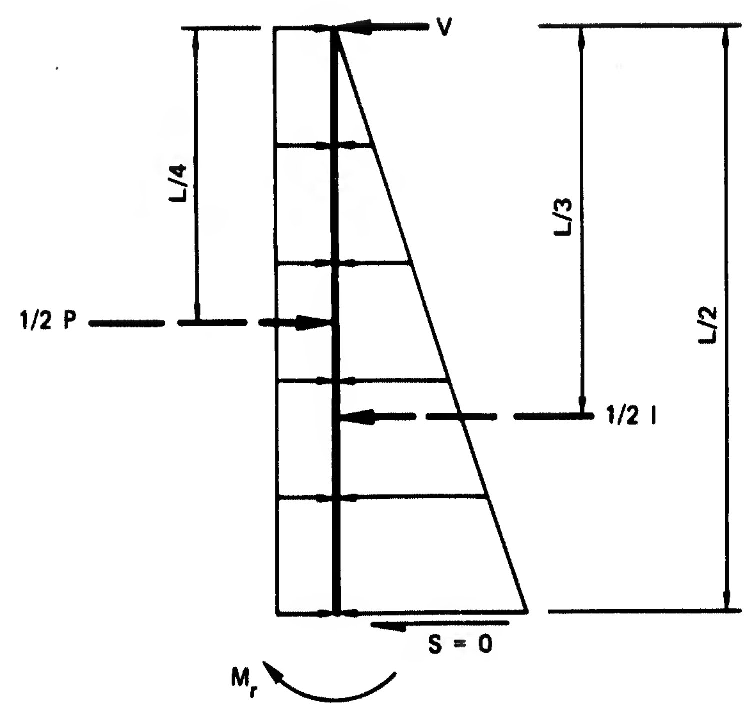


FIG. 17 DISTRIBUTION OF INERTIA FORCES ON ONE-HALF SIMPLY SUPPORTED WALL ELEMENT AFTER FLEXURAL FAILURE

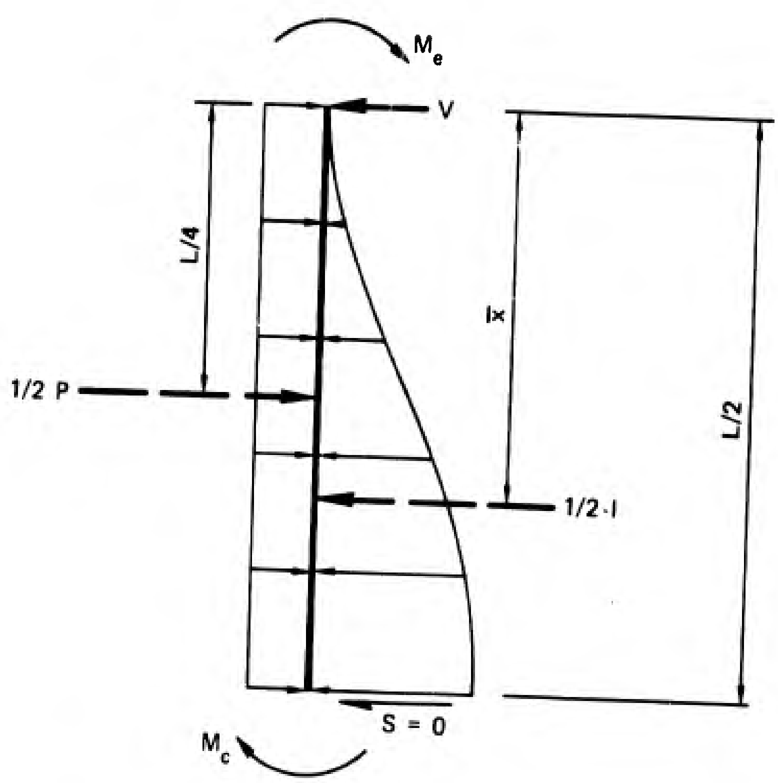


FIG. 18 DISTRIBUTION OF INERTIA FORCES ON ONE-HALF FIXED-END WALL ELEMENT BEFORE FLEXURAL FAILURE

After cracking (or yielding of the steel in a reinforced concrete wall), the wall deflects as a simply supported member and Eqs. 84 and 86 are used to determine the reactive forces.

Propped-Cantilever Wall

The reaction for the elastic phase of a one-way, propped-cantilever wall with a uniformly distributed lateral load is determined in a manner similar to that in the previous two subsections. For the wall element on Figure 19, it can be shown that the reactions during the elastic phase are equal to

$$V_1 = 0.292\ Q + 0.083\ P \tag{88}$$

and

$$V_2 = 0.459\ Q + 0.165\ P. \tag{89}$$

As noted above for fixed-end walls, after the elastic response of a propped-cantilever wall, Eqs. 84 and 86 for a simply supported wall are used to determine the wall reactions.

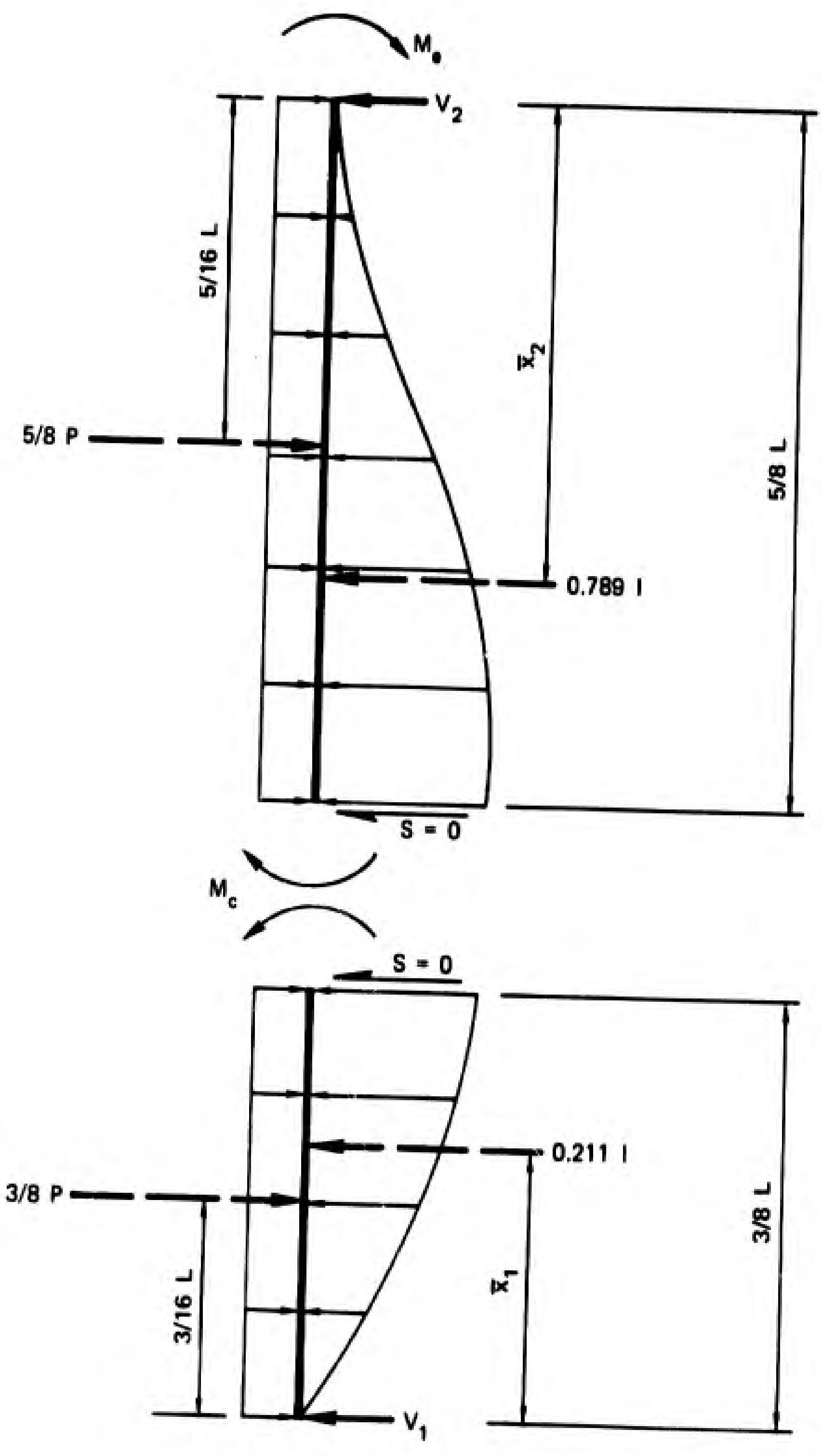


FIG. 19 DISTRIBUTION OF INERTIA FORCES ON WALL ELEMENT WITH ONE FIXED END AND ONE SIMPLY SUPPORTED END (PROPPED CANTILEVER)

BLANK PAGE

## V DISCUSSION

### Introduction

To determine the dynamic response of the various walls discussed, computer programs were developed using the Newmark $\beta$ Method (Ref. 8) to analyze numerically the walls having the resistance functions previously determined in Section III. These walls were subjected to the loadings presented in Section II. Transformation factors, as given in Ref. 7, were used to reduce the wall, which is in reality a distributed mass system, to an equivalent single-degree-of-freedom system. The input data required in the program consist of the wall and load properties, with the resulting output being a complete time-history of the response of the wall to failure, including reactions and midspan displacement, velocity, and acceleration. The time-history of the response may be determined for a wall subjected to a given loading or the magnitude of the load causing incipient collapse may be found for various load types. A more detailed discussion of the programs is given in Appendix D.

During the preparation of the computer programs for the three types of exterior wall models discussed in Section III, it was possible to analyze the response of selected walls up to collapse for the various loading conditions. The information from these computer runs permitted a comparison to be made between the limited experimental data on dynamically loaded walls and the mathematical models developed herein. In addition, it was possible to perform a variation-of-parameters study to evaluate the relative effect of the various factors on wall collapse. A brief discussion of each wall type is included in the following subsections.

## Unreinforced Concrete or Masonry Unit Wall (Without Arching)

### Experimental Correlation

Reference 11 reports on the air blast testing of two 8-1/2 ft high by 12 ft wide brick wall panels. The 8-in. thick panels were constructed of two courses of building brick and mortar, with every sixth row a bond course. The walls were mounted in a steel frame, which consisted of simple supports at the top and bottom while allowing the side edges to move. Each wall was mounted in the shock tunnel and subjected to an incident air blast pulse. Since the wall essentially blocked the cross section of the tunnel, it was subjected to the fully reflected overpressure on the front face, while a back face loading was prevented until collapse of the wall occurred. The pressure pulse was approximately as noted for Loading Case No. 4 in Section II, and consisted of "a sharp rise to the peak reflected overpressure value, a more or less flat top approximately 30 msec in duration, and then a linear decay to zero, with an overall pulse duration of approximately 90 msec" (Ref. 11). The loading on the test walls was about 3 psi peak reflected overpressure with a rise-time of a few milliseconds.

The failure mode of the panel consisted of the formation of a horizontal crack near the midheight, which extended across the entire width of the panel. This was followed by the rotation of the upper and lower sections about the supports. Complete collapse of the wall panels occurred in all tests.

From the standpoint of determining the adequacy of the anlytical model developed in this study to predict wall collapse, the information from the URS shock tunnel experiments was inconclusive. This was primarily because of the lack of incipient collapse data from the experiments, where all blast loadings were selected to assure a catastrophic wall collapse. In addition, for the preliminary tests, the dynamic deflection data were limited to measuring the first 1/8 in. of motion of the center of the wall panel. Although the computer program will provide deflection information to whatever precision desired, the model was developed primarily to predict the overpressure above which the collapse of the wall can be expected, and not necessarily precise deflection-time information. However, it would seem reasonable that if the model provided valid collapse pressures it should also provide realistic average deflection data. Although the small experimental deflections cannot be used to correlate the predicted analytical response for large deflections, the data from Ref. 11 for brick wall panels A and B are reproduced on Figure 20 for comparison with the model prediction for a similar wall and load-time function. This same information is shown in Figure 21 and indicates the importance of obtaining experimental data for the large deflections associated with wall collapse. At the present time, it cannot be ascertained whether the deviation shown by the figures would be less for larger deflections or whether it is a result of experimental errors or model inadequacies.

Another factor of interest in the prediction of wall behavior is the time for the wall to reach collapse. Figure 22 shows an analytical study of the wall model discussed above. To indicate the sensitivity of the collapse time of a wall to the magnitude of loading, the overpressure, $p_m$, was varied from a pressure of 0.72 psi, the predicted pressure at incipient collapse, to 20 psi. As noted, the predicted time of collapse varies from about 30 to 420 msec, whereas, the time to reach the initial crack, or initial flexural failure of the wall, varies from 2.5 to 16 msec for the same overpressures.

The curve for the 20 psi overpressure level shown on Figure 22 is included for illustrative purposes only. As noted in Ref. 24, the fracturing or failure mode of plates of brittle materials is sensitive to the pressure level; in general, the higher the overpressure, the greater the

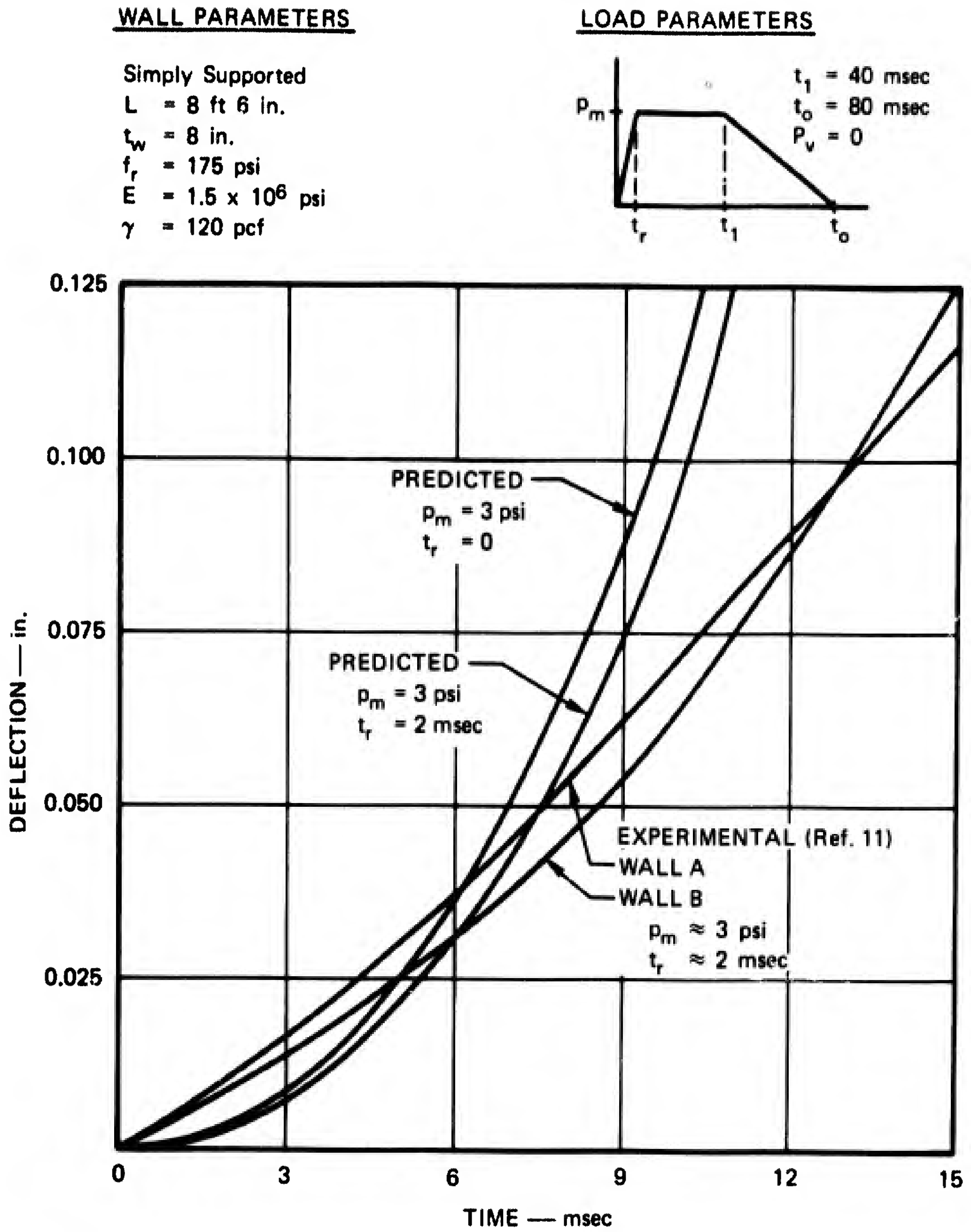


FIG. 20 COMPARISON OF EXPERIMENTAL WITH THEORETICAL PREDICTED DEFLECTIONS VERSUS TIME FOR ONE-WAY SIMPLY SUPPORTED BRICK WALL PANEL

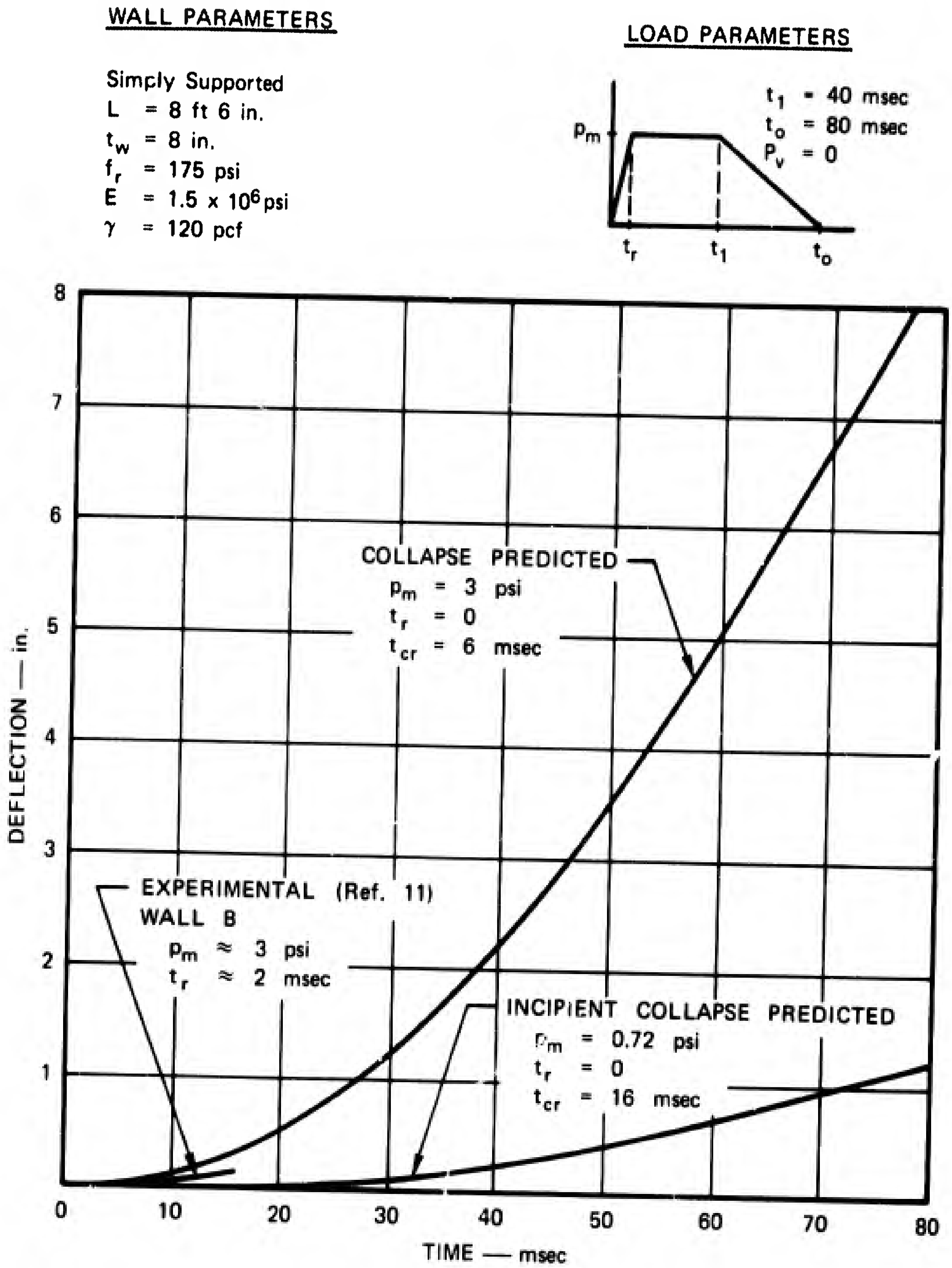


FIG. 21 DEFLECTION VERSUS TIME FOR ONE-WAY SIMPLY SUPPORTED BRICK WALL

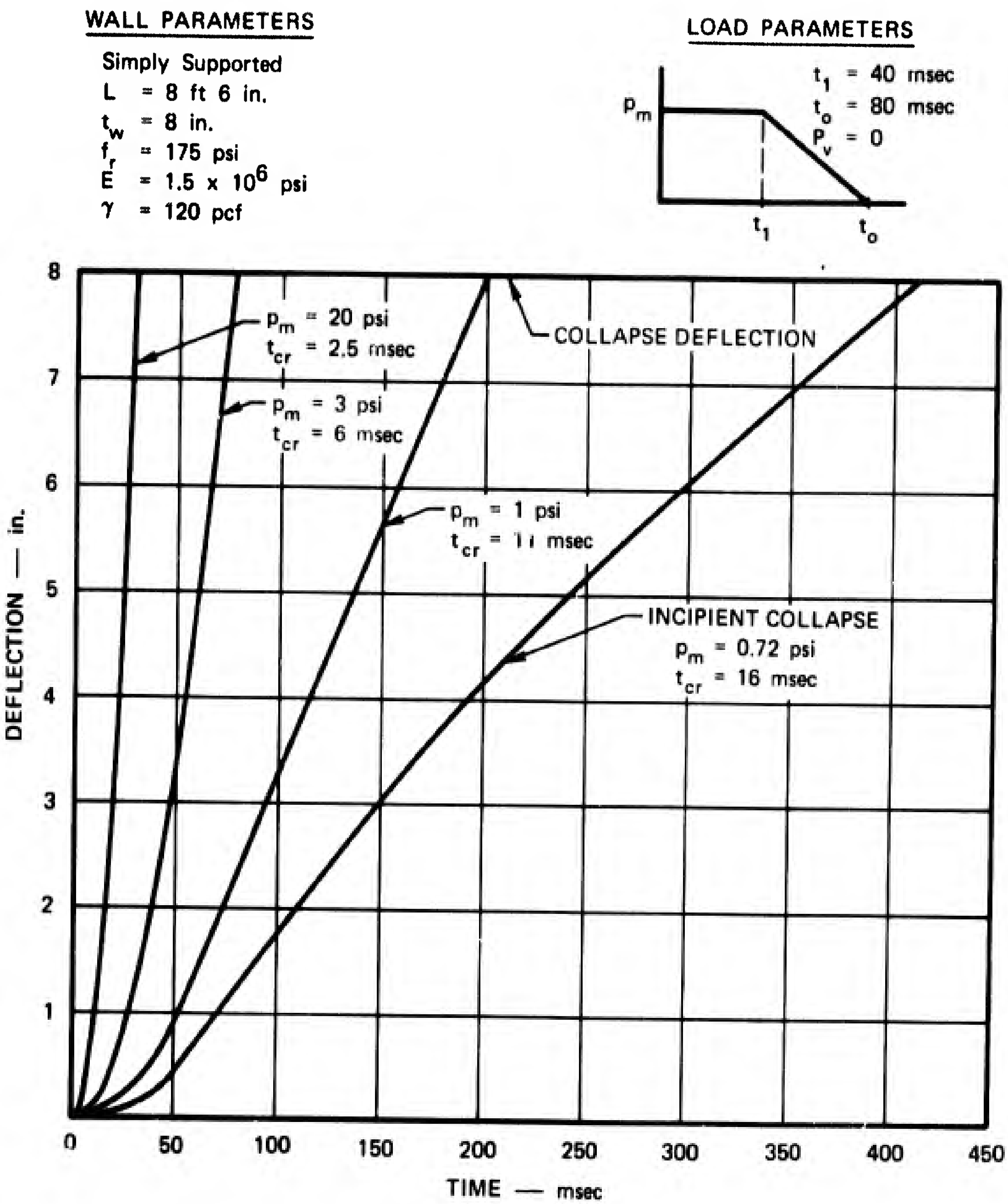


FIG. 22 TIME FOR BRICK WALL PANEL TO REACH INITIAL CRACK AND COLLAPSE FOR VARIOUS OVERPRESSURES

number of pieces. Since the experiments on walls reported in Ref. 11 were conducted in the 3-8 psi reflected overpressure region, it is not known at this time whether the response mode assumed in this study is applicable to the higher overpressures.

Variation of Parameters

To determine the individual effects of the parameters involved in the resistance of unreinforced masonry walls simply supported at top and bottom, several analyses were made in which the incipient collapse loads were calculated for various values of the parameters. These parameters were individually varied, so that any resulting changes in the collapse load would be caused by the parameter being considered. Based on engineering judgment, a wall with the following properties was selected as the standard from which all variations were made:

Height, $L$ . . . . . . . . . . . . 96 in.

Thickness, $t_w$ . . . . . . . . . . 8 in.

Modulus of elasticity, $E$ . . . 1,000,000 psi

Modulus of rupture, $f_r$. . . . . 50 psi

Unit Weight, $\gamma$ . . . . . . . . . 120 pcf

Vertical load, $P_v$ . . . . . . . . 0

The type of loading acting on the wall (Loading Case No. 1, Section II) for this variation of parameters was that corresponding to an idealized nuclear blast. Standard values of ambient atmospheric pressure, $P_o$, and ambient sound velocity ahead of the shock, $c_o$, were taken as 14.7 psi and 1120 fps, respectively. A study of the effect of the clearing distance, S, which results in a clearing time, $t_c$, was made for various yields. These results are shown in Figure 23. As can be seen for walls without vertical load, the results for yields of greater than 10 kt lie on approximately the same curve. For these higher yields, the effect of $t_c$ on the incipient collapse pressure is negligible for values larger than about

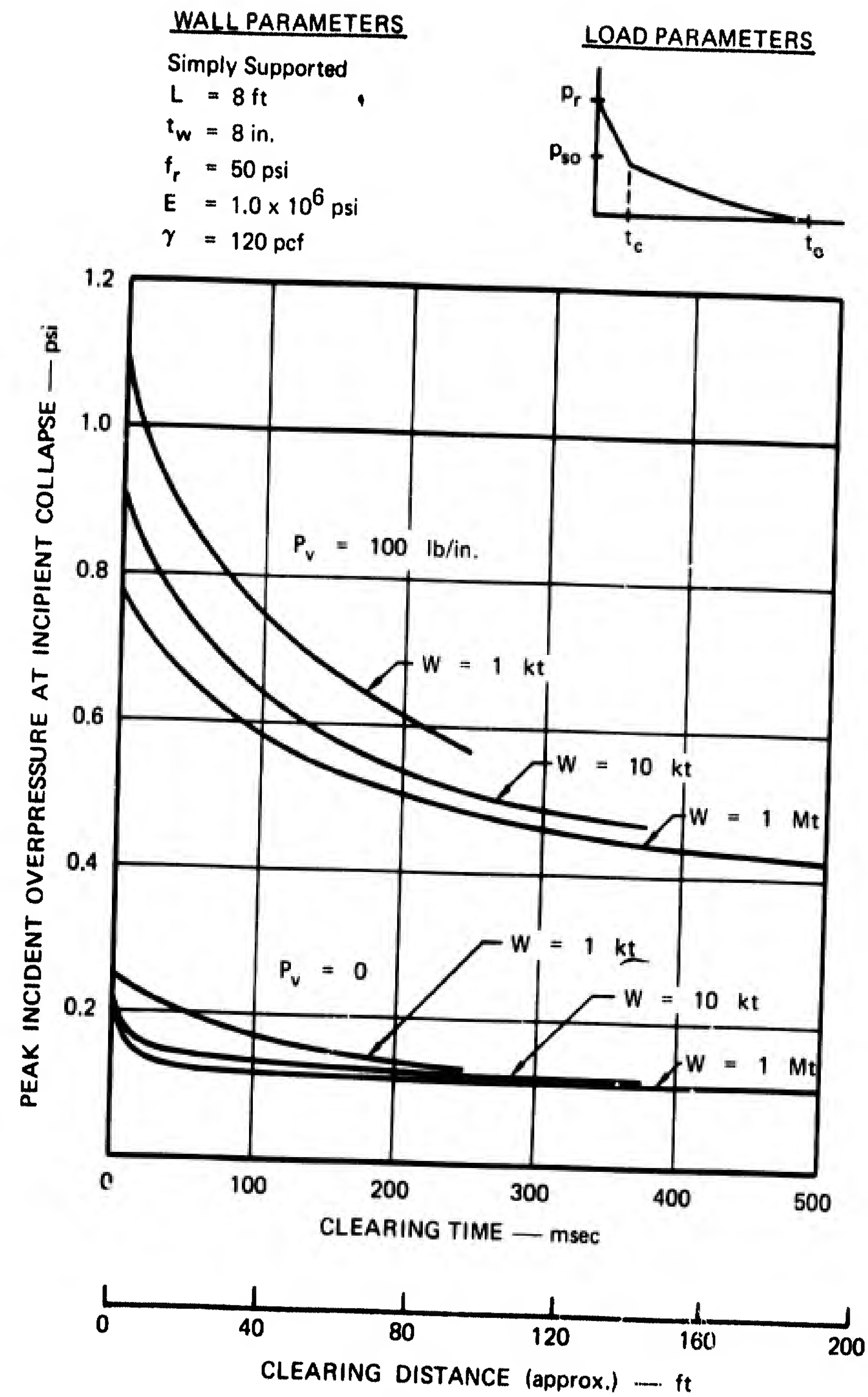


FIG. 23 PEAK INCIDENT OVERPRESSURE AT INCIPIENT COLLAPSE VERSUS CLEARING TIME
Unreinforced Wall Without Arching

50 milliseconds. As can also be noted from the figure, for walls with vertical load, the effect of the clearing time becomes more significant.

A value of S equal to 30 ft, which results in a clearing time of approximately 80 milliseconds, and a yield of 1 Mt were chosen as the standard values for the study of the other parameters. These values essentially eliminate the effect of a variable clearing time and yield on the behavior of the walls without vertical load. The effect of the other parameters on the incipient collapse load of the wall are summarized as follows.

Duration of Load, $t_o$ (Figure 24). To determine the effect of the duration of the load on the magnitude required to cause failure, a triangular load of varying duration was used. The duration of the load is seen to have an important effect at the shorter times, causing the magnitude of the collapse pressure to increase significantly. As the duration becomes longer, however, the magnitude of the load approaches a constant value.

Height, L (Figure 25). As the height of the wall is increased, the load required to cause incipient collapse decreases. This decrease tends to flatten out as the height increases. The effect was found to be similar for all thicknesses, i.e., the percentage change over the range of heights shown is similar for the three thicknesses.

Thickness, $t_w$ (Figure 26). As the thickness of the wall is increased, the load required to cause incipient collapse increases. This increase becomes more pronounced as the thickness is increased. The percentage change in the incipient collapse pressure over the range of thickness shown is similar for the three heights.

Modulus of Elasticity, E (Figure 27). For values ranging from 750,000 to 3,000,000 psi, the modulus of elasticity was seen to have little effect on the load required to cause incipient collapse, regardless of the magnitude of the modulus of rupture.

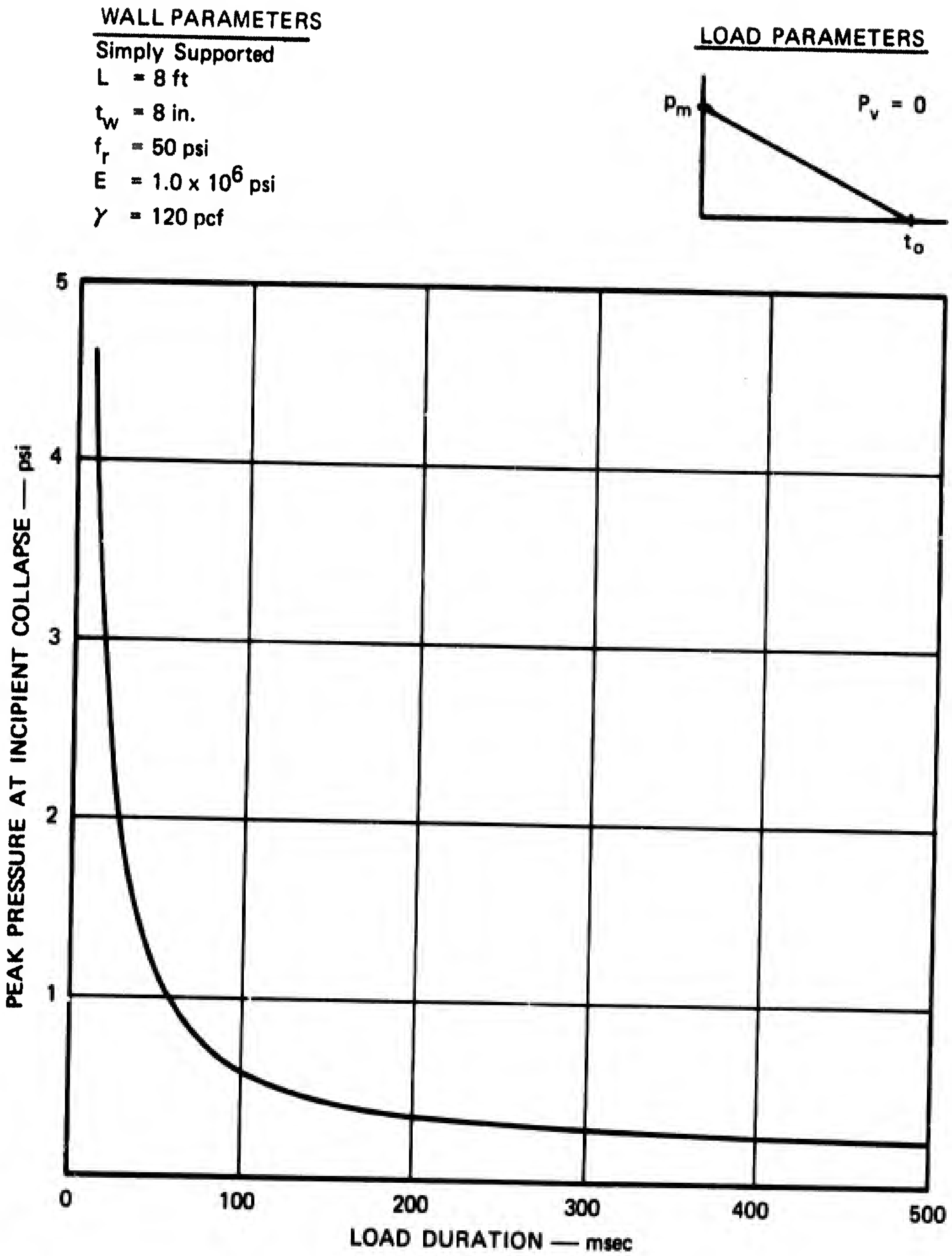


FIG. 24 PEAK PRESSURE AT INCIPIENT COLLAPSE VERSUS LOAD DURATION
Unreinforced Wall Without Arching

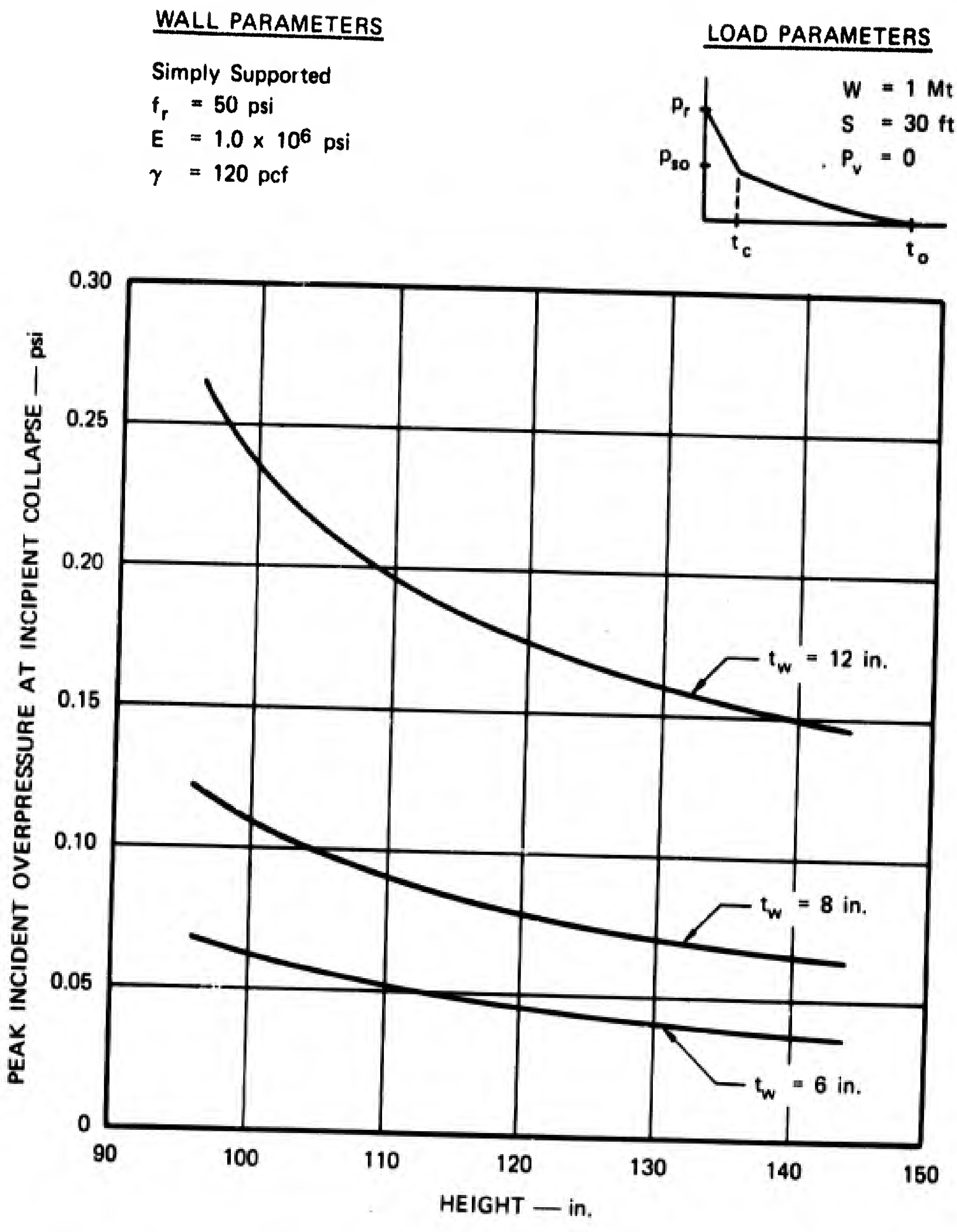


FIG. 25 PEAK INCIDENT OVERPRESSURE AT INCIPIENT COLLAPSE VERSUS HEIGHT
Unreinforced Wall Without Arching

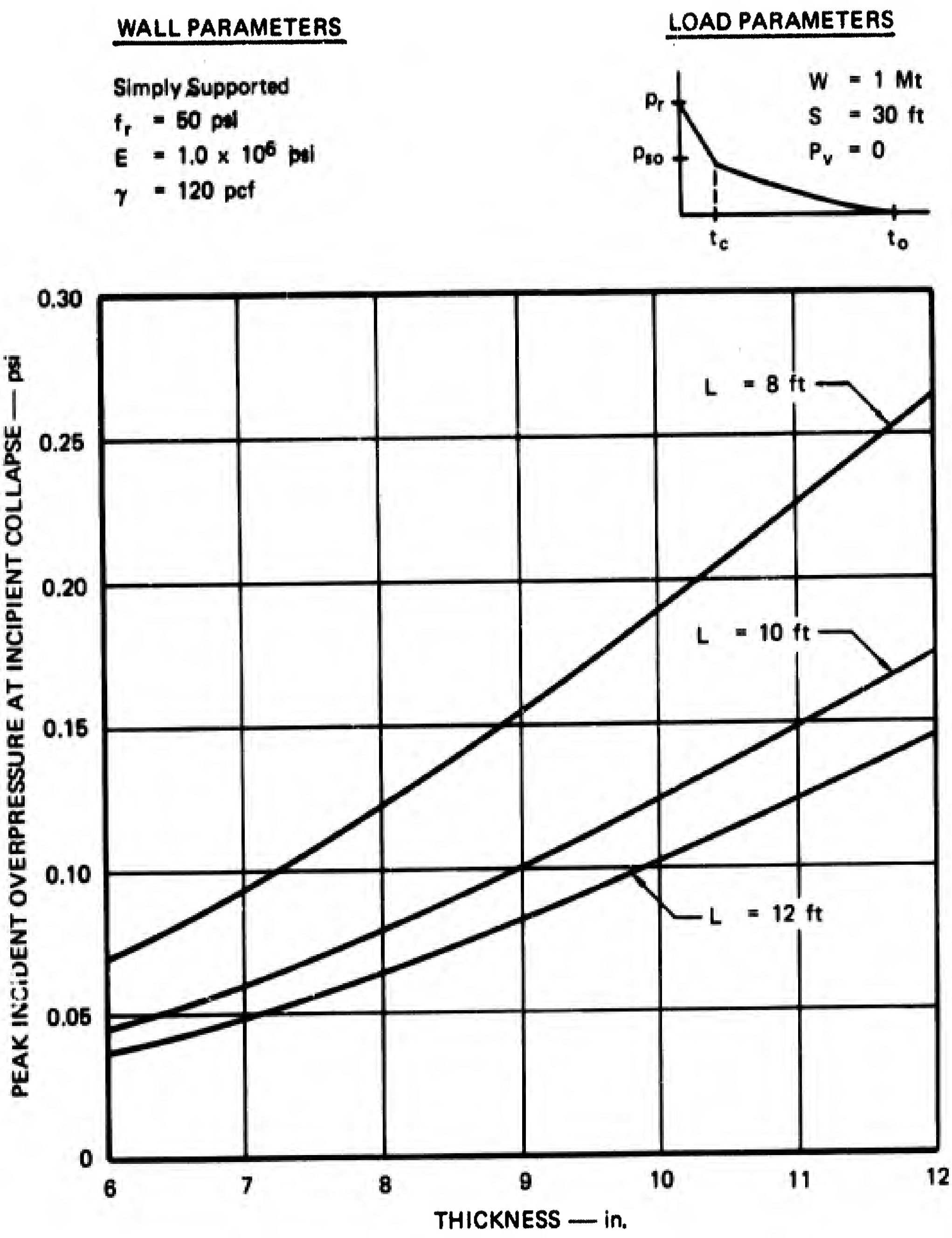


FIG. 26 PEAK INCIDENT OVERPRESSURE AT INCIPIENT COLLAPSE VERSUS THICKNESS
Unreinforced Wall Without Arching

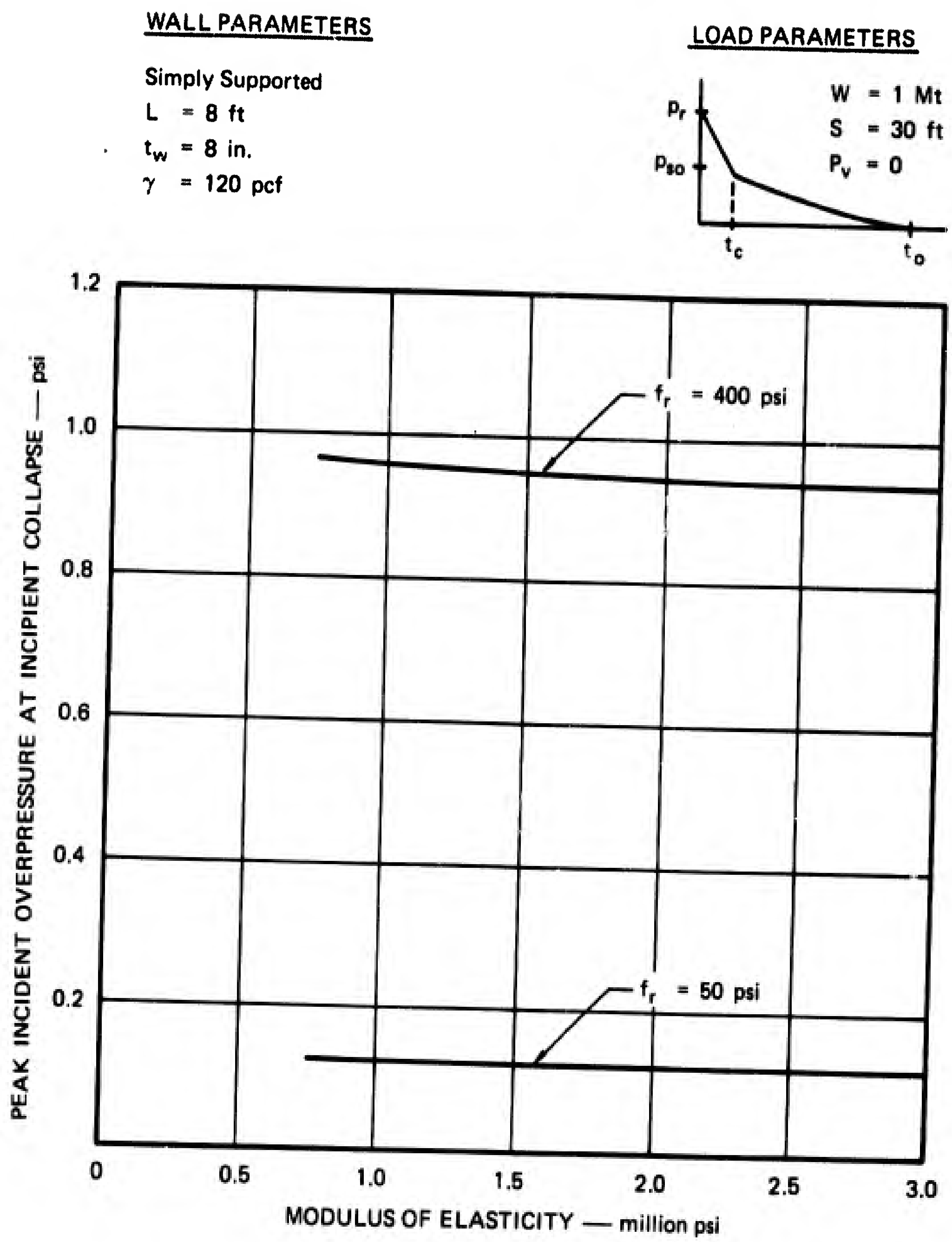


FIG. 27 PEAK INCIDENT OVERPRESSURE AT INCIPIENT COLLAPSE VERSUS MODULUS OF ELASTICITY
Unreinforced Wall Without Arching

Unit Weight, $\gamma$ (Figure 28). For values ranging from 80 to 150 pcf, the unit weight of the wall material has practically no effect on the value of the load required to cause incipient collapse.

Modulus of Rupture, $f_r$ (Figure 29). For the case of no vertical load, the lateral load required to cause incipient collapse increases in direct proportion to the modulus of rupture for values ranging from 50 psi (typical tensile bond strength of brick wall) to 800 psi (corresponding to a fairly high strength concrete).

Vertical Load, $P_v$ (Figure 29). The vertical load is seen to have an important effect on the value of the lateral load required to cause incipient collapse, especially for walls having a low modulus of rupture. This effect becomes more important at values of the vertical load that provide a resistance in the secondary phase (see Figure 8) approximately equal to the resistance resulting from the modulus of rupture in the elastic bending phase. After this value is reached, the lateral load required to cause incipient collapse is directly dependent on the value of the vertical load, the relationship being approximately linear.

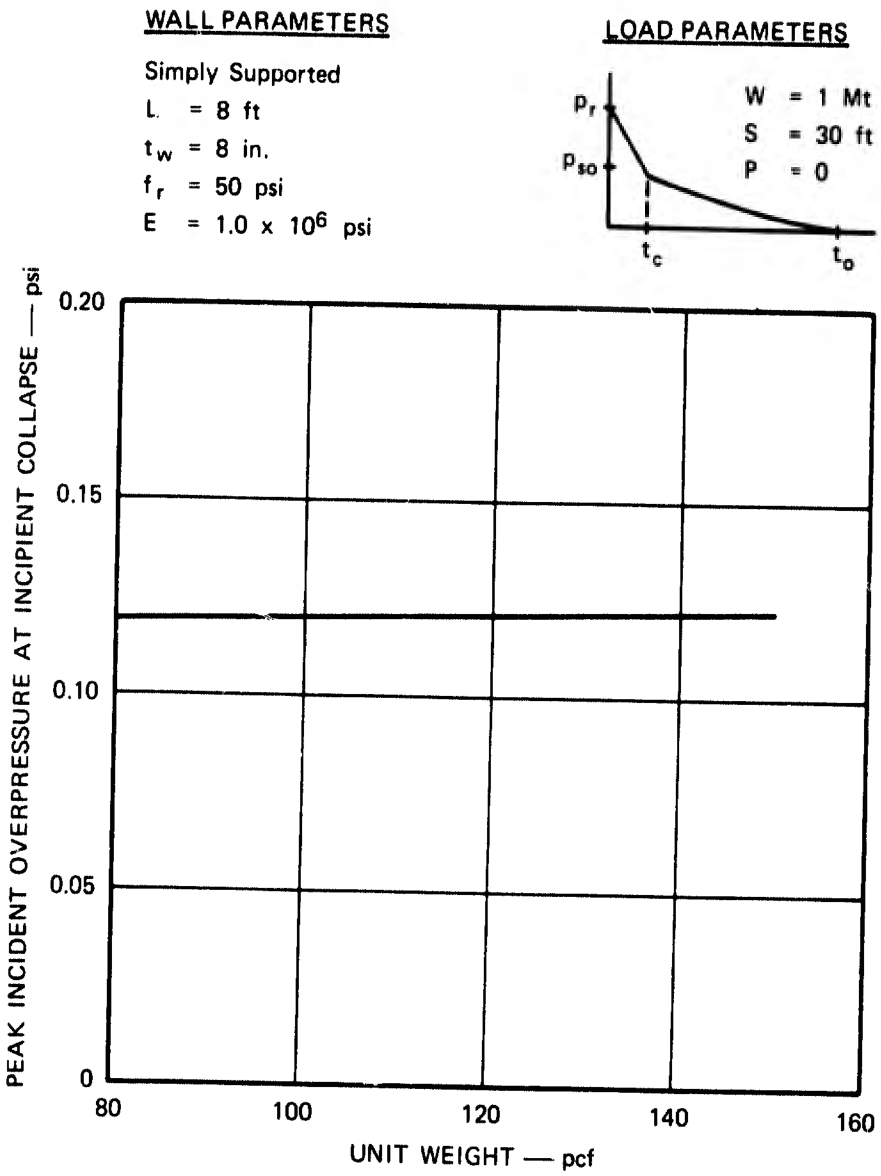


FIG. 28 PEAK INCIDENT OVERPRESSURE AT INCIPIENT COLLAPSE VERSUS UNIT WEIGHT
Unreinforced Wall Without Arching

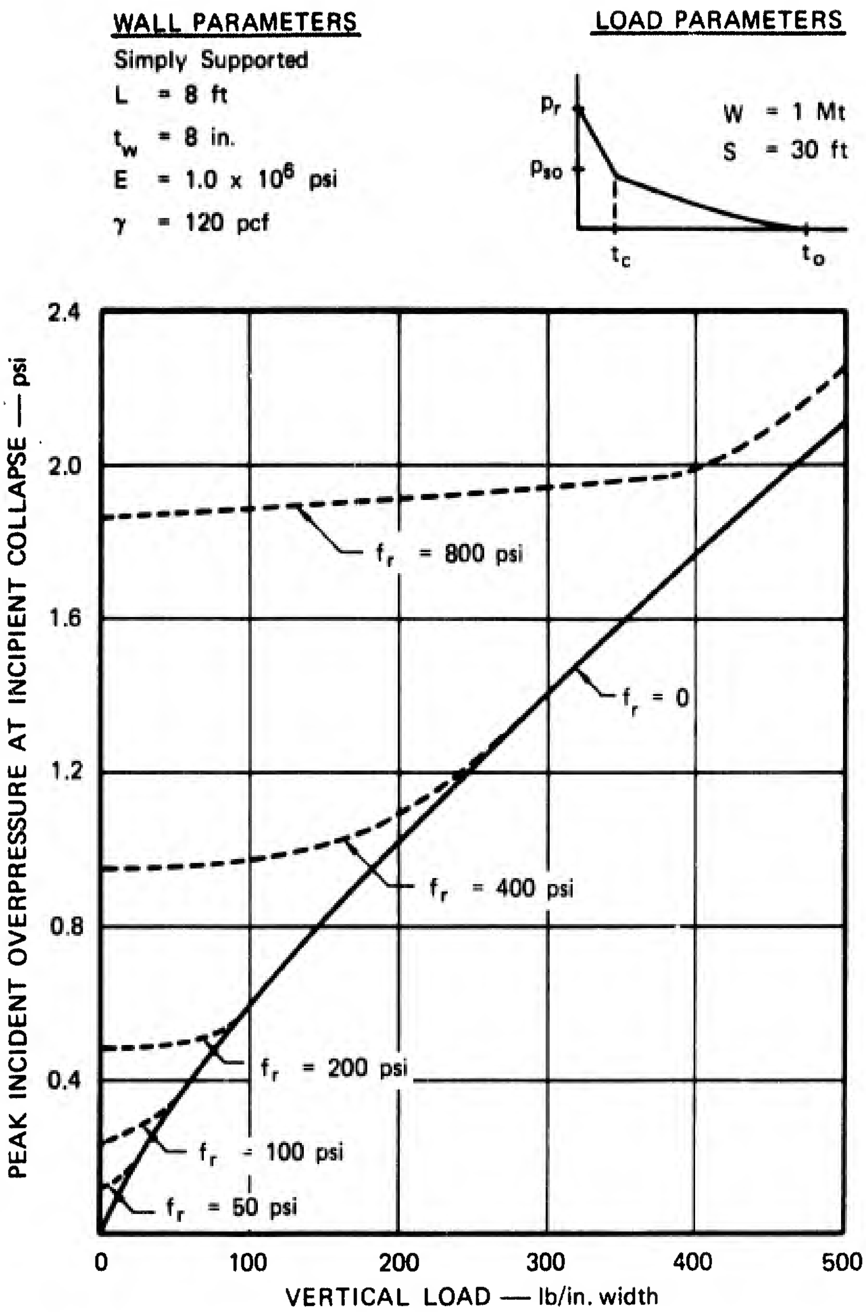


FIG. 29 PEAK INCIDENT OVERPRESSURE AT INCIPIENT COLLAPSE VERSUS VERTICAL LOAD AND MODULUS OF RUPTURE
Unreinforced Wall Without Arching

Reinforced Concrete Wall

A wall similar to that used for the standard unreinforced masonry wall was chosen to serve as the standard for reinforced concrete walls, from which a variation of parameters was made. These values were changed slightly so as to reflect the properties of concrete. The properties of the standard wall are summarized as follows:

| | |
|---|---|
| Height, $L$ . . . . . . . . . . . . . . . | 96 in. |
| Thickness, $t_w$ . . . . . . . . . . . . | 8 in. |
| Modulus of elasticity | |
| Concrete, $E_c$ . . . . . . . . . . . | $3 \times 10^6$ psi |
| Reinforcing steel, $E_s$ . . . . . . | $30 \times 10^6$ psi |
| Ultimate strength (dynamic) | |
| Concrete, $f'_{dc}$ . . . . . . . . . . . . | 3,750 psi |
| Reinforcing steel, $f_{dy}$ . . . . . . | 42,000 psi |
| Unit weight, $\gamma$ . . . . . . . . . . . . . | 145 pcf |
| Percent reinforcing steel | 0.0025 |
| Tension, $p$ ($d$ = 7 in.) . . . . . . . | 0.0025 |
| Compression, $p'$ ($d'$ = 1 in.) . . . . | 0 |
| Vertical load, $P_v$ . . . . . . . . . . . . | 0 |
| Support conditions . . . . . . . . . . | Simply supported |

The type of loading acting on the wall was the same as that used for the unreinforced masonry wall, i.e., Loading Case No. 1, Section II.

The effect of the parameters studied on the incipient collapse load are as follows.

Clearing Time, $t_c$ (Figure 30). The clearing time, $t_c$, is seen to have significant effect on the collapse pressure for much longer durations than was found to be the case for the unreinforced walls without arching. This effect becomes relatively minor at a value of approximately 250 milliseconds. The yield is also seen to have an important effect throughout the range of 1 kt to 1 Mt studied.

Load Duration, $t_o$ (Figure 31). A triangular loading (Loading Case No. 2, Section II) of varying duration was used to determine the effect of load duration on the incipient collapse pressure. The effect of the load duration is seen to be significant for durations up to about 300 milliseconds, after which the incipient collapse pressure decreases only slightly. The effect of the load duration is significant for much longer durations than was the case for unreinforced masonry walls (Figure 24). This is undoubtedly because of the resistance being maintained at a constant value with deflection for the reinforced walls, whereas unreinforced walls had a decaying function.

Tension Reinforcement, p (Figure 32). As a percentage of tension reinforcement is increased, the load required to cause incipient collapse increases significantly. This increase is nearly linear for the range of values studied.

Vertical Load, $P_v$ (Figure 33). The load required to cause incipient collapse increases as the axial load increases. This increase is nearly the same for all three types of support conditions.

Support Conditions (Figure 33). The type of support conditions is seen to have a significant effect on the load required to cause incipient collapse, with the fixed-end wall being the strongest, followed by the propped-cantilever wall, and the simply supported wall being the weakest. This effect is approximately the same for each value of the vertical load.

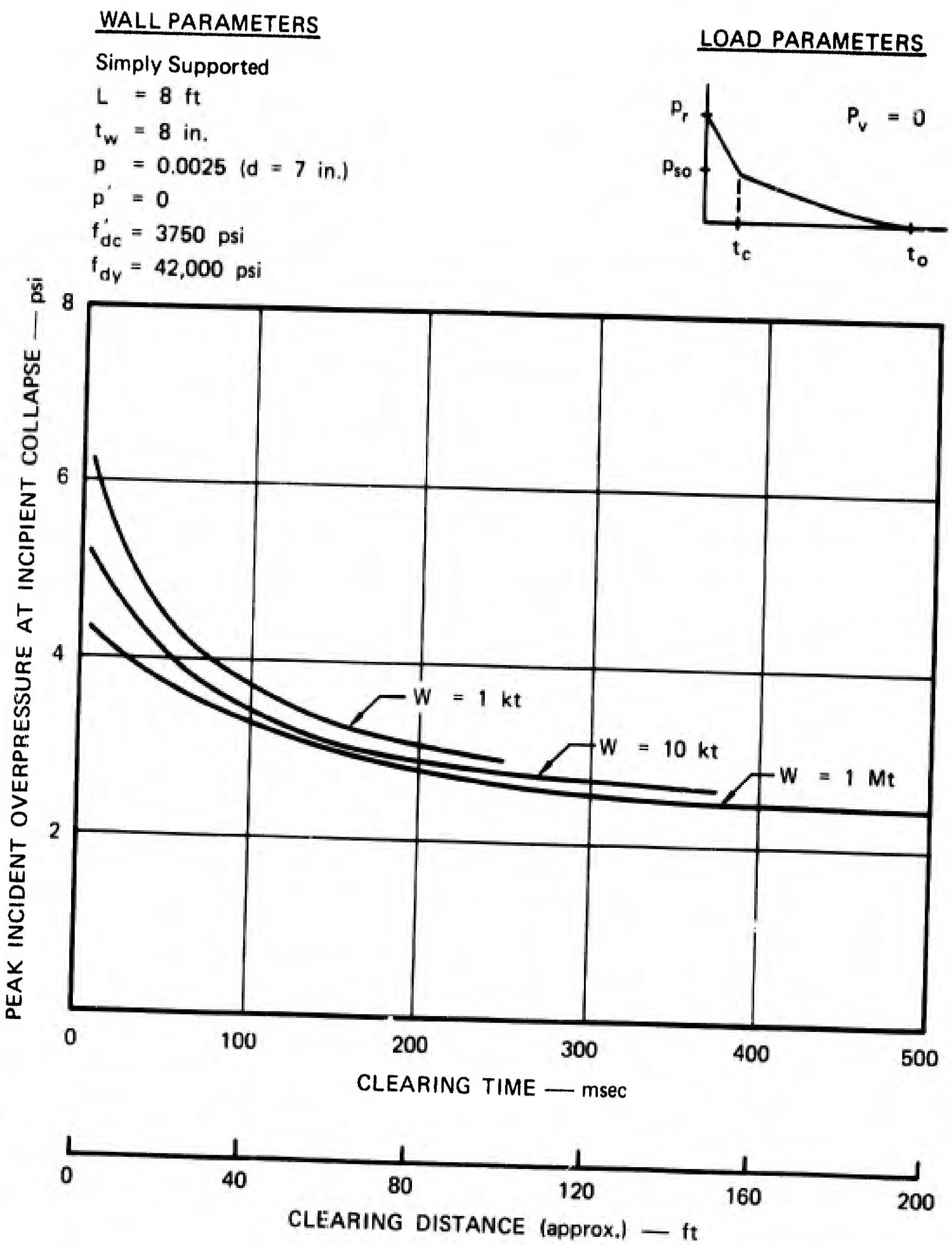


FIG. 30 PEAK INCIDENT OVERPRESSURE AT INCIPIENT COLLAPSE VERSUS CLEARING TIME
Reinforced Concrete Wall

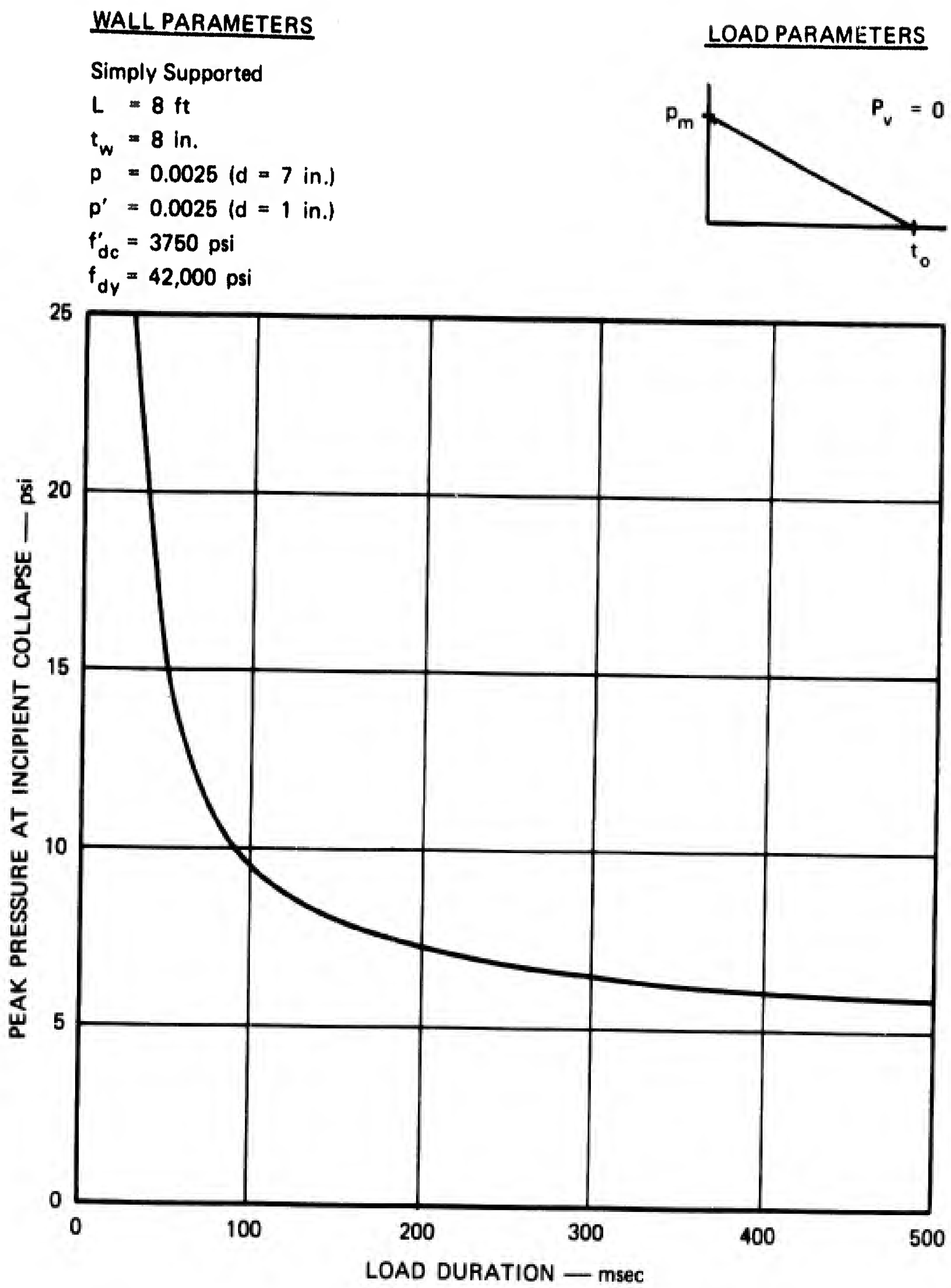


FIG. 31 PEAK PRESSURE AT INCIPIENT COLLAPSE VERSUS LOAD DURATION
Reinforced Concrete Wall

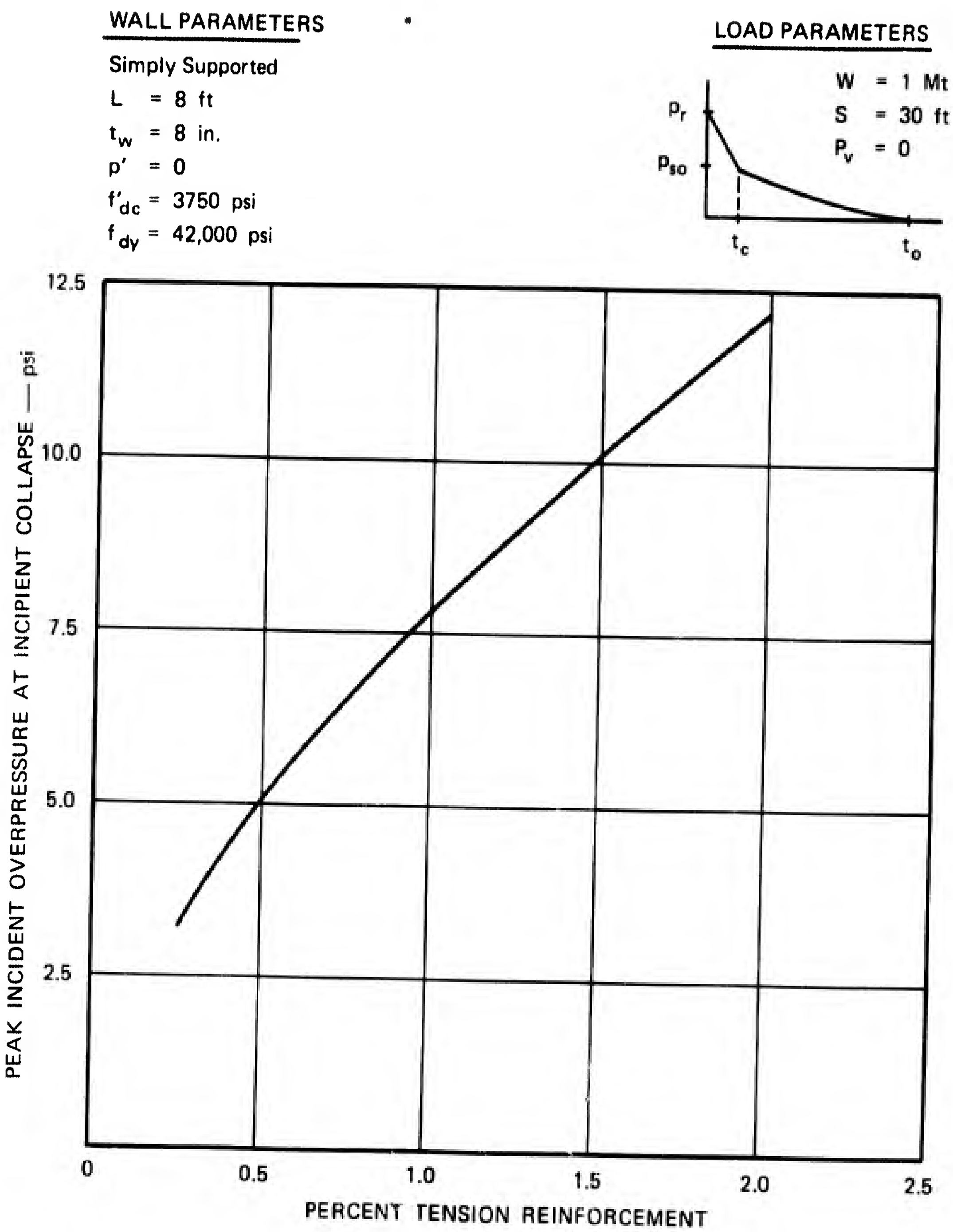


FIG. 32 PEAK INCIDENT OVERPRESSURE AT INCIPIENT COLLAPSE VERSUS PERCENT TENSION REINFORCEMENT
Reinforced Concrete Wall

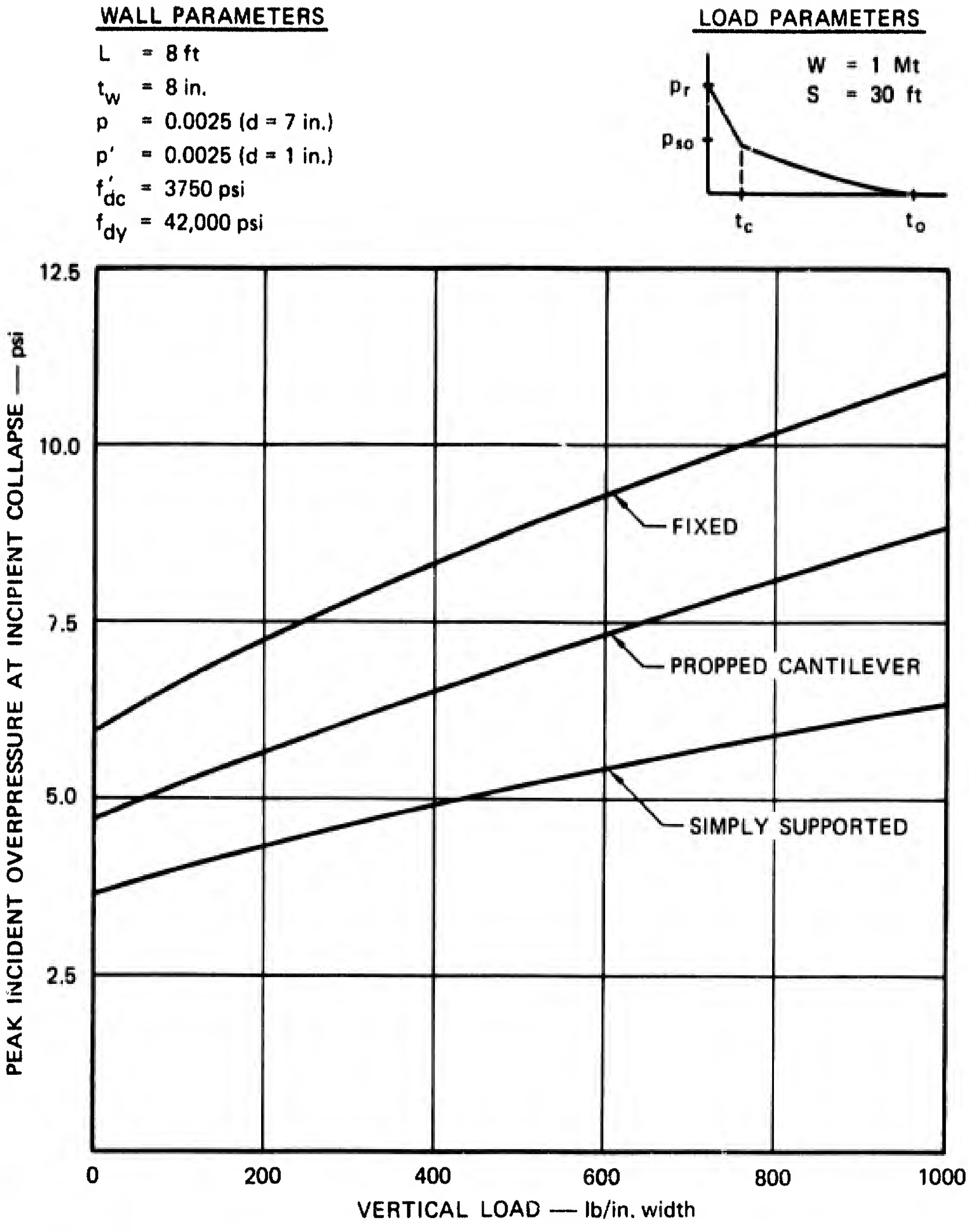


FIG. 33 PEAK INCIDENT OVERPRESSURE AT INCIPIENT COLLAPSE VERSUS VERTICAL LOAD
Reinforced Concrete Wall

Failure Deflection, $y_f$ (Figure 34). Because of the uncertainty of the deflection at which reinforced concrete walls collapse (see page 55), the effect of varying $y_f$ was studied. Values of ductility ($\mu = y_f/y_u$) ranging from 2 to 35 were investigated, with the resulting incipient collapse pressures ranging from 2.5 psi to 3.5 psi. For the most probable range of $y_f$--between a $\mu$ of 10 and 30--the incipient collapse pressure varied between 2.9 and 3.5 psi. This represents a maximum possible error of 20 percent based on the lower value. Thus, any error introduced in choosing a value for $y_f$ is within a tolerable limit.

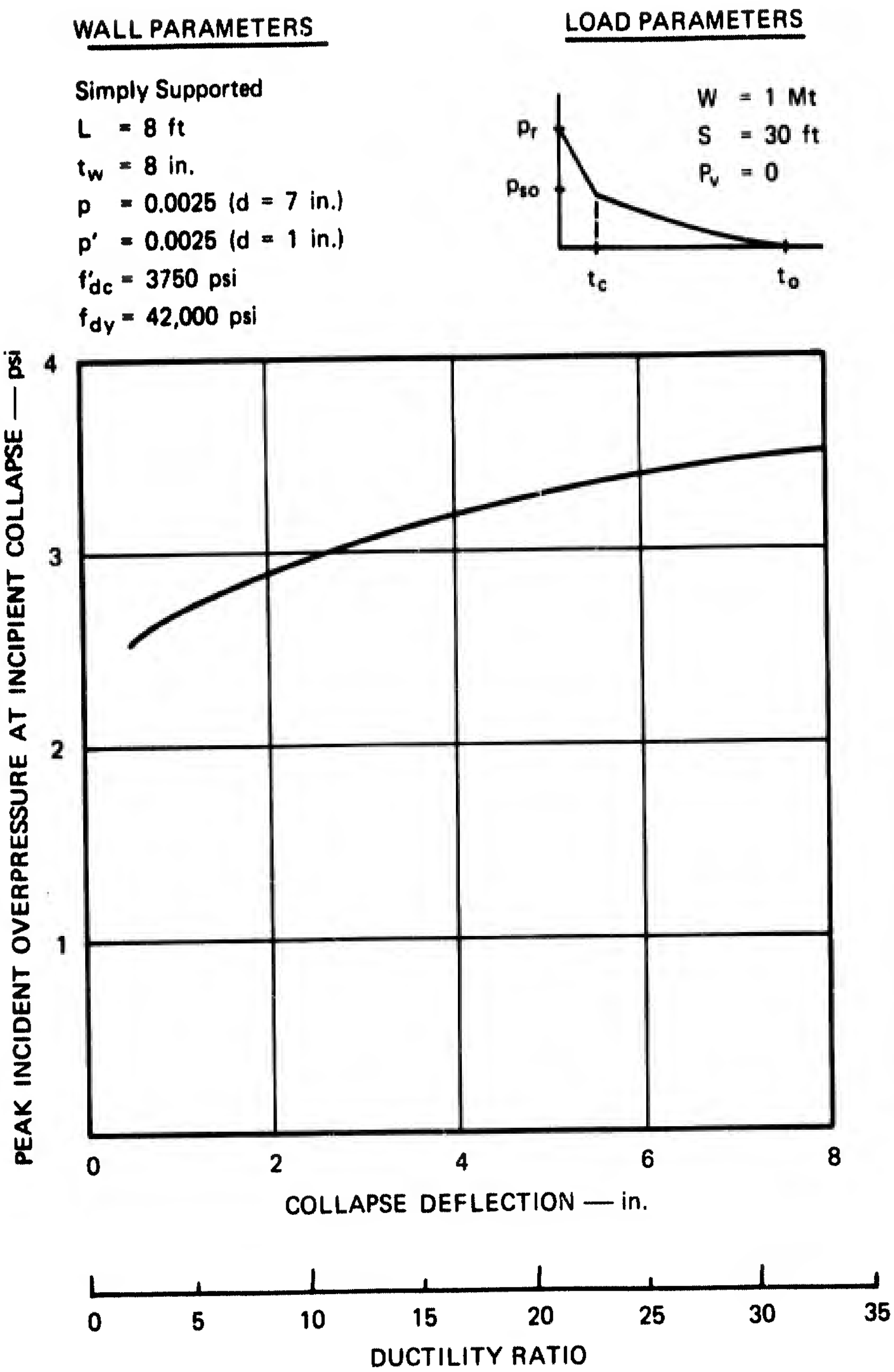


FIG. 34 PEAK INCIDENT OVERPRESSURE AT INCIPIENT COLLAPSE VERSUS COLLAPSE DEFLECTION
Reinforced Concrete Wall

## Unreinforced Concrete or Masonry Unit Wall (With Arching)

### Experimental Correlation

The time-deflection behavior of an unreinforced masonry wall, as predicted by the arching action theory in Section III, was compared with results obtained from experimental tests during Operation UPSHOT-KNOTHOLE (Ref. 25). The particular case compared was a solid brick curtain wall 12 in. thick and 120 in. high. The roof and floor slabs of the structure supporting the wall were 10 and 12 in. thick, respectively, and for the purposes of this comparison, were assumed to be infinitely stiff (rigid) against in-plane movement of the wall. The ultimate compressive strength of the wall was assumed to be 1,000 psi and the unit weight was taken as 120 pcf. The wall was subjected to the loading shown in Figure 35 (a), which approximates the field measurements.

The midspan deflection was calculated using the resistance function presented in Section III and is compared with the test data in Figure 35 (b). As can be seen, the arching method predicts the behavior fairly well up to the initial peak deflection, after which time the predicted and recorded behavior begin to deviate.* This deviation is probably because of the fact that the arching theory assumes that the properties of the masonry materials maintain constant, a condition that probably does not exist due to the crushing at the supports and center. Subsequent behavior past this initial peak, as predicted by the arching theory, is thus felt to be incorrect because of this breakdown of material properties, as well as because of the fact that the dynamic analysis used does not include damping. This neglect of damping is felt to

---

* The test wall used here to check the arching behavior did not collapse.

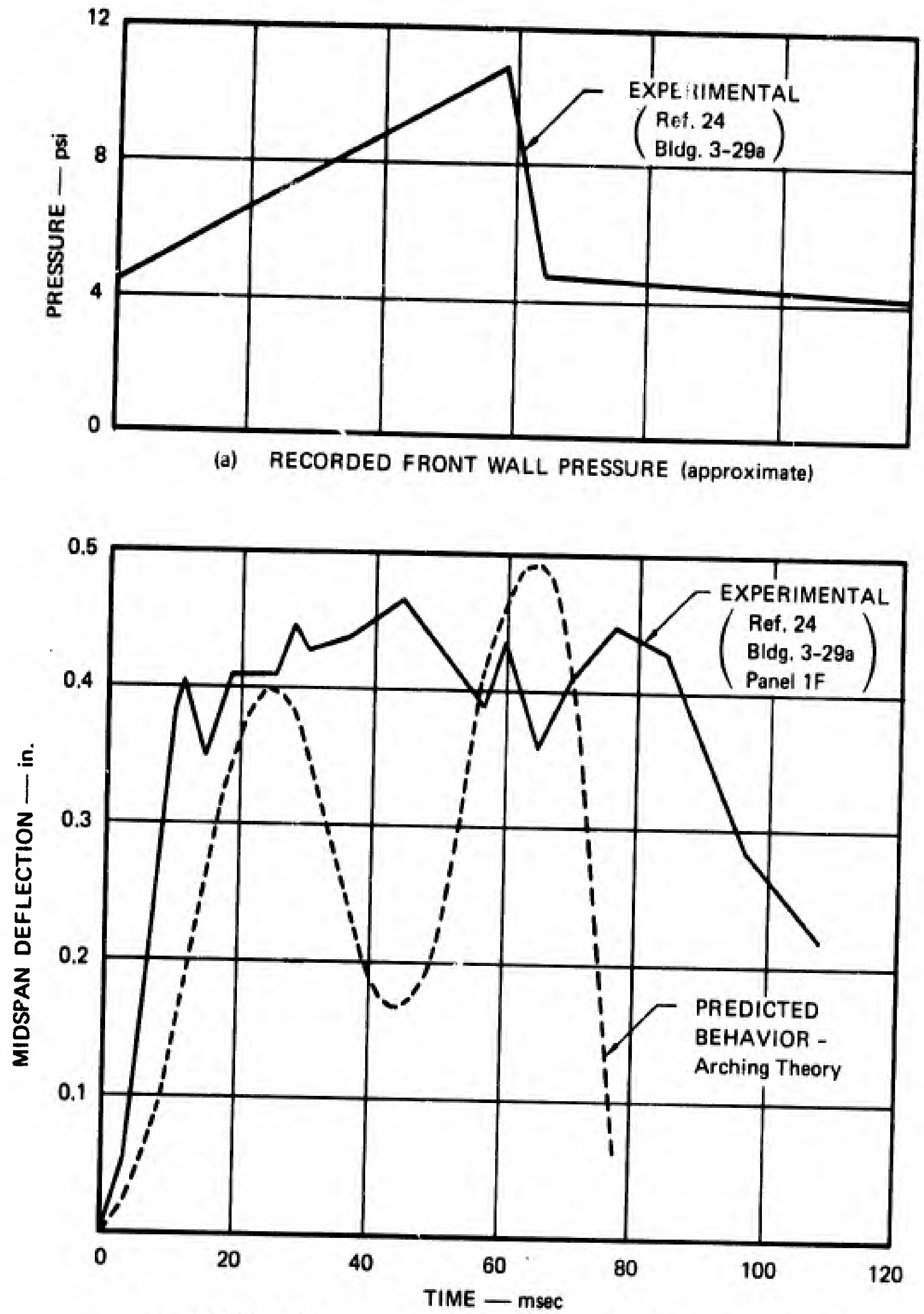


(a) RECORDED FRONT WALL PRESSURE (approximate)



(b) RECORDED AND PREDICTED TIME-DEFLECTION BEHAVIOR

FIG. 35 COMPARISON OF RECORDED AND PREDICTED ARCHING BEHAVIOR be minor up to the initial peak deflection. However, in predicting subsequent motion, the effect of damping would be significant because of the large dissipation of energy resulting from the crushing of the masonry material. Therefore, if damping had been included in the dynamic analysis, the initial peak deflection would have been greater than subsequent wall deflections.

From these results, it can be concluded that the arching theory adequately represents the time-deflection behavior of the wall up to the initial peak deflection. Since damping would decrease subsequent deflections, a wall subjected to a decreasing load function would not fail if the initial peak deflection was less than the collapse deflection. Thus, the fact that the arching analysis is incorrect for deflections past this initial peak is unimportant for predicting the collapse of blast loaded walls.

Variation of Parameters

The wall chosen as the standard for the arching analysis from which a variation of parameters was made had the same physical dimensions as used previously for unreinforced masonry walls without arching. These properties were:

| | |
|---|---|
| Height, $L$ . . . . . . . . . . . . . . . . . | 96 in. |
| Thickness, $t_w$ . . . . . . . . . . . . . . . . | 8 in. |
| Modulus of elasticity, $E_m$ . . . . . . . . . | 1,000,000 psi |
| Unit weight, $\gamma$ . . . . . . . . . . . . . . | 120 pcf |
| Ultimate compressive strength, $f'_m$ . . . | 1,000 psi |

The type of loading acting on the wall was again the same as used previously (Loading Case No. 1, Section II).

The effect of the parameters studied on the incipient collapse load of the wall for the arching action case is as follows.

<u>Height, L (Figure 36)</u>. The effect of the height of the wall is similar to that found for the case of unreinforced concrete or masonry walls without arching. That is, as the height is increased, the incipient collapse pressure is increased.

<u>Thickness, $t_w$ (Figure 37)</u>. The effect of the thickness is also very similar to that for the unreinforced masonry wall without arching, with the incipient failure collapse increasing as the thickness is increased.

<u>Unit Weight, $\gamma$ (Figure 38)</u>. For values ranging from 80 to 150 pcf, the unit weight of the wall material had very little effect on the pressure required to cause incipient collapse.

<u>Ultimate Compressive Strength, $f_m'$ (Figure 39)</u>. The incipient collapse pressure increased linearly with the ultimate strength of the masonry material for values ranging from 1,000 to 2,000 psi. This effect is seen to be very significant.

<u>Load Duration, $t_o$ (Figure 40)</u>. A triangular load (Loading Case No. 2) was used to determine the effect of the load duration on the incipient collapse pressure. This effect was seen to be significant for durations up to about 150 milliseconds. Comparing this wall with the two previous wall types, the effect of load duration is significant for durations to about three times as long as the unreinforced masonry wall without arching; it is only about half as long as for the reinforced concrete case. This is undoubtedly again because of the fact that the resistance is of a decreasing nature as the deflection is increased. The magnitude, however, is greater for a wall with arching.

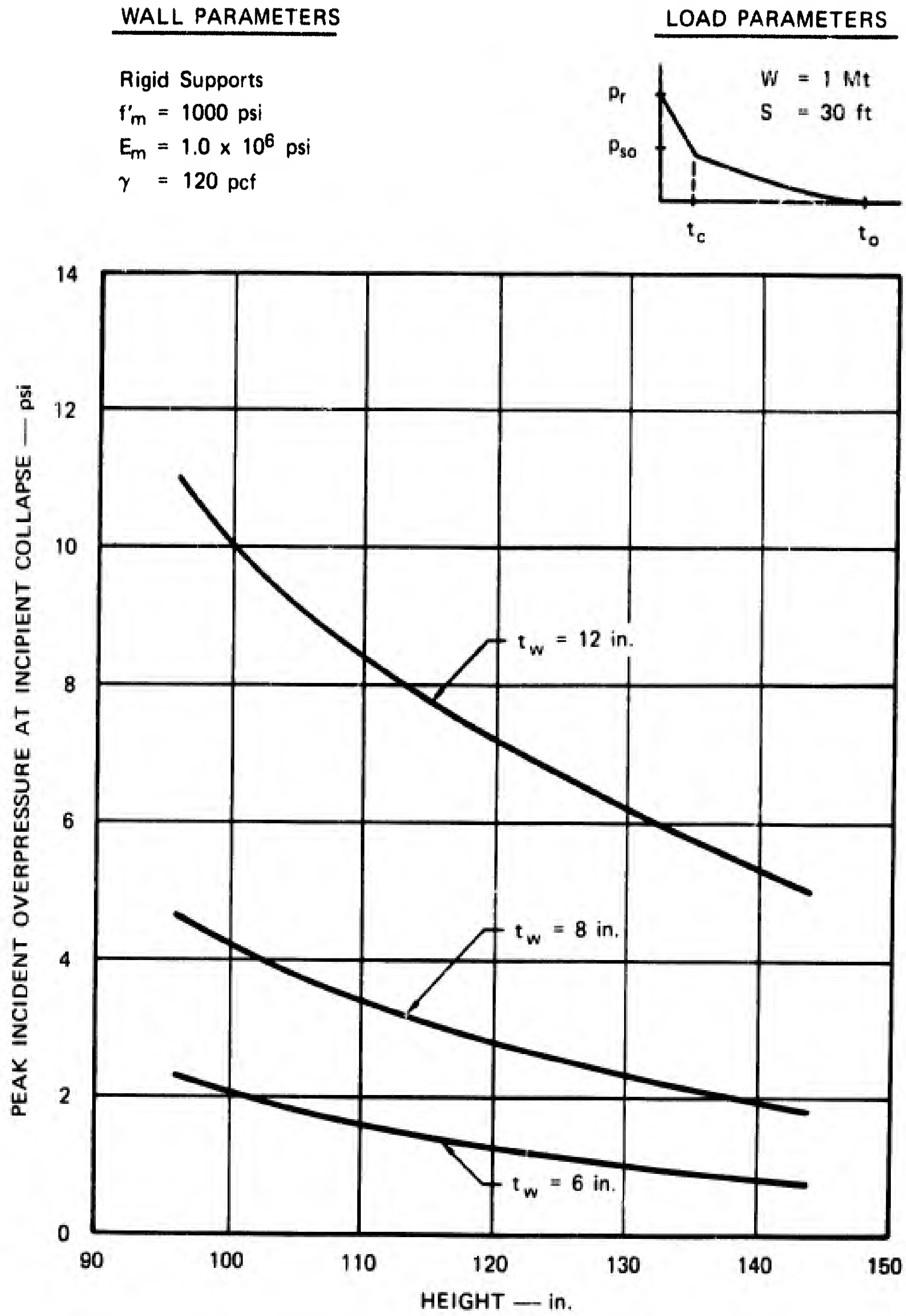


FIG. 36 PEAK INCIDENT OVERPRESSURE AT INCIPIENT COLLAPSE VERSUS HEIGHT
Unreinforced Wall With Arching

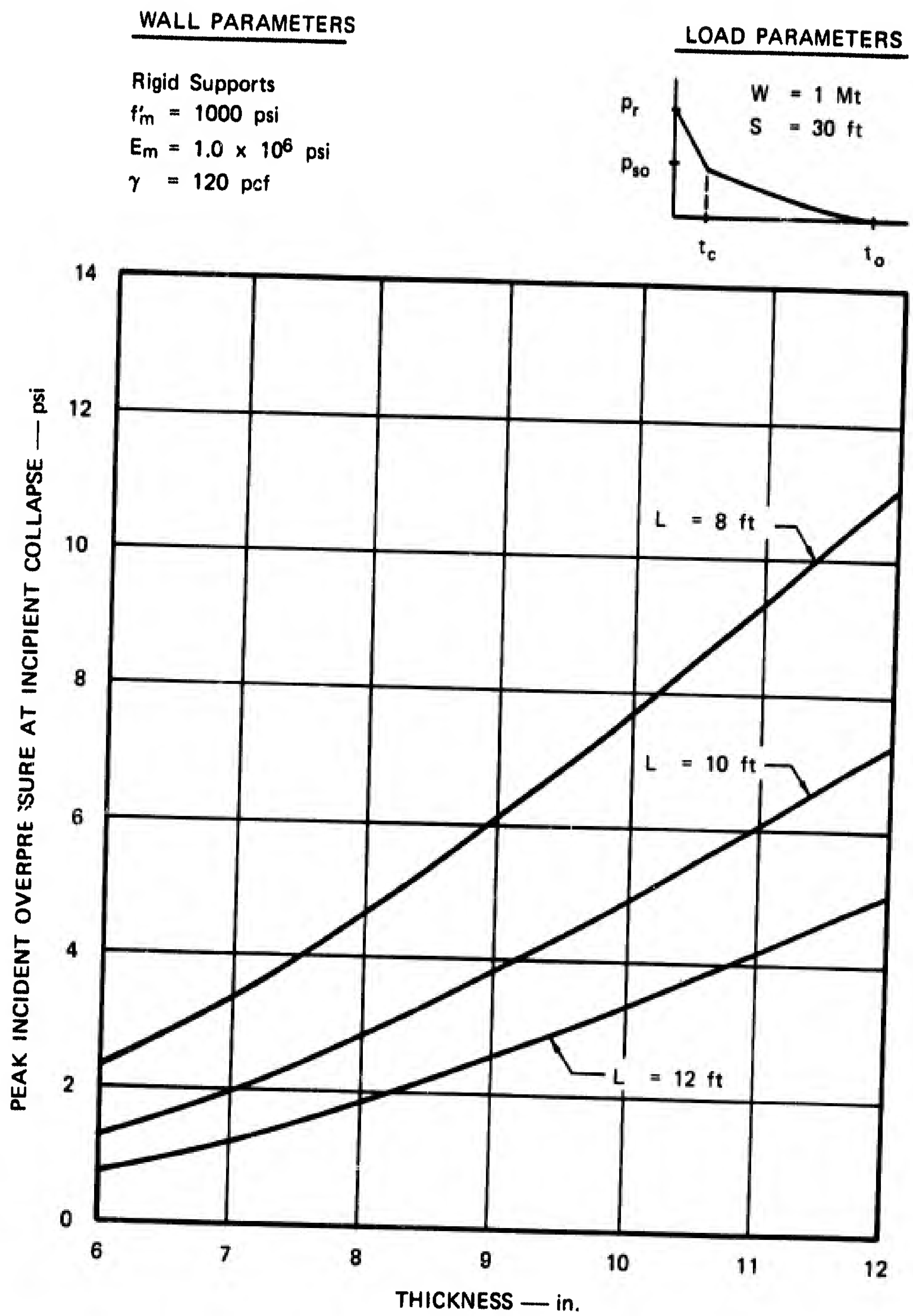


FIG. 37 PEAK INCIDENT OVERPRESSURE AT INCIPIENT COLLAPSE VERSUS THICKNESS
Unreinforced Wall With Arching

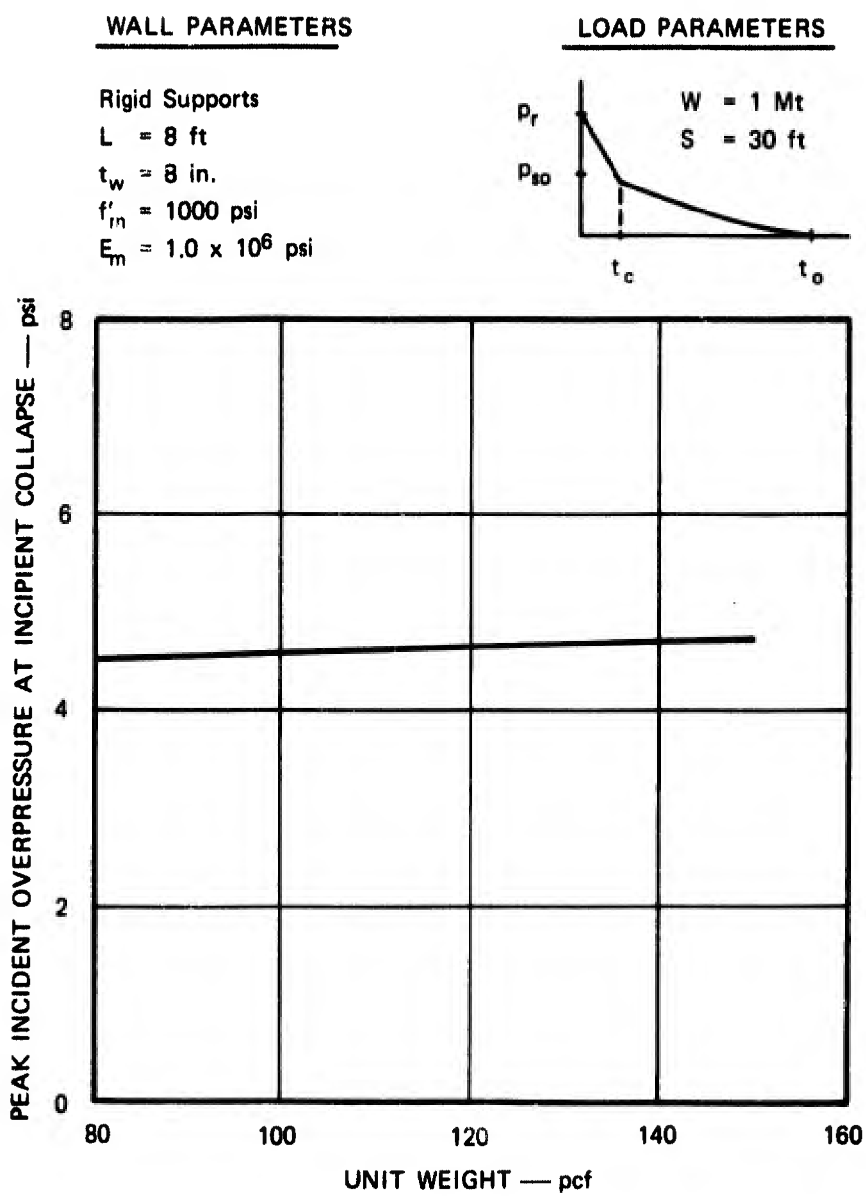


FIG. 38 PEAK INCIDENT OVERPRESSURE AT INCIPIENT COLLAPSE VERSUS UNIT WEIGHT
Unreinforced Wall With Arching

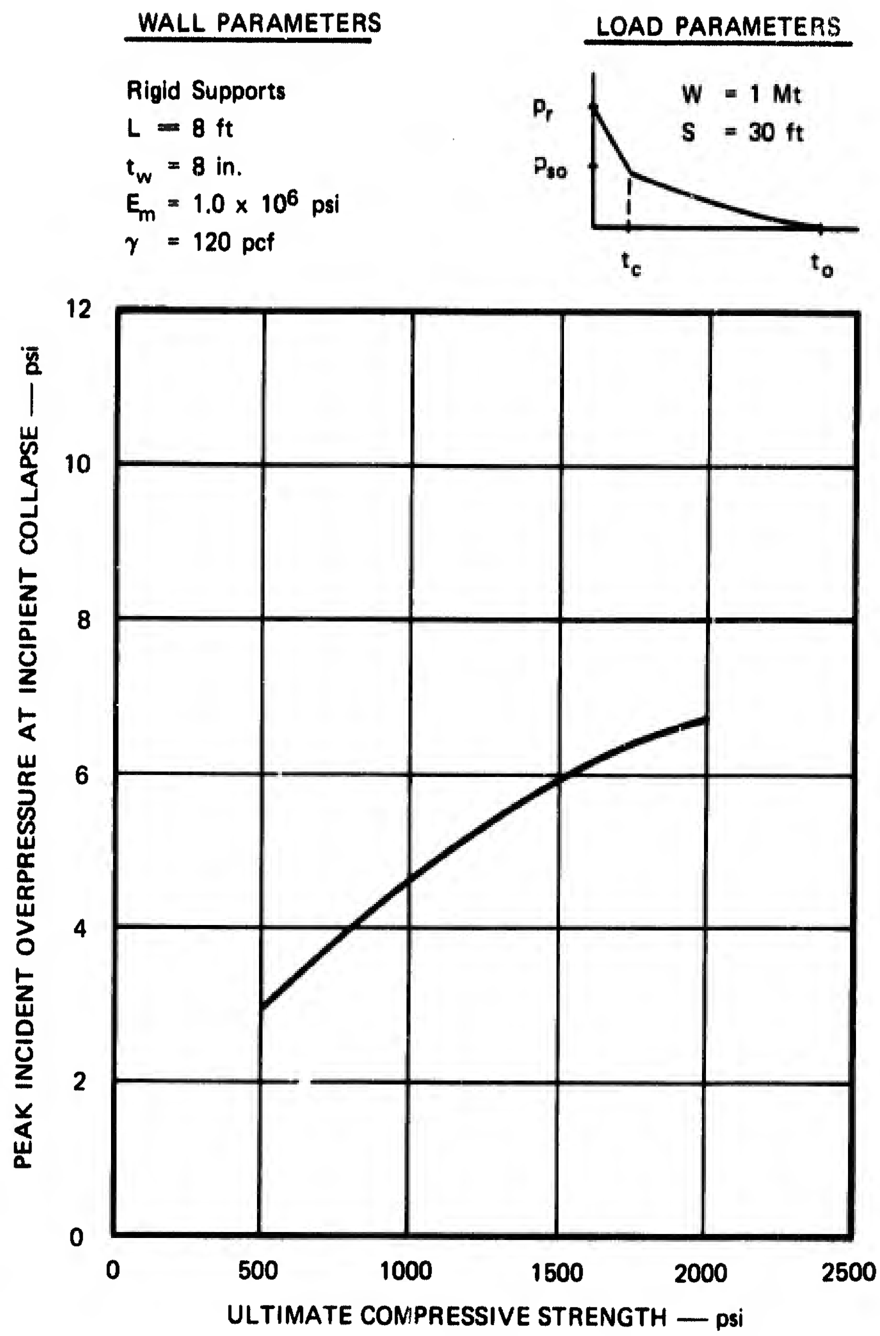


FIG. 39 PEAK INCIDENT OVERPRESSURE AT INCIPIENT COLLAPSE VERSUS ULTIMATE COMPRESSIVE STRENGTH
Unreinforced Wall With Arching

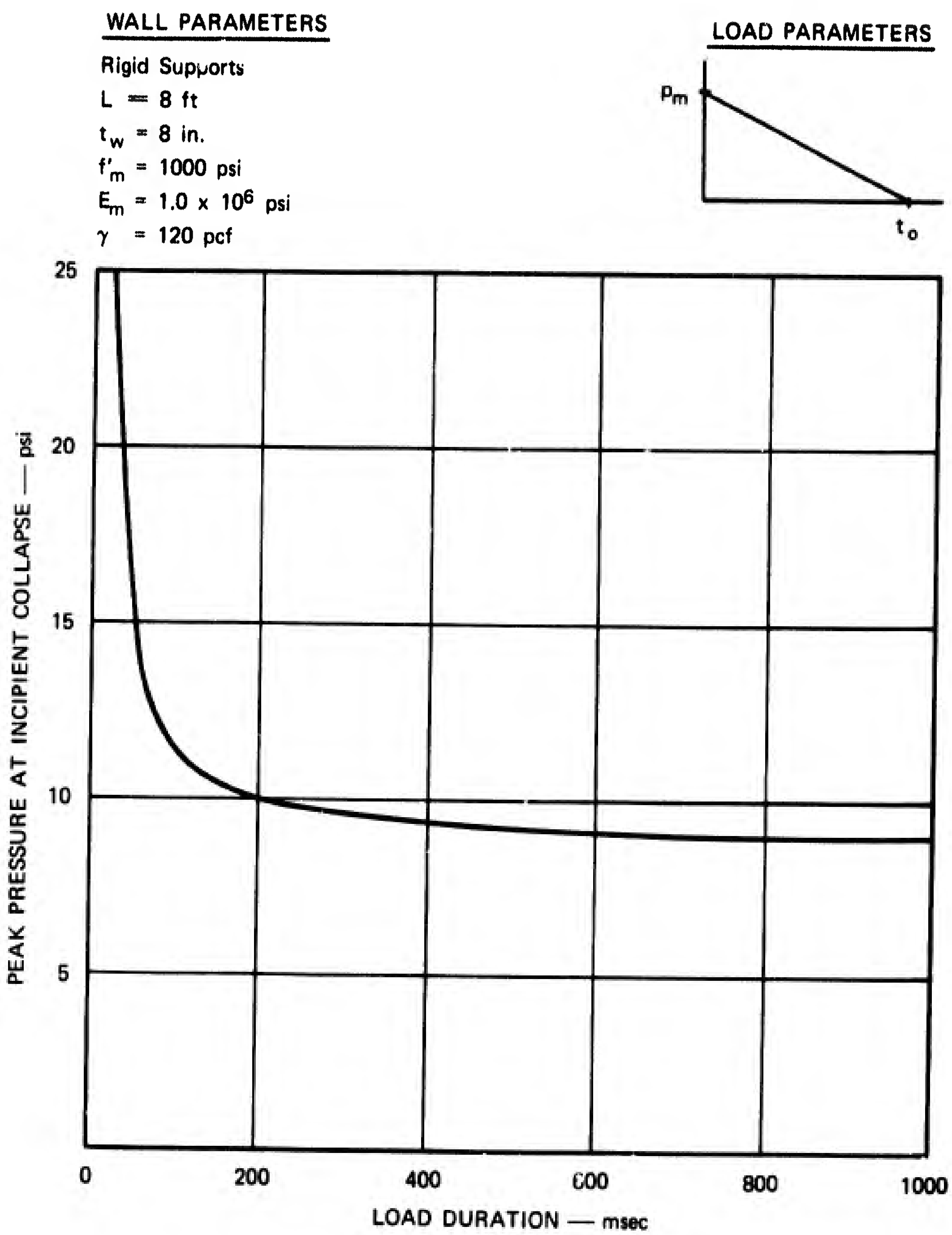


FIG. 40 PEAK PRESSURE AT INCIPIENT COLLAPSE VERSUS LOAD DURATION
Unreinforced Wall With Arching

Support Stiffness, $k_s$ (Figure 41). The effect of the stiffness of the supports on the resistance curve and the subsequent incipient collapse pressure is of considerable importance. As the support stiffness is decreased, the peak resistance is also decreased, with the deflection at which this occurs increasing (see Figure 15). The effect is to decrease the pressure at which incipient collapse is predicted as shown by Figure 41. For the sample wall studied, this effect was seen to be most important for stiffness of less than $10^5$ lb/in. For stiffnesses greater than this value, the effect was much less, with the resistance curve for the case of $k_s = 10^7$ lb/in. being indistinguishable from the case of rigid supports.

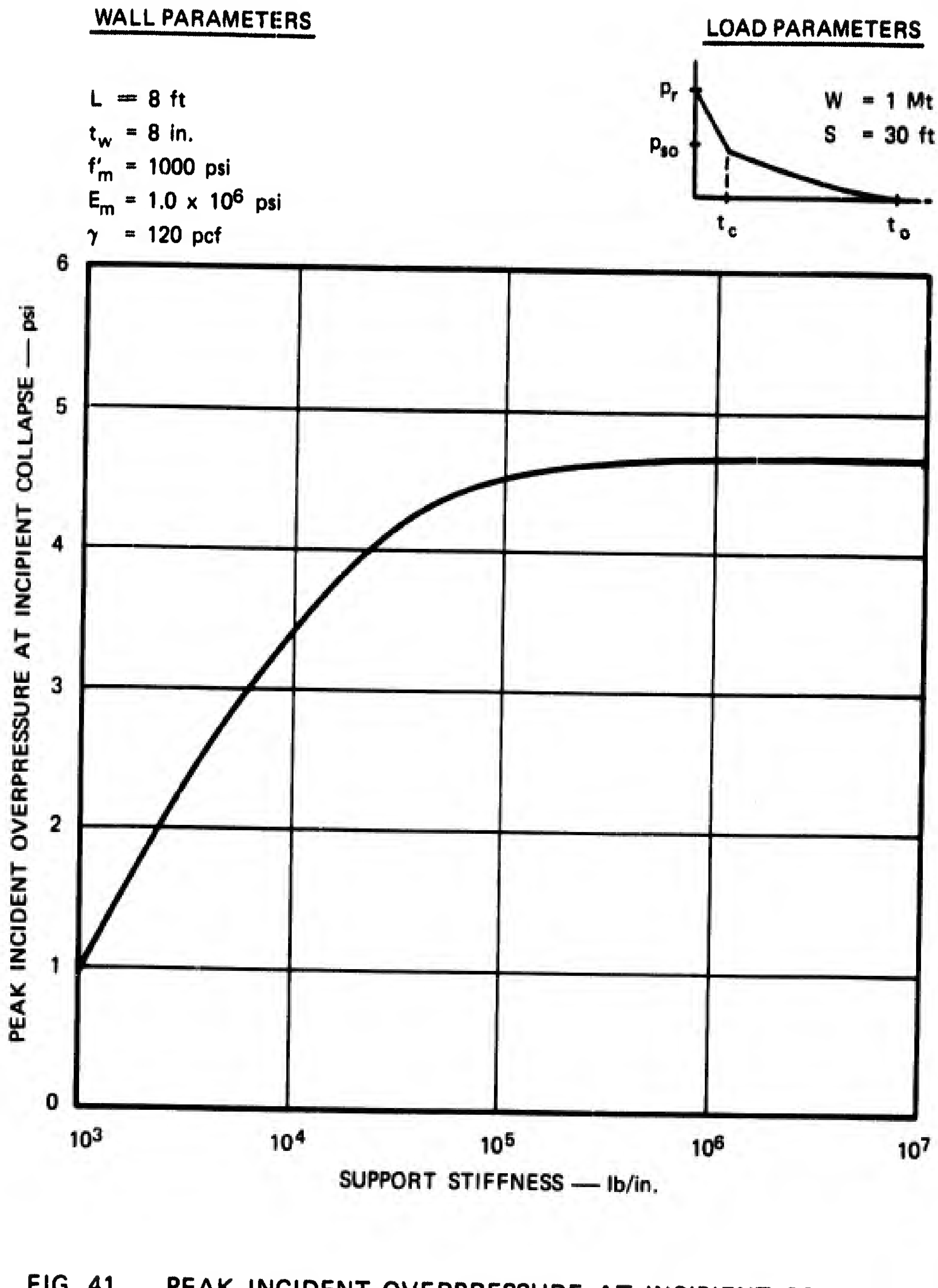


FIG. 41 PEAK INCIDENT OVERPRESSURE AT INCIPIENT COLLAPSE VERSUS SUPPORT STIFFNESS
Unreinforced Wall With Arching

## Reactions

The analytical model used in this study to determine the reactions of dynamically loaded structural walls was discussed in Section IV. The method, although simplified, is well-established in dynamic analysis and has been used to predict reasonable values for the peak dynamic reactions measured in limited experiments (e.g., Ref. 26). For the purpose of the evaluation of existing structures, however, the magnitude of the reactions without the time-distribution is of limited application, since the reactive force of a wall is the input load on the structure, and both its magnitude and duration are important to the response of the structural framing. It was therefore necessary to determine whether the time-dependent reactions predicted by the method were realistic. A correlation of the reaction time function from the analytical model and from the limited experimental information is presented in the following pages. Also, a comparison is made between the reactions determined by the method used in this study and those obtained by the method given in Ref. 1.

### Experimental Correlation

Reference 26 presents the results of laboratory experiments to determine the response of beams to transient loads. The dynamic information was given in sufficient detail to permit a comparison to be made between the experimentally measured reactive forces from two beams and those predicted by the mathematical model presented in Section IV. The beams were simply supported, with a 78-in. span length, and were dynamically loaded with a concentrated load at midspan. Although the reaction equations developed in Section IV considered only distributed loads, the reactions for a simply supported beam with a concentrated load can be obtained in a similar manner or from Ref. 7:

$$V = 0.78\,Q - 0.28\,P \quad .$$

By substitution of the experimental resistance and load values from Ref. 26 in the above equations, the reaction-time history for the beams can be determined. This information is shown on Figure 42, together with the reaction-time forces measured in the tests. It is apparent that there is a good correlation between the theory and the limited experimental data.

Unreinforced Masonry Unit Wall (Without Arching)

A study of the total reaction imparted to the supporting frame by the failing wall was made to check the method suggested in Ref. 1 for failing frangible walls to see whether such a method applies in the case of unreinforced masonry walls. The method outlined in Ref. 1 treats the reaction from the frangible wall as an impulse of magnitude equal to 0.04 times the area of the wall, regardless of the load applied to the structure (as long as load is sufficient to cause failure). As can be seen from the plot of the reactions for the airblast loadings studied shown in Figure 43, the total reaction, $R_t$, imparted to the frame is not constant, but depends on the magnitude of the applied load. For the load corresponding to incipient collapse ($p_{so}$ = 0.12 psi), the total reaction applied to the frame is approximately 0.03 - 0.04 psi-sec., which agrees well with the value given in Ref. 1. However, for the range of loads studied, the total reaction ranged up to 0.09 - 0.10 psi-sec., which is well above the suggested value from Ref. 1. Thus, it may be concluded that the total reaction from masonry walls cannot be treated as a constant, but is some function oi the applied load.

There is also some question as to whether the reaction of masonry walls can be treated as an impulse loading on the frame, especially for loads near the incipient collapse load. As can be seen in Figure 43, times associated with incipient collapse are in the hundreds of milliseconds, and it is doubtful whether reactions of these durations can be

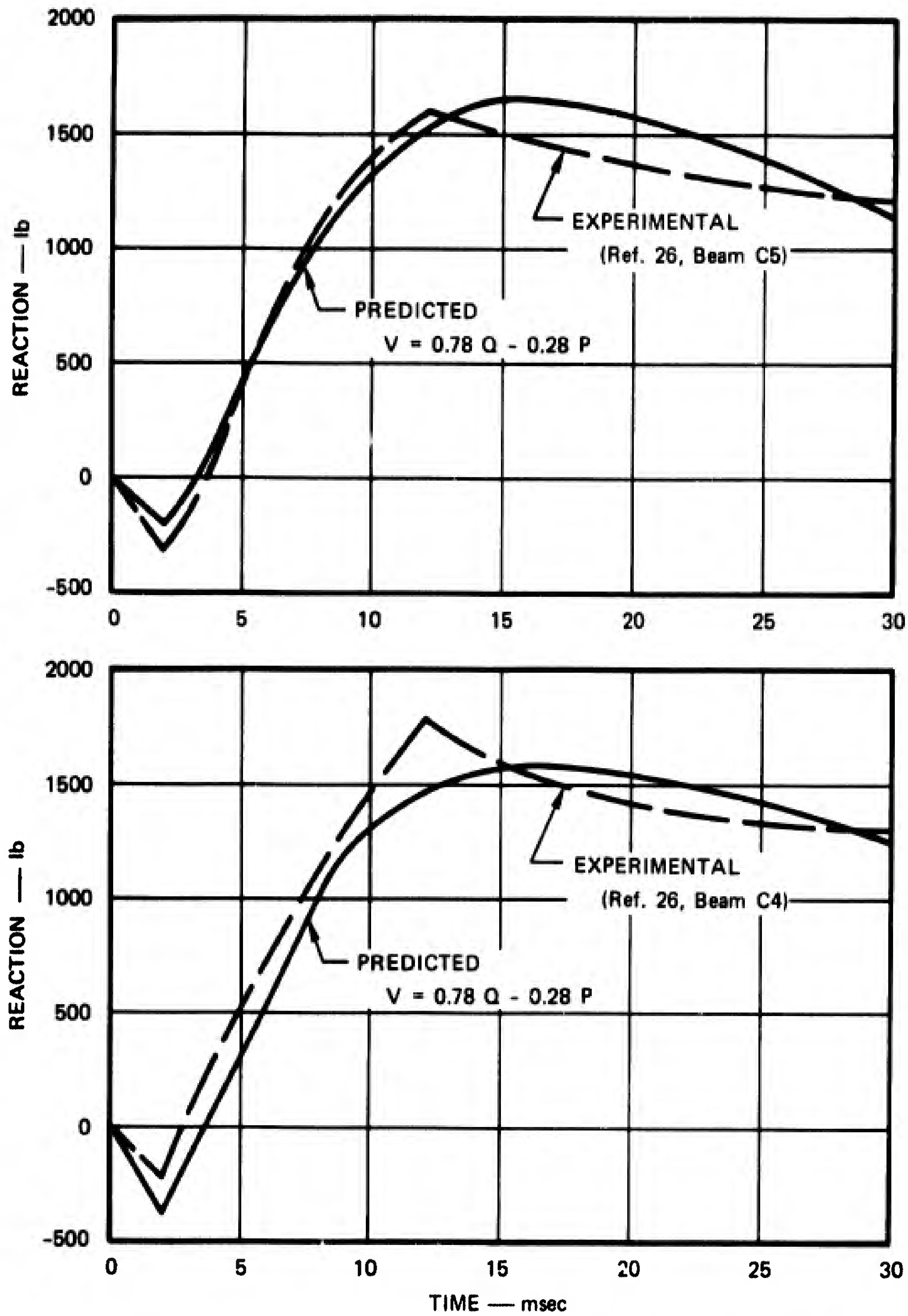


FIG. 42 BEAM REACTION VERSUS TIME

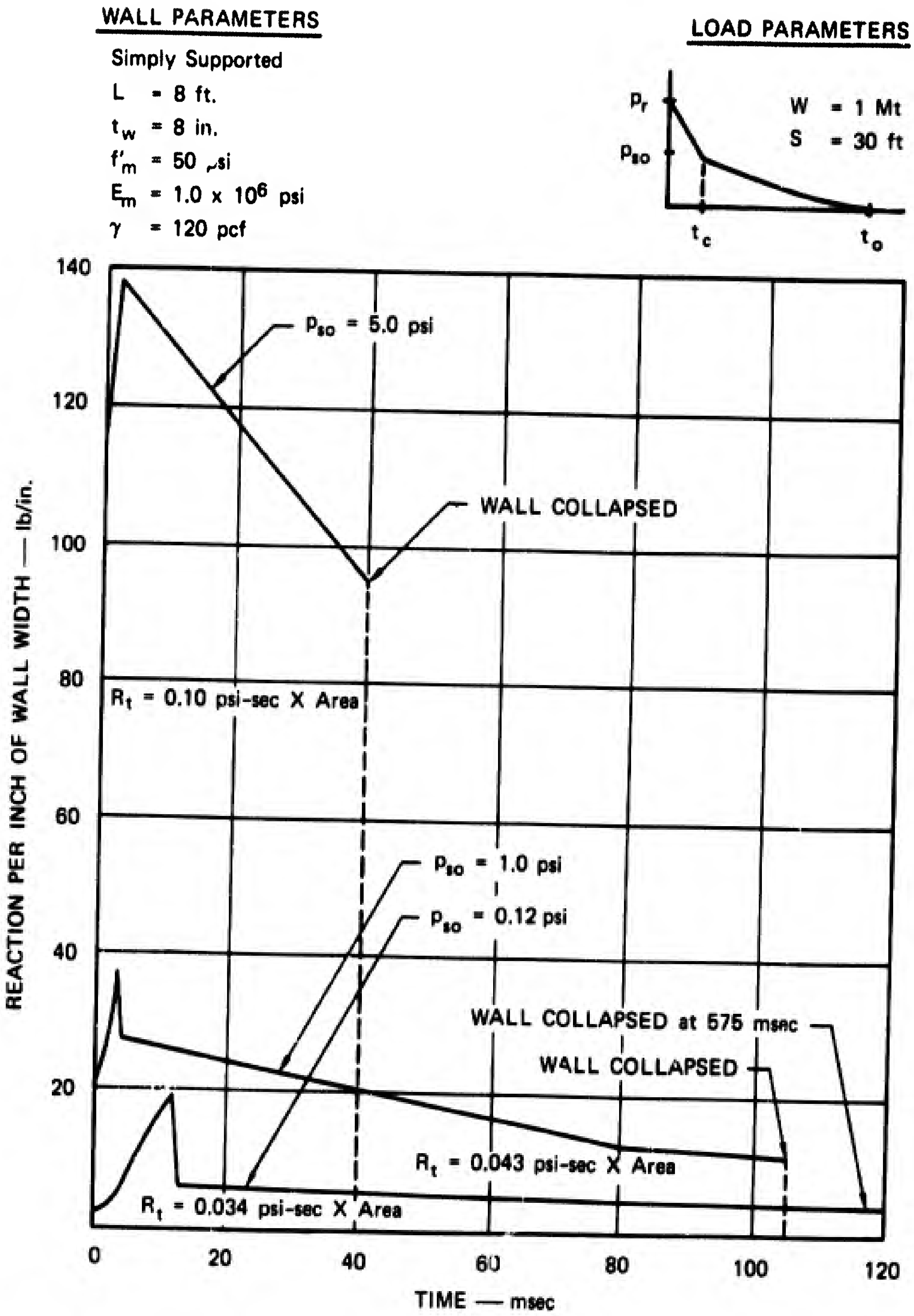


FIG. 43 REACTION-TIME HISTORY FOR WALL SEGMENT
Unreinforced Wall Without Arching

considered as impulses applied to the frame. For loads of higher magnitude, this assumption may be more nearly correct, since the times to failure are reduced significantly, being in the range of 40 milliseconds for the highest load considered. Loads of these durations may probably be treated as impulses in relation to the natural period of the supporting frame, although as pointed out above, the applied load must be considered when determining the magnitude of the impulse.

# VI SUMMARY AND RECOMMENDATIONS

## Introduction

This report covers the first phase of a program to develop a procedure for the evaluation of existing structures subjected to nuclear air blast. The initial effort was concerned with the behavior of exterior walls.

From the study herein, it is apparent that the determination of the failure of exterior walls is a complex problem involving the elastic and inelastic response of the wall, its mode of collapse, and the load-time function. The approach used to solve this problem was to develop a resistance function for each of three basic types of walls; unreinforced concrete or masonry unit, both with and without arching, and reinforced concrete. The collapse pressure for a wall element was then determined by treating the dynamic response of the wall model as a simplified single-degree-of-freedom system. Since only limited experiemntal data were available to verify the validity of the procedure, specific wall elements were selected to examine the sensitivity of the predicted collapse pressure over a range of the various parameters. Although the results of the parametric study are not conclusions in the usual sense, a summary of the findings presented in Section V are included in this section.

In addition, a short discussion of the recommendations for further research related to predicting the collapse of exterior walls is included.

## Summary

### Unreinforced Concrete or Masonry Unit Wall (Without Arching)

The foregoing parametric study makes it apparent that only certain factors appreciably affect the prediction of the collapse pressure for unreinforced concrete or masonry unit walls without arching. For example, it was found that the incipient collapse pressure of walls subjected to dynamic loads does not depend either on the modulus of elasticity or the unit weight for a rather wide range of practical values. This is of interest for the evaluation of existing structures, since both parameters are difficult to determine in situ.

Another factor, which has limited influence on the collapse of unreinforced walls, is the overall size of the structure. The bottom curves in Figure 23 indicate that for clearing distances greater than about 20 ft ($t_c \approx 50$ msec), the clearing time of ideal nuclear blast waves does not significantly affect the predicted collapse pressure of a windowless wall without vertical load. This is especially true for weapon yields above 10 kt, which include the range of primary interest to OCD; i.e., the clearing time is more important for predicting the collapse of walls in small buildings or for small weapon yields. For buildings of the dimensions usually found in NFSS-type structures, the clearing time would not be an important factor for walls without vertical load. However, as noted in the upper curves in Figure 23, for walls with a vertical load as low as 100 lb/in. of width, the clearing time influences the incipient collapse pressure of the wall for a wide range of values. Also, a wall with a vertical load is more sensitive to a variation in weapon yield.

As can be seen in Figure 24, for a triangular load pulse, the duration of the load on the wall is very important for the prediction of collapse. This emphasizes, therefore, that for most buildings that contain windows the net load (front loading minus back loading) on the wall governs the predicted collapse pressure, and the interior shock wave diffraction and room filling processes become important considerations in any evaluation procedure.

An important factor in determining the incipient collapse pressure of unreinforced walls is the magnitude of the vertical load in the plane of the wall. As Figure 29 indicates, an 8-in. thick wall with a modulus of rupture of about 150 psi, but without a vertical load, would collapse at peak incident overpressure of about 0.35 psi. This collapse pressure is equivalent to that for a wall with zero modulus of rupture, but with a vertical load of less than 50 lb/in. of wall width. It is of interest that a 50 lb/in. vertical load is about equal to the dead load from an additional 8 ft height of the wall.

Reinforced Concrete Wall

The limited parametric study showed also that only certain factors appreciably affected the predicted collapse pressure of reinforced concrete walls. For example, although not shown on the figures in Section V, it was found that a variation in the modulus of elasticity of concrete from 2 to 3 million psi resulted in less than 1 percent change in the predicted incipient collapse pressure for walls subjected to typical nuclear blast loading. Also, changing the ultimate concrete compressive strength from 2,000 to 4,000 psi resulted in less than 3 percent change in the incipient collapse pressure, and a change in the unit weight of the concrete from 100 to 145 pcf resulted in about a 5 percent change in the incipient collapse pressure.

As might be expected, it was found that a vertical load on reinforced concrete walls has less effect on the incipient collapse pressure than was found for unreinforced walls. Figure 33 shows that the addition of a vertical load of 100 lb/in. of wall width increases the wall incipient collapse pressure about 11 percent. However, factors that significantly influence the predicted incipient collapse pressure for reinforced concrete walls include the percent tension steel, shown in Figure 32, and the duration of the net wall loading, as indicated by Figures 30 and 31.

Unreinforced Concrete or Masonry Unit Wall (With Arching)

The results of the limited parametric study conducted for unreinforced walls with arching were very similar to those obtained for the case without arching. However, the magnitude of the predicted incipient collapse pressures was significantly higher. It was again found that the unit weight of the wall had very little influence on the predicted incipient collapse pressure (Figure 38). The predicted incipient collapse pressure was determined, however, to be greatly dependent on the height and thickness of the wall element, as well as upon its ultimate compressive strength (Figures 36, 37, and 39).

As shown in Figure 40, for a triangular load, the effect of the load duration was found to be similar to that for the walls without arching, (Figure 24) with the wall being able to sustain much higher pressures as the load duration becomes shorter.

The stiffness of the supports against in-plane movement of the wall as seen in Figures 15 and 41, significantly affects the predicted incipient collapse pressure, with the pressure being greatly reduced as the support stiffness is reduced. It can also be seen that for larger values of the stiffness, the predicted incipient collapse pressure remains nearly constant at a value corresponding to that obtained for the case where rigid supports are assumed. For these values, the supports may thus be assumed to be rigid, with very little resultant error in the predicted incipient collapse pressure.

## Wall Reactions

As noted on Figure 42, a good correlation was obtained between the predicted reaction-time history of one-way wall elements and the measured reactions from a limited number of reinforced concrete beam tests. On the other hand, an examination of the reaction-time history for an unreinforced masonry wall showed that the total reaction applied to the supporting frame was not a constant as sometimes assumed. Rather, as noted on Figure 43, the total area under the reaction-time curve, or impulse, increases with increasing load magnitude. This indicates that the assumption that exterior walls can be treated as frangible elements for determining the reactive forces, or input load to the structural frame, is incorrect for most of the walls in NFSS-type structures. Therefore, for the purpose of evaluating existing structures in the overall program, the method outlined in Section IV will be used for determining the reaction-time history.

## Computer Programs

Computer programs were developed for analyzing the dynamic behavior of the three types of exterior walls previously discussed. The programs use the resistance functions presented in Section III and are capable of accepting any arbitrary type of lateral load-time function, including the net loading on walls with openings.

The programs were designed to solve for the magnitude of the load causing incipient collapse of the wall if the shape of the load function is given. In addition, the time-history of the wall response up to collapse can be determined for a given loading. The computer output data includes the wall reaction and the displacement, velocity, and acceleration of the midheight of the wall. For loads above the incipient collapse pressure, this information can be used, together with the wall properties, to obtain an average velocity of the two half-wall elements. The average velocity can then be used to approximate the translation of the wall for use in casualty and debris studies.

<u>Recommendations</u>

In addition to a continuation of the effort on exterior walls to include such factors as two-way structural action, it became apparent during this investigation that information was needed in related areas to supplement the analytical effort to develop a procedure for the evaluation of existing structures. Recommendations for such research are given below.

- It is recommended that sufficient static and dynamic tests of typical exterior walls be conducted to permit an examination of the validity of the mathematical models presented in this report or to establish the basis for additional or substitute procedures. The specific areas of interest for which experimental information is needed include the resistance function for various types of walls, the effect of two-way wall action, the effect of shear and connections on wall failure, the reaction of walls through the collapse phase, and the effect of support stiffness for walls where arching occurs. In addition, information should be obtained on the collapse mechanism of walls to establish the primary collapse mode and to determine a realistic failure criterion for each wall type. The tests should provide information on the collapse mechanism at various pressure levels above the incipient collapse, and the test parameters should include various support conditions and vertical in-plane wall loads. Instrumentation should provide data on the loading, deflection, velocity, and reactive force versus time throughout the total range of wall response.

- Because of the importance of the net pressure for predicting the collapse of wall elements, it is recommended that air blast studies be made to establish more definitive load-time prediction techniques than are now available. Such studies should include at least two factors. First, the conventional air blast load schemes provide the average load-time relationship on the exterior surface of various geometric shapes. These procedures, although generally satisfactory for design purposes, are inadequate for describing the external load-time function needed to predict the collapse of various wall elements in a large multistory building. Therefore, a rational method is needed for determining the load-time function at any point of interest on the surface of a structure. Second, the net load on a wall with openings is influenced by the back face loading, which is a function of the wave propagation into the room and the subsequent pressure build-up resulting from room-filling. At the present time, techniques are available for predicting the average pressure build-up during the room-filling phase for limited geometries and for the lower overpressure levels. These methods should be extended to include other geometries of interest and the higher overpressures. In addition, techniques should be developed for estimating the loading on the interior wall surfaces as a result of the wave front propagation into the room.

# Appendix A

## ULTIMATE STRENGTH OF REINFORCED CONCRETE MEMBERS

## Appendix A

## ULTIMATE STRENGTH OF REINFORCED CONCRETE MEMBERS

### Introduction

To use the formulas presented in Section III to calculate the resistance function for a specific reinforced concrete wall, it is necessary to determine the ultimate moment of the section of interest. Although ultimate strength concepts for reinforced concrete are well-documented (e.g., Refs. 27-29), they are summarized in this appendix for convenience and also because there were several modifications made herein in the usual formulations for application to lightly reinforced concrete walls. The ultimate strength concept used in this study is based on the assumption that the concrete stress-strain relationship in the compression zone is parabolic in shape as shown on Figure A-1. Also, it is assumed that the strain distribution across a section in flexure is linear. The relationship among the various factors used in the following ultimate strength formulas are shown in Figure A-2 and A-3.

### Coefficients

The use of the ultimate strength equations developed for the assumed parabolic shape of the concrete stress-strain curve requires the determination of three coefficients and the ultimate concrete strain. As noted on Figure A-2, these coefficients are related to the magnitude and position of the internal compressive force in the concrete compression zone.

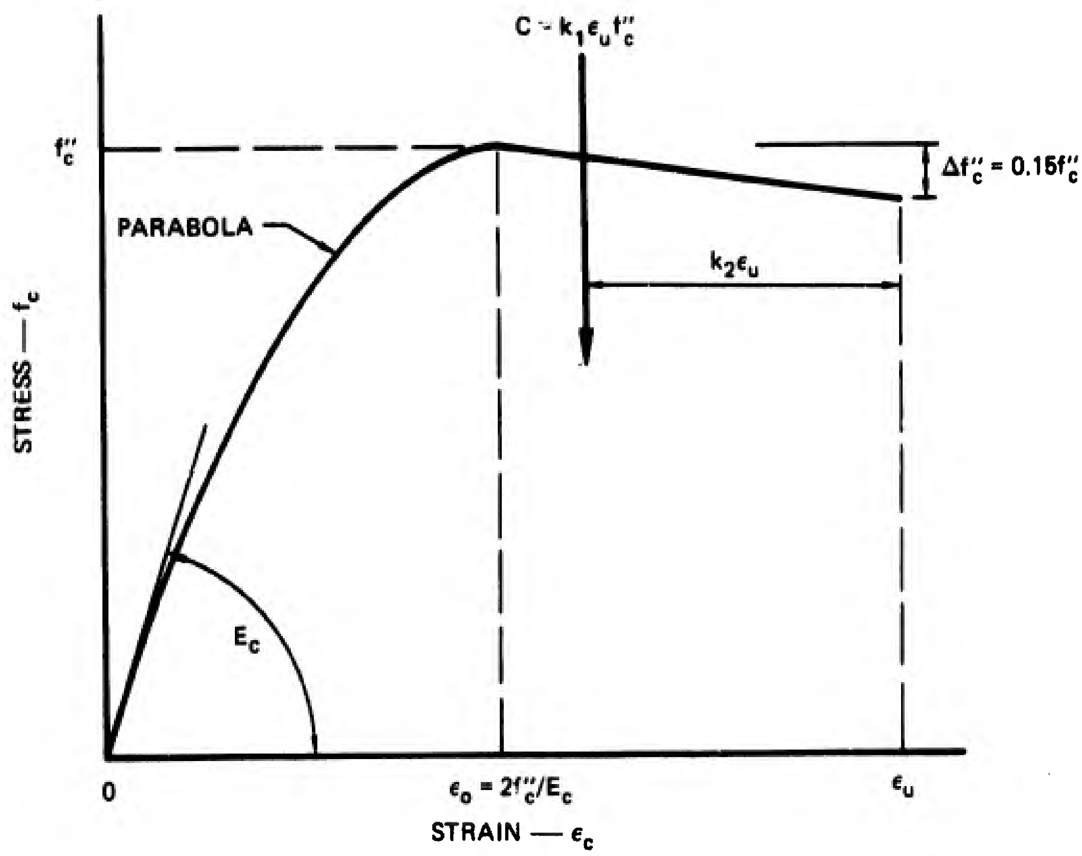


Source: Ref. 29

FIG. A-1 ASSUMED STRESS-STRAIN RELATIONSHIP FOR CONCRETE IN FLEXURE

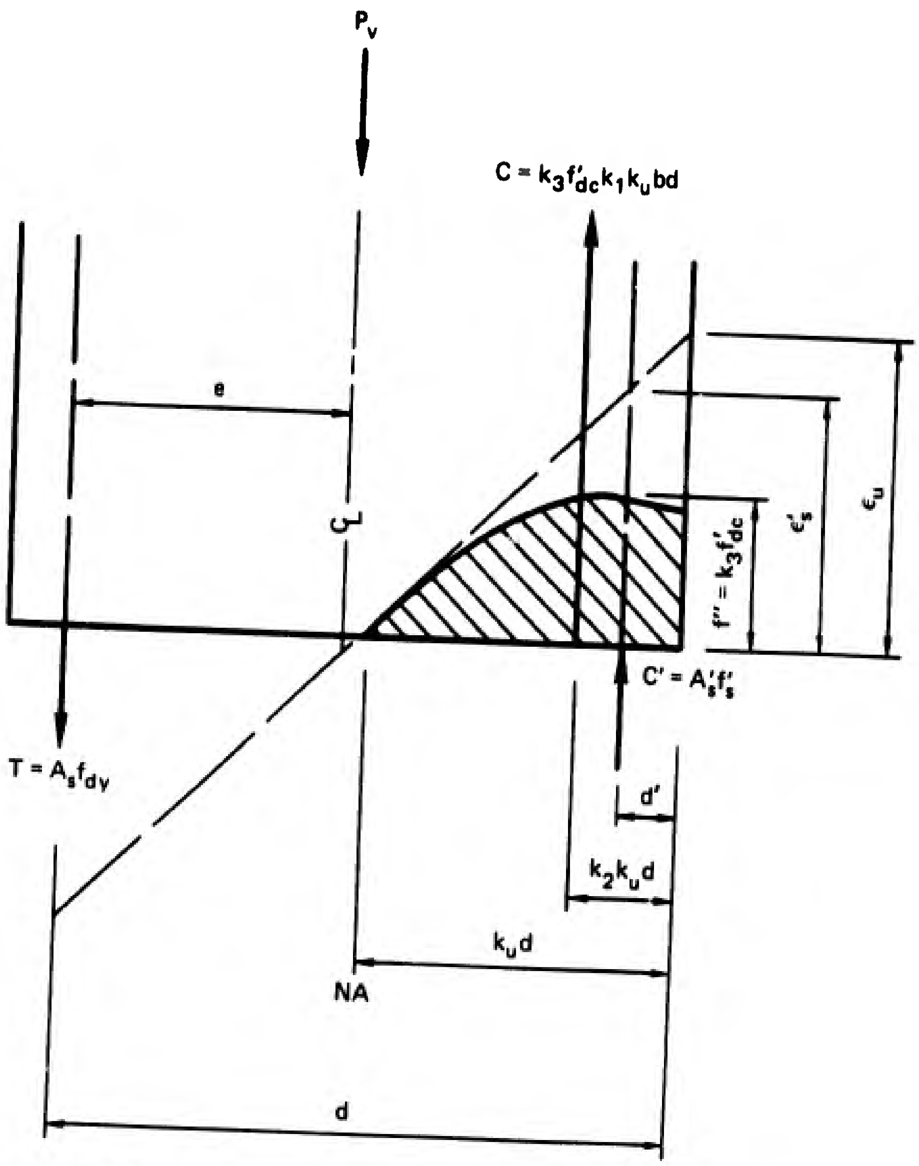


Source: Ref. 29

FIG. A-2 SECTION OF REINFORCED CONCRETE WALL USED IN ANALYSIS FOR $k_u d > d'$

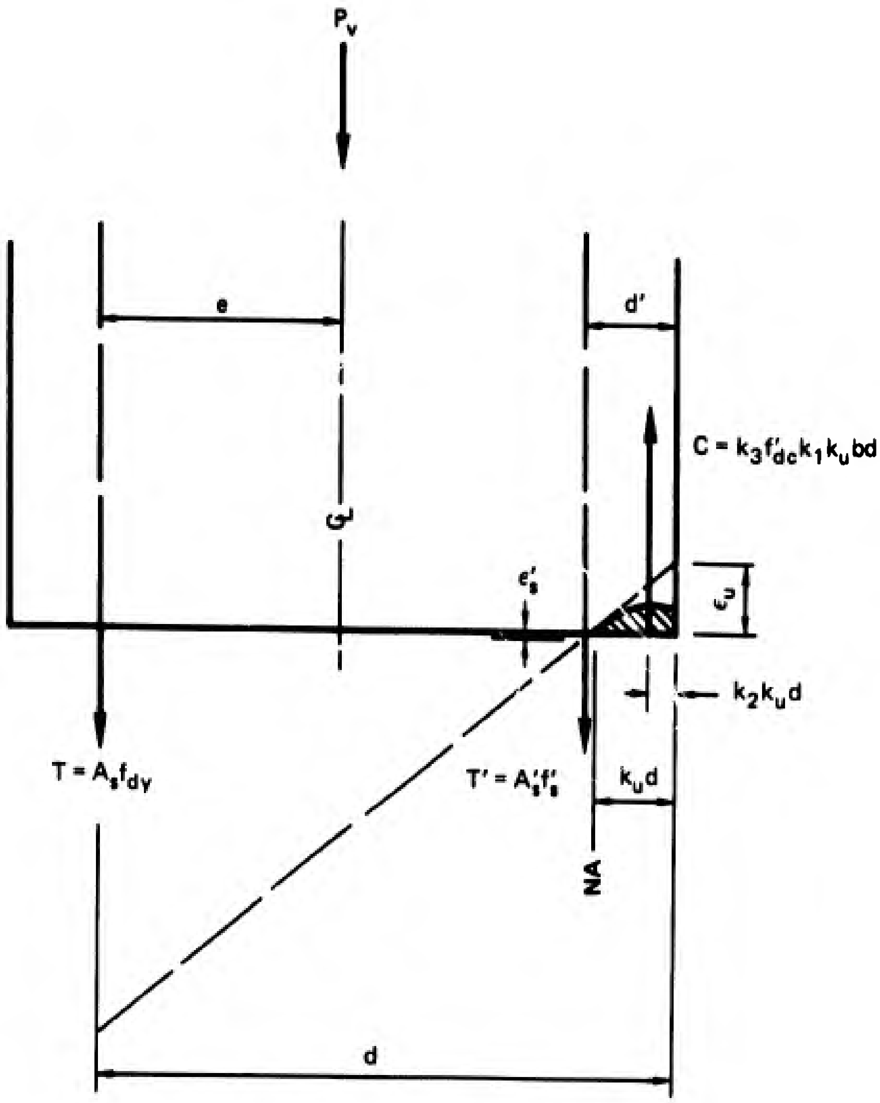


FIG. A-3 SECTION OF REINFORCED CONCRETE WALL USED IN ANALYSIS FOR $k_u d < d'$

The following relationship for the coefficients used in this study was obtained from the published experimental results in Ref. 28:

$$k_1 = 0.94 - \frac{f_c'}{26,000} \tag{A-1}$$

$$k_2 = 0.50 - \frac{f_c'}{80,000} \tag{A-2}$$

$$k_3 = \frac{3900 + 0.35\ f_c'}{3000 + 0.82\ f_c' - \frac{f_c'^2}{26,000}} \tag{A-3}$$

$$\epsilon_u = 0.004 - \frac{f_c'}{6.5 \times 10^6} \tag{A-4}$$

Rectangular Members (Simple Bending, Without Vertical Load)

Without Compressive Reinforcement

$$M_u = A_s\ f_{dy}\ d \left(1 - p\ \frac{k_2\ f_{dy}}{k_1 k_3\ f_{dc}'}\right) \tag{A-5}$$

With Compressive Reinforcement

For the usual ultimate strength equations for flexural members with compression reinforcement, it is assumed that the neutral axis is a greater distance from the compression face than the compressive reinforcement, as noted on Figure A-2 (Ref. 29). Since the steel reinforcement reaches its yield point at about one-third the ultimate strain of the concrete, it is also assumed that the stress in the compressive reinforcement, $f_s'$, is equal to the yield stress of the steel. In lightly reinforced concrete members, neither the assumed location of the neutral axis nor the magnitude and direction of the stress in the compression steel is necessarily correct. Therefore, in a subsection following the ultimate strength equations, a method is presented for determining the location of the netural axis in a lightly reinforced wall. Once the neutral axis location is known, the magnitude and direction of the stress in the compressive reinforcement can be determined:

$\underline{k_u d > d'}$

$$M_u = \left[A_s f_{dy} - A_s'\left(f_s' - k_3 f_{dc}'\right)\right] d \left[1 - \frac{k_2}{k_3 f_{dc}' k_1}\left(p\, f_{dy} - p'\left(f_s' - k_3 f_{dc}'\right)\right)\right]$$

$$+ A_s'\left(f_s' - k_3 f_{dc}'\right)\left(d - d'\right) \qquad \text{(A-6)}$$

where $f_s'$ is determined by Eq. A-20

$\underline{k_u d < d'}$

$$M_u = \left(A_s f_{dy} + A_s' f_s'\right) d \left[1 - \frac{k_2}{k_1 k_3 f_{dc}'}\left(p f_{dy} + p' f_s'\right)\right]$$

$$- A_s' f_s' \left(d - d'\right) \qquad \text{(A-7)}$$

where $f_s'$ is determined by Eq. A-16.

### Rectangular Members (Combined Bending and Vertical Load)

#### Without Compressive Reinforcement

$$M_u = \left(P_v + A_s\ f_{dy}\right)\left[d - k_2\left(\frac{P_v + A_s\ f_{dy}}{k_3\ f'_{dc}\ k_1\ b}\right)\right] \quad \text{(A-8)}$$

#### With Compressive Reinforcement

$k_u d > d'$

$$M_u = \left[P_v + A_s\ f'_{dy} - A'_s\left(f'_s - k_3\ f'_{dc}\right)\right]\left[d - k_2\left(\frac{P_v + A_s f_{dy} - A'_s(f'_s - k_3 f'_{dc})}{k_3\ f'_{dc}\ k_1\ b}\right)\right]$$

$$+ A'_s\ (f'_s - k_3\ f'_{dc})\ (d - d') \quad \text{(A-9)}$$

where $f'_s$ is determined by Eq. A-25

$k_u d < d'$

$$M_u = \left(P_v + A_s f_{dy} + A'_s f'_s\right)\left[d - k_2\left(\frac{P_v + A_s\ f_{dy} + A'_s\ f'_s}{k_3\ f'_{dc}\ k_1\ b}\right)\right]$$

$$- A'_s\ f'_s\ (d - d') \quad \text{(A-10)}$$

where $f'_s$ is determined by Eq. A-23.

### Determination of Neutral Axis

In general, the neutral axis for doubly reinforced concrete members designed by ultimate strength concepts will be located between the tension and compressive steel. However, for lightly reinforced concrete members such as walls the concrete compression zone at ultimate strength may not intersect the reinforcing steel, as noted on Figure A-2, when the wall is subjected to a lateral load. For such cases, the compression steel is actually in tension when the ultimate strength of the section is developed, rather than in compression as usually assumed. Therefore, the prediction of the resistance of laterally loaded wall members must include an examination of the location of the neutral axis before the equilibrium equations can be established. In addition, once the direction of the stress in the compressive steel is established, it is necessary to determine its magnitude. For this study the following procedure was used.

Rectangular Member with Tension and Compression Steel (Without Vertical Load)

Calculate the maximum concrete compressive force, which can be obtained by assuming that the tension steel is at yield and that the compressive steel has zero stress, i.e., $k_u d = d'$,

$$T = A_s f_{dy} \quad . \tag{A-11}$$

Using the ultimate strength concepts, as presented in Refs. 27-29, the maximum potential compressive force available is calculated for a concrete stress block that does not extend beyond the compressive reinforcement, i.e., with the neutral axis located at the centerline of the compressive reinforcement. From Figure A-2.

$$C = k_3 f'_{dc} k_1 k_u db$$

or for $k_u d = d'$

$$C_m = k_3 f'_{dc} k_1 bd' \tag{A-12}$$

<u>If $C_m > T$</u>. For this case, $k_u d < d'$, and $k_u d$ can be determined in the following manner. From the equilibrium of forces on the section shown on Figure A-3,

$$k_u d = \frac{A_s f_{dy} + A'_s f'_s}{k_3 f'_{dc} k_1 b} . \tag{A-13}$$

By assuming a linear distribution of strain across the section

$$k_u d = \frac{\epsilon_c}{\epsilon'_s} (d' - k_u d) . \tag{A-14}$$

By factoring and substitution of $\epsilon'_s = \frac{f'_s}{E_s}$

$$k_u d = \frac{d' E_s \epsilon_c}{E_s \epsilon_c + f'_s} . \tag{A-15}$$

By equating Eqs. A-13 and A-15, rearranging terms, and factoring, it can be shown that

$$f'_s = -\frac{1}{2}\left(E_s \epsilon_c + \frac{A_s}{A'_s} f_{dy}\right)$$
$$+ \frac{1}{2}\sqrt{\left(E_s \epsilon_c + \frac{A_s}{A'_s} f_{dy}\right)^2 - \frac{4 E_s \epsilon_c}{A'_s}\left(A_s f_{dy} - d' k_3 f'_{dc} k_1 b\right)} \tag{A-16}$$

where the maximum $f'_s = f'_{dy}$ .

If $C_m < T$. For this case, $k_u d > d'$ (Figure A-3) and from Ref. 27

$$k_u d = \frac{A_s f_{dy} - A_s' \left(f_s' - k_3 f_{dc}'\right)}{k_3 f_{dc}' k_1 b} \quad . \qquad \text{(A-17)}$$

By assuming a linear distribution of strain across the section

$$k_u d = \frac{\epsilon_c}{\epsilon_s} (k_u d - d') \quad . \qquad \text{(A-18)}$$

By factoring and substitution of $\epsilon_s' = \dfrac{f_s'}{E_s}$

$$k_u d = \frac{d' E_s \epsilon_c}{E_s \epsilon_c - f_s'} \quad . \qquad \text{(A-19)}$$

By equating Eqs. A-17 and A-19, rearranging terms, and factoring, it can be shown that

$$f_s' = \frac{1}{2} \left( E_s \epsilon_c + \frac{A_s}{A_s'} f_{dy} + k_3 f_{dc}' \right)$$

(A-20)

$$- \frac{1}{2} \sqrt{\left( E_s \epsilon_c + \frac{A_s}{A_s'} f_{dy} + k_3 f_{dc}' \right)^2 - \frac{4 E_s \epsilon_c}{A_s'} \left( A_s f_{dy} + A_s' k_3 f_{dc}' - d' k_3 f_{dc}' k_1 b \right)}$$

where the maximum $f_s' = f_{dy}'$.

Rectangular Member with Tension and Compression Steel (With Vertical Load)

Calculate the maximum concrete compressive force, which can be obtained by assuming that the tension steel has yielded and that the compressive steel has zero stress, i.e., $k_u d = d'$,

$$T_p = A_s f_{dy} + P_v \quad . \tag{A-21}$$

The maximum potential compressive force available is calculated for a concrete stress block with the neutral axis located at the centerline of the compressive steel and the concrete strain equal to its ultimate value; the force is given by Eq. A-12.

If $C_m > T_p$. For this case, $k_u d < d'$ and $k_u d$ can be determined by considering the equilibrium of forces on the section shown on Figure A-2

$$k_u d = \frac{P_v + A_s f_{dy} + A_s' f_s'}{k_3 f_{dc}' k_1 b} \quad . \tag{A-22}$$

By the same manner as previously, it can be shown that by equating Eqs. A-15 and A-22

$$f_s' = -\frac{1}{2}\left(\frac{P_v}{A_s'} + \frac{A_s}{A_s'} f_{dy} + E_s \epsilon_c\right)$$

$$+ \frac{1}{2}\sqrt{\left(\frac{P_v}{A_s'} + \frac{A_s}{A_s'} f_{dy} + E_s \epsilon_c\right)^2 - \frac{4 E_s \epsilon_c}{A_s'}\left(P_v + A_s f_{dy} - k_3 f_{dc}' k_1 b d'\right)} \tag{A-23}$$

where the maximum $f_s' = f_{dy}'$.

If $C_m < T_p$. For this case, $k_u d > d'$, and from the equilibrium of forces on the section shown on Figure A-3

$$k_u d = \frac{P_v + A_s f_{dy} - A_s' (f_s' - k_3 f_{dc}')}{k_3 f_{dc}' k_1 b} \quad . \qquad \text{(A-24)}$$

By the same manner as previously, it can be shown that by equating Eqs. A-19 and A-24,

$$f_s' = \frac{1}{2}\left(\frac{P_v}{A_s'} + \frac{A_s}{A_s'} f_{dy} + E_s \epsilon_c + k_3 f_{dc}'\right)$$

$$- \frac{1}{2}\sqrt{\left(\frac{P_v}{A_s'} + \frac{A_s}{A_s'} f_{dy} + E_s \epsilon_c + k_3 f_{dc}'\right)^2 - \frac{4E_s \epsilon_c}{A_s'}\left(P_v + A_s f_{dy} + A_s' k_3 f_{dc}' - d' k_3 f_{dc}' k_1 b\right)} \qquad \text{(A-25)}$$

where the maximum $f_s' = f_{dy}'$.

# Appendix B

## FAILURE OF LIGHTLY REINFORCED MEMBERS DUE TO CRUSHING OF THE CONCRETE

BLANK PAGE

## Appendix B

### FAILURE OF LIGHTLY REINFORCED MEMBERS DUE TO CRUSHING OF THE CONCRETE

As discussed in Section III on failure, or collapse, criteria of lightly reinforced concrete members, there is almost no test information available on which to base such criteria. Thus, as stated, the establishment of failure criteria must be considered to be rather arbitrary, and based more on judgment than on fact. In addition to the three criteria presented in Section III, one other criterion was considered as a possible failure mode. This was failure of the wall resulting from crushing of the concrete in the compression zone of a bending wall element. This crushing is not the same as that which occurs in overreinforced beams before yielding of the reinforcement steel, but is rather a "secondary compression failure" that occurs after yielding of the steel. It results from a shift of the neutral axis toward the compressive surface with increasing elongation of the reinforcement, causing the strains in the remaining compression zone to increase beyond the strain corresponding to the ultimate of the concrete and crushing occurs. It is not known whether this crushing results in actual collapse of the member. This doubt exists since the reinforcing steel still is intact, and without an actual separation of the steel, collapse would probably not occur. However, it is possible that crushing of the concrete in lightly reinforced members could result in the entire load being transferred instantaneously to the steel. This could lead to a large reduction in the resistance and could result in a rapid elongation of the reinforcement, followed by collapse of the wall. If this occurred, the crushing of the concrete could be considered as the primary failure mechanism. Another possibility is that as crushing occurs, the area of concrete in compression may increase due to redistribution of the compressive stress and may result in little or no change in the load resistance of the wall. Because of this lack of knowledge of the actual nature of the concrete crushing during the failure process, it was not included as a collapse criterion.

It was believed worthwhile, however, to examine the failure of lightly reinforced walls due to concrete crushing, in the event that failure studies indicate that such behavior may actually be the case. As presented in Section III, it was assumed that after the initial tensile cracking of the concrete at the section of maximum moment, the wall rotates around the supports and the cracked section as two rigid bodies. Crushing of the concrete may be assumed to occur when the extreme concrete fiber strain reaches some limiting value, $\epsilon_u$. This may be related to the wall properties through the moment-curvature (M-$\phi$) relationship of the cross section (Ref. 30). The deflection at which this occurs may be determined by summing up the curvatures of the individual cross sections through use of a method such as the moment-area method.

For members with conventional percentages of reinforcement, this requires determining the entire moment-curvature relationship since the curvature, which is equal to the applied moment divided by the member stiffness, EI, varies throughout the length of the member. However, for the rigid body behavior assumed for lightly reinforced walls, this procedure is simplified since all the curvature is now taken as concentrated at the center. Thus, only the curvature corresponding to the ultimate concrete strain, $\epsilon_u$, and the length over which this curvature acts need be considered.

The curvature may be determined by computing the angle between the line representing the strain distribution, taken as linear across the section, and the zero strain line, as shown in Figure B-1. The curvature, $\phi_u$, in radius corresponding to the ultimate concrete strain is approximately equal to

$$\phi_u = \frac{\epsilon_u}{k_u d} \tag{B-1}$$

where $k_u d$ is the distance to the neutral axis and may be determined from the ultimate strength equations given in Appendix A.

The distance over which this curvature acts is taken to be the same as that assumed for the limiting steel strain criterion, i.e., a length, $\ell$, sufficient to develop the ultimate tensile strength of the reinforcing steel in bond

$$\ell = \frac{A_s f_u}{U_u'} \tag{B-2}$$

where $A_s$ is the cross-sectional area of the reinforcing bar under consideration and $U_u'$ is given in Ref. 13 by

$$U_u' = 30 \sqrt{f_c'} \ . \tag{B-3}$$

The deflection can then be obtained by taking the moment of the $\phi$ - diagram, assumed to be a constant value of $\phi_u$ over the length and zero elsewhere, about the end for the half-length of the member, as shown in Figure B-2. This results in the following equation for the failure deflection

$$y_f = \frac{\ell \phi_u}{2} (L - \ell) \ . \tag{B-4}$$

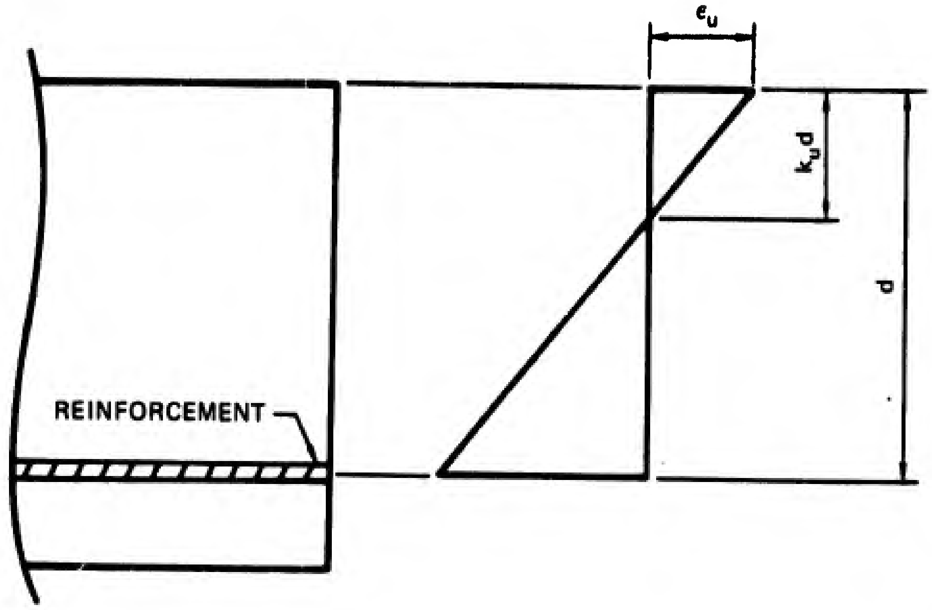


FIG. B-1 STRAIN DISTRIBUTION ON WALL CROSS SECTION

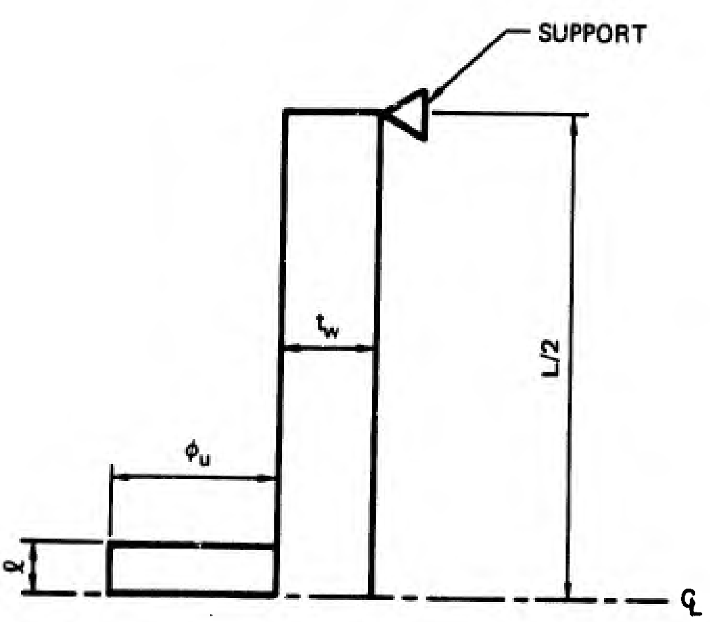


FIG. B-2 $\phi$-LOADING ON HALF-SPAN OF WALL

There is some question as to a realistic value of the strain at which crushing of the concrete sufficient to cause collapse may occur. Some argument may be presented that this crushing of the concrete corresponds to the ultimate concrete strain used in ultimate strength design of approximately $\epsilon_u = 0.0038$ (Ref. 28), since final collapse of compression test specimens often takes place shortly after the maximum stress is reached. It has been recognized, however, that an ultimate strain can be developed that is greater than the above value, since it has been shown that sudden failures observed in compression tests are related to the release of energy stored in the testing machines. This in turn may be challenged by the argument that a plain concrete specimen that has been strained beyond the maximum compressive load is generally cracked and therefore useless for load-carrying purposes. If the strain is limited to the value corresponding to the ultimate moment, one would thereby eliminate the descending branch of the stress-strain curve beyond $\epsilon_u$. If this branch were actually caused by irreversible microcracking as argued, this may be a desirable measure. It can thus be seen that the problem of establishing a failure criterion due to the crushing of the concrete is made even more complicated by having to choose a value for the ultimate concrete strain.

This criterion based on the crushing of the concrete in lightly reinforced concrete walls may perhaps be best illustrated through an example. The predicted failure deflection will be calculated for a simply supported wall having the following properties:

| | |
|---|---|
| $L = 96$ in. | $t_w = 8$ in. |
| $p = 0.0026$ (No. 3 @ 6) | $d = 7$ in. |
| $p' = 0$ | $d' = 0$ |
| $f'_{dc} = 3750$ psi | $E_c = 3 \times 10^6$ psi |
| $f_{dy} = 42{,}000$ psi | $E_s = 30 \times 10^6$ psi |
| $P_v = 0$ | |

Using $f'_c = f'_{dc}$, the ultimate bond strength is found from Eq. B-3 to be

$$U'_u = 1837 \text{ lb/in.}$$

For the case using No. 3 reinforcing bars ($A_s = 0.11$ sq. in.) and the conservative value of $f_u = f_{dy}$, the length required to develop the ultimate strength in bond is calculated from Eq. B-2 as

$$\ell = 2.51 \text{ in.}$$

The distance to the neutral axis, $k_u d$, for the case of no compression steel can be determined from the following equation (Ref. 29)

$$k_u d = \frac{A_s f_u}{k_1 f'_{dc} k_3 b} .$$

In this example, $A_s$ is the area of the tension steel corresponding to the width b = 6 in. Values for $k_1$ and $k_3$ were determined from Eqs. A-1 and A-3 to be equal to 0.796 and 0.942, respectively. This results in a value of

$$k_u d = 0.27 \text{ in.}$$

Using a value of $\epsilon_u = 0.0038$ and substituting this along with the above values for $\ell$ and $k_u d$ into Eqs. B-1 and B-4, the following results are obtained

$$\phi_u = 0.0141 \text{ radians}$$

and

$$y_f = 1.65 \text{ in.}$$

However, if a value of $\epsilon_u = 0.008$ (Ref. 14) is used instead, these values become

$$\phi_u = 0.0296 \text{ radians}$$

and

$$y_f = 3.47 \text{ in.}$$

It can be seen that the collapse deflection, as determined by the above method, is highly dependent on the values of the concrete strain, $\epsilon_u$, at which collapse is assumed to occur.

These values can be compared with the collapse deflections for the same wall, as determined by the three failure criteria given in Section III.

1. Limiting steel strain criterion (failure elongation of 20%): $y_f = 6.96$ in.
2. Instability criterion: Not applicable, since $P_v = 0$
3. Ductility criterion: $y_f = 6.12$ in.

As can be seen, the collapse deflection predicted by the crushing of the concrete is considerably less than that predicted by the other failure criteria, even for the case where the concrete strain at crushing was assumed to be twice the usual value. Because of this rather large discrepancy in values and the uncertainty as to whether crushing of the concrete results in an immediate reduction of the load resistance and collapse of the wall, this criterion was not included among those used in this study for predicting wall collapse.

## Appendix C

## ARCHING OF MASONRY WALLS

## Appendix C

## ARCHING OF MASONRY WALLS

### Introduction

Masonry walls, under conditions where they are constrained between essentially rigid supports, have been observed to have greater resistance to lateral loads than would be predicted by conventional bending analysis. It therefore seems logical to compute the behavior of a panel on the basis of edge restraint, compressive strength, and geometry of deflection rather than the flexural properties. This approach is the basis for the so-called arching action theory (Ref. 22).

### Resistance Function: Rigid Supports

Various approaches based on different assumptions have been followed in previous developments of this theory, e.g., Refs. 22, 23, 33. The assumed mode of response is the same in all cases, however, and may be described as follows. The wall is idealized as a beam of solid, uniform, rectangular cross section constrained between rigid supports on two opposite edges. The masonry material is assumed to have no tensile strength. Therefore, immediately on loading, cracks develop on the tension side and extend to the centerline. During subsequent motion, each half of the beam is assumed to remain rigid and rotate about its end support and the center. This rotation is resisted by a force couple developed as a result of the two halves being wedged between the rigid supports, thus causing crushing at the ends and center. This rotation continues until either the load is removed or the resisting couple vanishes, in which case the wall collapses. This assumed behavior is illustrated in Figure C-1.

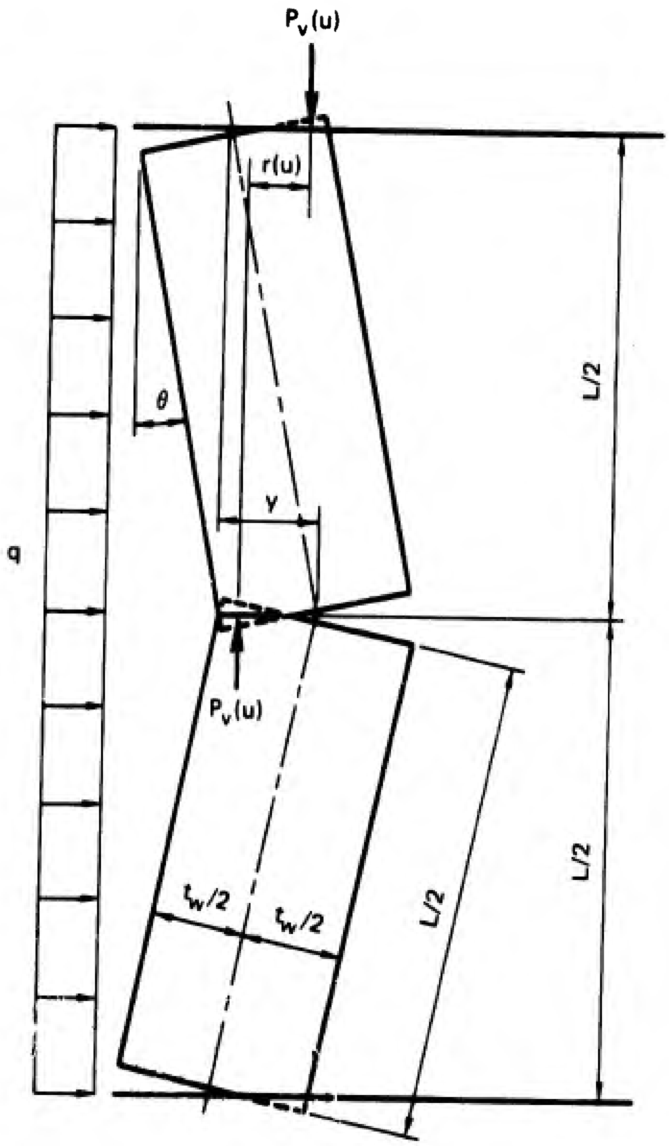


FIG. C-1 SCHEMATIC REPRESENTATION OF ARCHING ACTION

The magnitude of the resisting couple is seen to depend on the magnitude of the compressive forces developed at the ends and center and on the moment arm between these forces. Both these values, in turn, depend on the stress-strain properties of the masonry material. Various assumptions have been made for these stress-strain properties. The most accurate of these is probably that of elastic-plastic behavior.

### Elastic-Plastic Stress-Strain Relationship

This method was originally presented in Ref. 22. Further developments were given in Refs. 31 and 32.

Expressions for the strain along the contact area at the ends and center of the beam are developed in terms of the midspan deflection of the centerline. The geometry at the contact area is shown in detail in Figure C-2. Each half of the wall rotates about the inner edge of the wall at the support. Equilibrium requires that the contact areas at the ends and center be equal. As the center deflection increases, this contact area decreases. This decrease can be determined by considering compatibility of vertical dimensions,

$$\frac{L}{2} + 2z \tan \theta = \frac{L}{2} \sec \theta$$

or

$$z = \frac{L}{4} \times \frac{(\sec \theta - 1)}{\tan \theta} = \frac{L}{4} \times \frac{(1 - \cos \theta)}{\sin \theta} = \frac{L}{4} \tan \frac{\theta}{2} \quad . \qquad \text{(C-1)}$$

The center deflection is related to the angle of rotation by

$$y = \left( \frac{L}{2} - z \sin \theta \right) \tan \theta \quad .$$

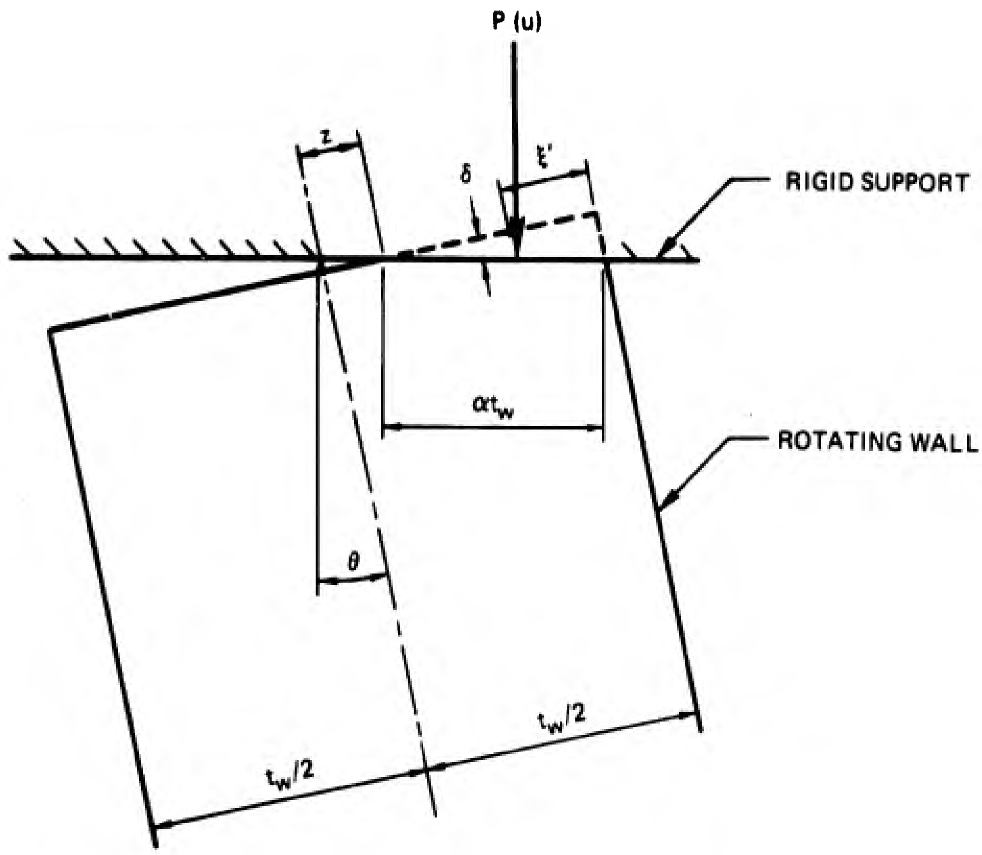


FIG. C-2 CONDITIONS AT WALL SUPPORT

Substituting "z" from Eq. C-1, gives

$$y = \left[\frac{L}{2} - \left(\frac{L}{4} \times \frac{1 - \cos\theta}{\sin\theta}\right) \sin\theta\right] \tan\theta$$

$$= \frac{L}{2} \tan\theta \left[1 - \frac{1}{2}(1 - \cos\theta)\right] .$$

For small values of θ,

$$\cos\theta \approx 1 \text{ and } \tan\theta \approx 2 \tan\theta/2.$$

Then, by substitution

$$y \approx \frac{L}{2} \times 2 \tan\frac{\theta}{2} \left[1 - \frac{1}{2}(1 - 1)\right] \approx L \tan\frac{\theta}{2} . \quad \text{(C-2)}$$

Using Eqs. C-1 and C-2 gives the relationship

$$z \approx \frac{y}{4} . \quad \text{(C-3)}$$

The contact width is now given by

$$\alpha t_w = \left(\frac{t_w}{2} - z\right) \sec\theta . \quad \text{(C-4)}$$

The shortening of a vertical fiber a distance ξ from the edge is given by

$$\delta = (\alpha t_w \cos\theta - \xi) \tan\theta = \left(\frac{t_w}{2} - z - \xi\right) \tan\theta . \quad \text{(C-5)}$$

The average strain along a fiber of the beam at distance ξ from the surface can be defined as

$$\epsilon_{avg} = \frac{\delta}{L/2} . \quad \text{(C-6)}$$

As seen in Figure C-1, each fiber of the half span is unstressed at one end. Assuming the variation of strain along the fiber to be linear, the strain at the stressed end is then

$$\epsilon = 2\,\epsilon_{avg} = \frac{4\,\delta}{L} \quad . \qquad \text{(C-7)}$$

Substituting for $\delta$ from Eq. C-5 gives

$$\epsilon = \frac{4}{L}\left(\frac{t_w}{2} - z - \xi\right)\tan\theta \quad . \qquad \text{(C-8)}$$

Again using the approximation, $\tan\theta \approx 2\tan\theta/2$, and substituting for this value from Eq. C-2 gives

$$\epsilon = \frac{4}{L}\left(\frac{t_w}{2} - z - \xi\right)\frac{2y}{L} = \frac{8y}{L^2}\left(\frac{t_w}{2} - z - \xi\right) . \qquad \text{(C-9)}$$

At this point, it is convenient to introduce a nondimensional center deflection, u, equal to $y/t_w$. Using this term and Eq. C-3, Eq. C-9 can be rewritten in the nondimensional form,

$$\epsilon = \frac{8y}{L^2} \times \frac{t_w}{2} \times \frac{t_w}{t_w}\left(1 - \frac{2z}{t_w} - \frac{2\xi}{t_w}\right) = \frac{4t_w^2}{L^2}\,\frac{y}{t_w}\left(1 - \frac{2}{t_w}\,\frac{y}{4} - \frac{2\xi}{t_w}\right)$$

$$\epsilon = \frac{4t_w^2}{L^2}\,u\left(1 - \frac{u}{2} - \frac{2\xi}{t_w}\right) . \qquad \text{(C-10)}$$

To determine the resisting forces and moments from this distribution of strain along the contact area, it is necessary to look in more detail at the stress-strain relationship of the masonry material.

In addition to the previously stated assumption of inability of the material to withstand tensile stress, the following compressive properties are assumed:

1. Stress-strain curve is elastic up to a limiting stress, $f'_m$ (and corresponding strain $\epsilon_y$).

2. At strains greater than $\epsilon_y$, the stress remains constant at $f'_m$.

3. Material exhibits no strength recovery beyond the elastic range.

This is essentially the classical elastic-plastic relationship, with the plastic strength corresponding to the crushing strength of the masonry material. However, it has a modified property in that once the crushing strength is exceeded and the strain decreases, the stress drops instantly to zero.

Thus the state of stress along the contact area initially increases linearly with the midspan deflection. At some point, the stress reaches the crushing strength and remains constant with increasing strain. With still greater deflections, the strain begins to decrease at certain points resulting from the continual decrease in the contact area, whereupon if the crushing strength has been reached, the stress instantly vanishes. This behavior results in a compressive force at the contact area that increases nearly linearly to a maximum value and then gradually decreases to zero. This is illustrated in Figure C-3, where the arching force per unit width, $P_v(u)$, is plotted in terms of the nondimensional parameters u and $8\, P_v(u)/f'_m\, t_w$.

Curves are shown on the figure for several values of the nondimensional variable, R, where

$$R = \frac{\epsilon_y L^2}{4t_w^2} \quad . \qquad \text{(C-11)}$$

The analytical expressions involving $P_v(u)$ are given in Figure C-4.

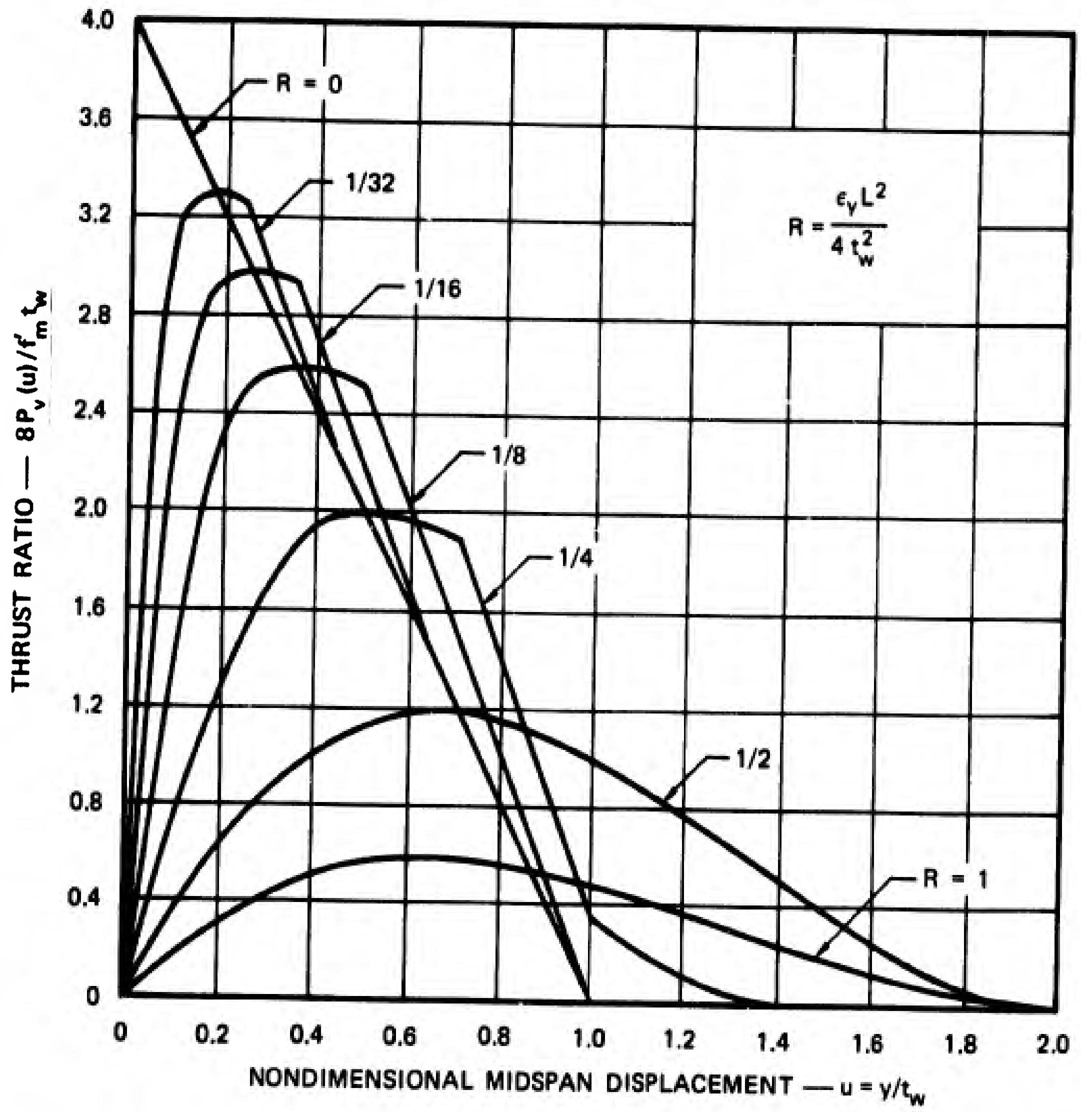


Source: Ref. 22

FIG. C-3 VARIATION OF THRUST FORCE WITH WALL DEFLECTION

| Range of R | Range of u | Stress Distribution Along Contact Area | $\frac{8\,P_v(u)}{f'_m\,t_w}$ | $\frac{16\,M(u)}{f'_m\,t_w^2}$ |
|---|---|---|---|---|
| $R \geqq 1/2$<br>$R < 1/2$ | $u \geqq 0$<br>$0 \leqq u \leqq 1-\sqrt{1-2R}$ | 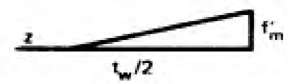  | $\frac{2u}{R}\left(1-\frac{u}{2}\right)^2$ | $\frac{8u}{3R}\left(1-\frac{5u}{4}\right)\left(1-\frac{u}{2}\right)^2$ |
| $R < 1/2$ | $1-\sqrt{1-2R} \leqq u < \sqrt{2R}$ |  | $4\left(1-\frac{u}{2}-\frac{R}{2u}\right)$ | $4\left(1+\frac{R}{2}+\frac{3u^2}{4}-2u-\frac{R^2}{3u^2}\right)$ |
| $1/8 \leq R < 1/2$ | $\sqrt{2R} \leqq u < 1$ | 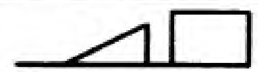 | $4(1-u)+\frac{u}{2R}\,(2\sqrt{2R}-u)^2$ | $4(1-u)^2-\frac{u}{6R}\,(2\sqrt{2R}-u)^2(5u-4\sqrt{2R})$ |
| | $1 \leqq u < 2\sqrt{2R}$ |  | $\frac{u}{2R}\,(2\sqrt{2R}-u)^2$ | $\frac{u}{6R}\,(2\sqrt{2R}-u)^2(5u-4\sqrt{2R})$ |
| | $u \geqq 2\sqrt{2R}$ |  | 0 | 0 |
| $R < 1/8$ | $\sqrt{2R} \leqq u < 2\sqrt{2R}$ | 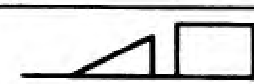 | $4(1-u)+\frac{u}{2R}\,(2\sqrt{2R}-u)^2$ | $4(1-u)^2-\frac{u}{6R}\,(2\sqrt{2R}-u)^2(5u-4\sqrt{2R})$ |
| | $2\sqrt{2R} \leqq u < 1$ | 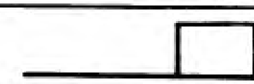 | $4(1-u)$ | $4(1-u)^2$ |
| | $u \geqq 1$ |  | 0 | 0 |

Source: Ref. 22

FIG. C-4 ANALYTIC FORMS FOR THRUST FORCE, $P_v(u)$, AND MOMENT, $M(u)$

The moment resistance, $M(u)$, is now given by

$$M(u) = r(u) \times P_v(u) \tag{C-12}$$

where $r(u)$ is the moment arm shown in Figure C-1.

From the geometry

$$r(u) = 2 \left(\frac{t_w}{2} - \xi'\right) \sec\theta - y$$

where $\xi'$ locates the centroid of the stress distribution along the contact area as shown in Figure C-2. Using the approximation for small values of $\theta$, $\sec\theta \approx 1$, gives

$$r(u) = t_w \left(1 - \frac{2\xi'}{t_w} - \frac{2y}{t_w}\right) = t_w \left(1 - \frac{2\xi'}{t_w} - u\right) \quad . \tag{C-13}$$

The moment resistance, $M(u)$, is plotted in Figure C-5 in terms of the nondimensional parameters u and $16M(u)/f'_m t_w^2$ again for several values of R. The analytical expressions are also given in Figure C-4.

These moment resistance curves can be converted directly to load-deflection curves once the distribution of the lateral load is specified. For a uniform load per unit length, q, the load-deflection curve is obtained from the moment equation

$$\frac{qL^2}{2} = M(u) \quad .$$

Rewriting Eq. C-10 in terms of the nondimensional parameter R, gives

$$\frac{R\epsilon}{\epsilon_y} = u\left(1 - \frac{2\xi'}{t_w} - \frac{u}{2}\right). \tag{C-14}$$

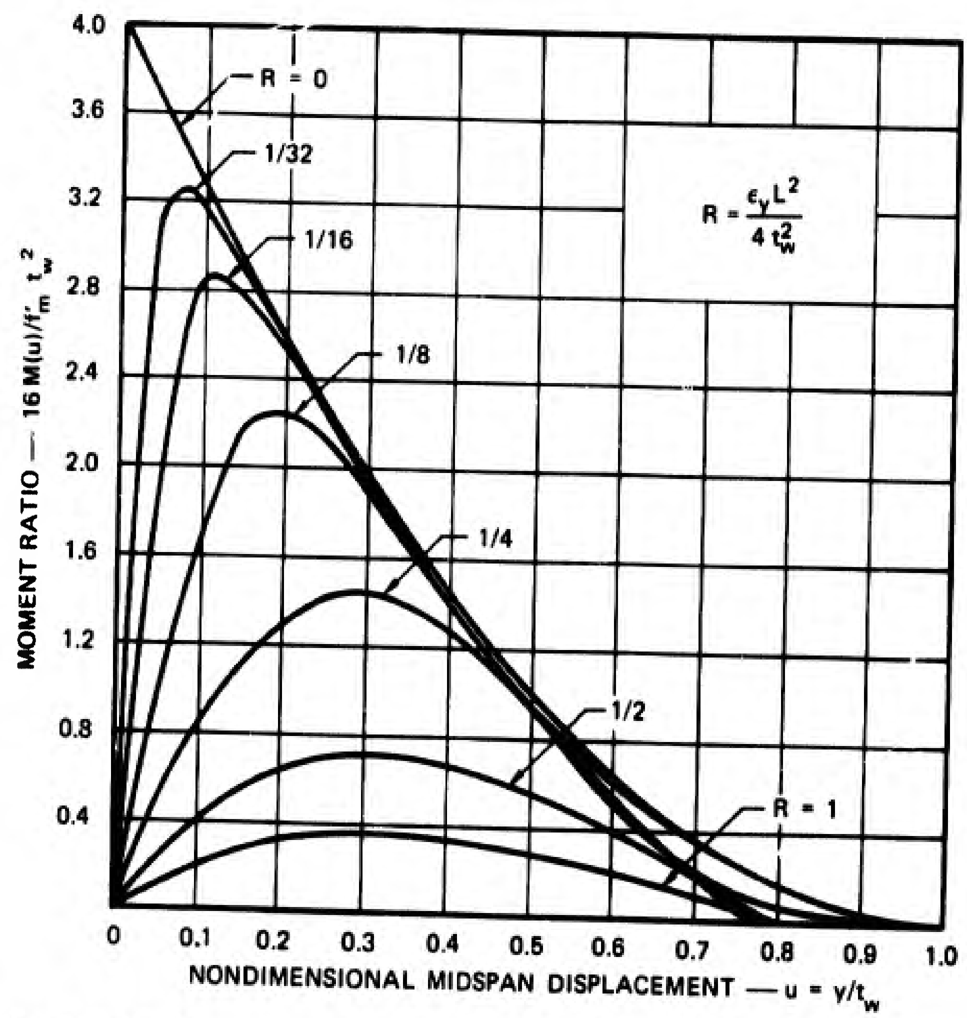


Source: Ref. 22

FIG. C-5 VARIATION OF MOMENT WITH WALL DEFLECTION

From this, it may be noted the $R > 1/2$ corresponds to the elastic state of stress throughout the deflection history since then $\epsilon < \epsilon_y$. Similarly, $R = 0$ corresponds to the plastic state of stress throughout the deflection history.

The rigid-plastic state of stress, $R = 0$, while hardly ever found in practice, presents a much simpler expression for the resisting moment, since it is not necessary to be concerned with the various possible stress distributions. Also the relation between the average strain and the strain at the contact surface need not be known. Moreover, if only the zone of complete failure is of interest, the differences between the rigid-plastic and elastic-plastic assumptions are minor.

The rigid-plastic assumption was developed in a slightly different manner in Ref. 33. This is shown as follows.

<u>Rigid-Plastic Stress-Strain Relationship</u>

Considering only small values of $\theta$ and using the approximations $\tan\theta \approx \sin\theta \approx \theta$ amd $\sec\theta \approx \cos\theta \approx 1$, one obtains from Eqs. C-1 and C-4

$$z = \frac{L\theta}{8} \tag{C-1a}$$

and

$$\alpha t_w = \frac{t_w}{2} - z = \frac{t_w}{2} - \frac{L\theta}{8} . \tag{C-4a}$$

With the rigid-plastic assumption, the width of the stress block, the magnitude of $P(\theta)$ can be computed from the geometry of the deformed panel, as shown in Figure C-6. Again using the approximations for small values of $\theta$, Eq. C-5 yields

$$\delta = (\alpha t_w - \xi)\,\theta = \left(\frac{t_w}{2} - \xi\right)\theta - \frac{L\theta^2}{8} . \tag{C-5a}$$

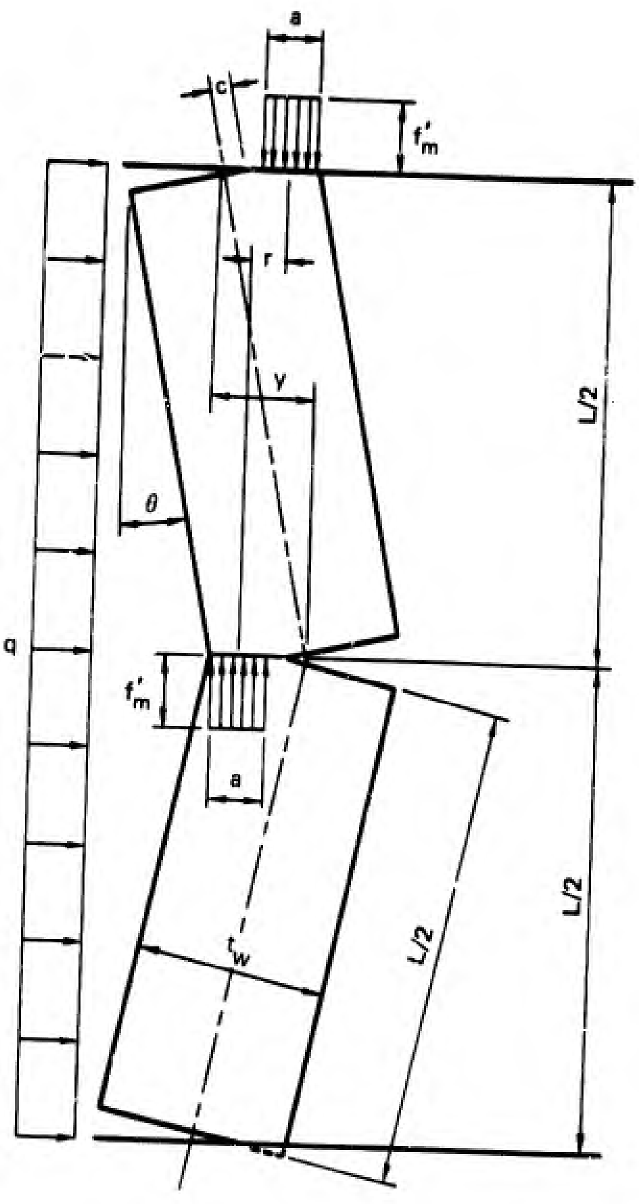


FIG. C-6 ASSUMED ARCHING BEHAVIOR OF MASONRY WALL
(Forces on Bottom Half Not Shown)

It is reasonable to assume that $\delta$ is related to compressive strain in such a way that compressive strain increases or decreases as $\delta$ increases or decreases. Differentiating Eq. C-5a

$$\frac{d\delta}{dt} = \frac{d\delta}{d\theta}\frac{d\theta}{dt} = \left(\frac{t_w}{2} - \xi - \frac{L\theta}{4}\right)\frac{d\theta}{dt} \quad . \qquad \text{(C-15)}$$

In the zone of panel failure, $d\theta/dt$ remains positive until the panel collapses. Therefore, if $t_w/2 - \xi < L\theta/4$, $d\delta/dt < 0$ and the force per unit area is zero. If $t_w/2 - \xi > L\theta/4$, $d\delta/dt > 0$ and the force per unit area is $f_m'$. Therefore the distance from the centerline to the inner edge of the stress block is

$$c = \frac{L\theta}{4} \qquad \text{(C-16)}$$

and the width of the stress block is

$$a = \left(\frac{t_w}{2} - c\right) \sec\theta \approx \frac{t_w}{2} - \frac{L\theta}{4} \quad . \qquad \text{(C-17)}$$

It follows that the compressive force $P(\theta)$ and the moment arm $r(\theta)$ are

$$P(\theta) = f_m' \times a = f_m' \left(\frac{t_w}{2} - \frac{L\theta}{4}\right) \qquad \text{(C-18)}$$

and

$$r(\theta) = 2\left(\frac{t_w}{2}\sec\theta - \frac{a}{2}\right) - \frac{L}{2}\tan\theta \approx \frac{t_w}{2} - \frac{L\theta}{4} \quad . \qquad \text{(C-19)}$$

The resisting moment is thus given by

$$M(\theta) = P(\theta) \times r(\theta) = f_m' \left(\frac{t_w}{2} - \frac{L\theta}{4}\right)^2 \quad . \qquad \text{(C-20)}$$

Either of the above procedures may be followed to determine the resistance of a wall with arching. The first of these, assuming elastic-plastic behavior, while giving a fairly accurate representation of the material properties, is a somewhat complicated procedure. On the other hand, the second, assuming rigid-plastic behavior, while being a simple procedure, overestimates the resisting moment, particularly during the initial stages of deflection. It thus appears advantageous to develop a procedure that more closely approximates the material behavior during the early deflection stages, while still remaining relatively simple to follow. Such a procedure, which essentially assumes a linearized elastic-plastic stress-strain behavior, was developed in Ref. 23.

## Linearized Elastic-Plastic Stress-Strain Relationship

As previously determined, the assumed rigid rotation type of behavior causes the fibers of each half of the wall to be shortened, thus developing compressive forces at the ends and center. The moment arm between these two forces reduces to zero at a deflection equal to the thickness of the wall, at which point there is no further resistance to deflection. At this point the diagonals of the half spans will be shortened by an amount

$$\delta = L_d - L/2 \qquad \text{(C-21)}$$

where $L_d$ is the original length of the diagonal and is given by

$$L_d = \sqrt{L/2^2 + t_w^2} \quad . \qquad \text{(C-22)}$$

The average unit strain is

$$\epsilon_m = \frac{\delta}{L_d} = \frac{L_d - L/2}{L_d} \qquad \text{(C-23)}$$

For a purely elastic material, this would cause a stress $f_m = E_m \epsilon_m$ where $E_m$ is the modulus of elasticity of the wall and $f_m$ is the elastic compressive stress corresponding to the strain $\epsilon_m$. In most cases, $f_m$ will be greater than the crushing stress of the wall, $f'_m$, and therefore cannot exist. Since with walls of normal height and thickness, each half of the wall undergoes a small rotation $\theta$ to reach a deflection equal to its thickness, the shortening of the diagonals can be considered a linear function of the displacement. The deflection $y_y$, at which a compressive stress of $f'_m$ exists, may therefore be found from the following relation.

$$\frac{y_y}{t_w} = \frac{f'_m}{f_m} = \frac{f'_m}{E_m \epsilon_m}$$

or

$$y_y = \frac{t_w f'_m}{E_m \epsilon_m} \qquad \text{(C-24)}$$

The corresponding resisting moment can be found by assuming rectangular compressive stress blocks to exist at the supports and center, similar to that shown in Figure C-6 for the rigid-plastic case.

The width "a" of the stress block is chosen so that the moment $M_y$ is a maximum. Thus differentiating $M_y$ with respect to "a" and setting the expression equal to zero, gives

$$\frac{dM_y}{da} = \frac{d}{da}\left[(a\ f'_m)\ (t_w - y_y - a)\right] = f'_m\ (t_w - y_y - 2a) = 0$$

for $f'_m \neq 0$

$$a = \frac{1}{2}\ (t_w - y_y)\ . \qquad \text{(C-25)}$$

Thus,

$$M_y = \frac{1}{4} f'_m (t_w - y_y)^2 \quad . \qquad \text{(C-26)}$$

When the midspan deflection is greater than $y_y$, the expression for the resisting moment becomes

$$M = \frac{1}{4} f'_m (t_w - y)^2 \qquad y > y_y \qquad \text{(C-27)}$$

As the deflection increases the resistance is reduced until at $y = t_w$, the resistance is zero. This expression is the same as for the rigid-plastic case. However, for deflections less than $y_y$, the resisting moment is taken to be linear between zero and $M_y$. This procedure also overestimates the actual resistance, but to a much smaller extent than for the rigid-plastic case.

Moment resistance curves determined from these three methods are shown in Figure C-7 for a typical wall.

Two other approaches, which will not be discussed in detail here, are given in Refs. 34 and 35. In Ref. 34 it is assumed that the stress block is defined by two parameters relating the total compressive force to the maximum stress and the distance from the neutral axis to the resultant compressive force. These parameters are similar to the $k_1$ and $k_2$ used in ultimate strength design of concrete. In Ref. 35, modifications that take into account the assumption of no tensile strength are developed for application to elastic plate theory.

In the foregoing developments, only the response of a one-way action wall (e.g., supported on two opposite edges) has been considered. The extension of two-way panels (supported on four sides) also needs to be considered, since these conditions exist in many cases.

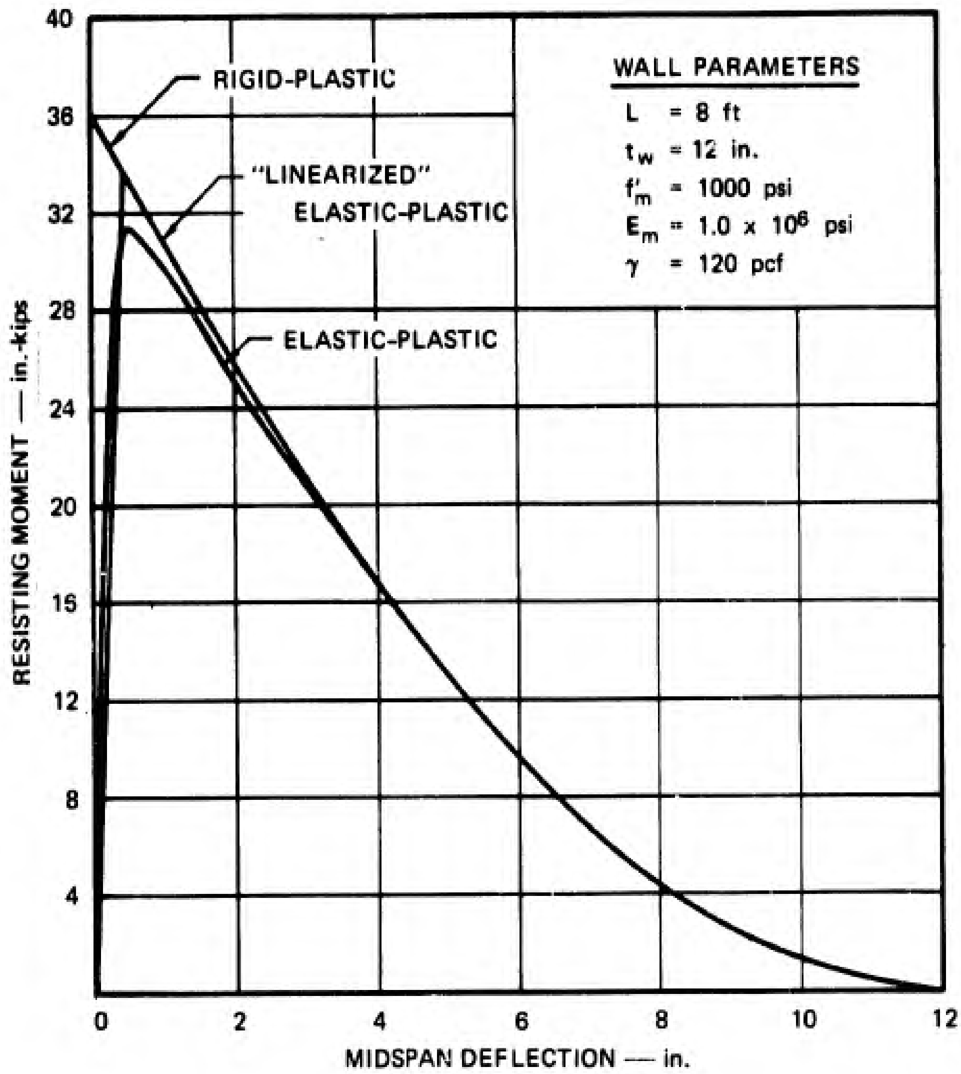


FIG. C-7 COMPARISONS OF MOMENT RESISTANCE CURVES

Two-Way Action

Little work has been done in this area. In Ref. 34, the expressions for the resisting moment of two-way action walls are based on dividing the wall into triangles and trapezoids based on yield line theory. Results presented in Ref. 35 also apply to two-way plate action. However, both these procedures are fairly complicated, and a simpler procedure that gives an approximate solution is discussed in Ref. 32. This requires the use of a so-called equivalent length, similar to that used in designing two-way reinforced concrete slabs. However, instead of keeping the length the same as one side of the two-way wall and determining an equivalent loading, it is more convenient to retain the loading and determine an equivalent one-way wall length. The equivalent length is determined so that a given uniform static load will produce the same center deflection in the one-way or in the two-way wall. Equivalent lengths were computed on the basis of two separate assumptions for the action of the two-way wall. The first assumption was that the wall deflects similarly to a simply supported homogeneous plate according to elastic theory. The second was that the wall deflects according to yield-line failure theory. The results obtained for each of these are shown in Figure C-8, in which the ratio $L_e/L_s$, is plotted against the ratio of the actual panel dimensions, $L_s/L_L$, where $L_s < L_L$. Because these curves agree fairly well, it seems plausible to use an average of the curves for determining equivalent beam lengths, as shown by the curve labeled "average."

All the results up to this point have been based on the assumptions of rigid supports. For the case where the wall is supported by elastic supports at top and bottom, the resistance curve must be constructed in a different manner. Since such a method was not available, the following method was developed in this study.

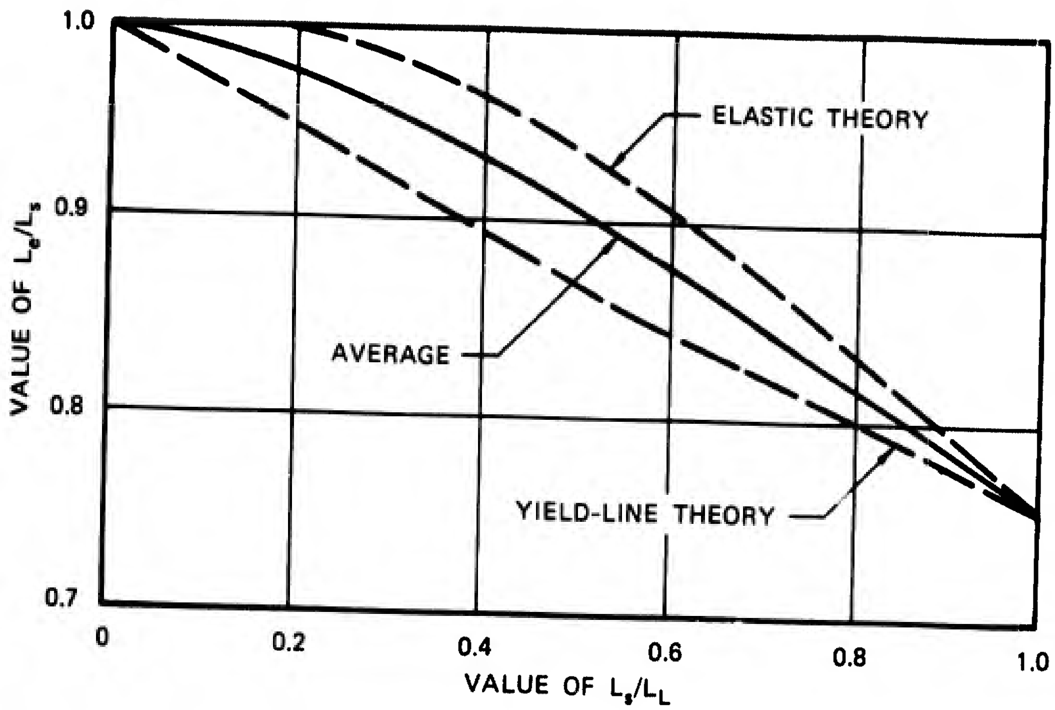


Source: Ref. 32

FIG. C-8 EQUIVALENT SPAN LENGTH

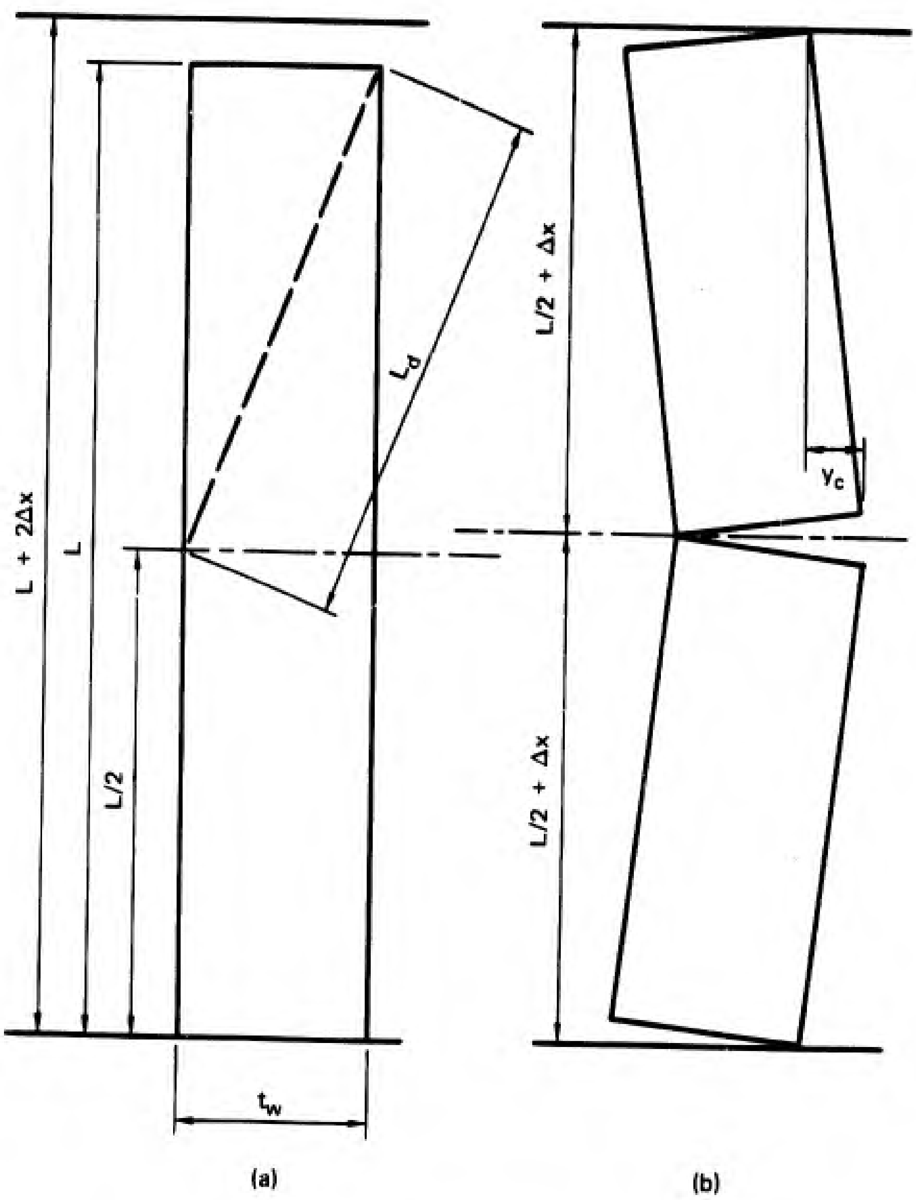


FIG. C-9 ARCHING OF MASONRY WALL WITH INITIAL GAP

## Resistance Function: Elastic Supports

Instead of remaining rigid against in-plane movement of the wall, supports move outward as the wall compresses against them. The magnitude of this movement is a function of the stiffness of the support, $k_s$, and the value of the compressive force, $P_v$, applied by the wall. Thus, for one-way action

$$\Delta x = P_v/k_s \tag{C-28}$$

where $\Delta x$ is the vertical deflection of the half wall and its support. However, the vertical movement of the support causes the compressive force $P_v$ to be reduced, in turn changing the previously determined vertical deflection. It can thus be seen that the procedure requiring an iterative process to determine the values of $P_v$ and $\Delta x$ that correspond to each other.

To perform the above iteration, it is first necessary to determine the effect of the vertical deflection $\Delta x$ on the value of $P_v$. One possible method in this regard is suggested by the solution to the problem of a gap initially existing between the top of the wall and the rigid support, as discussed in Ref. 23, and shown in Figure C-9 (a). The wall is assumed to be laterally supported at the top and bottom, so that lateral motion at these edges is prevented, and the wall will rotate as a rigid body as assumed previously. However, since the wall has zero tensile strength, no resistance to motion will develop until the upper corner just touches the support, as shown in Figure C-9 (b). The lateral deflection at the center, $y_c$, for this position can be determined from the geometry.

$$(t_w - y_c)^2 = (L_d)^2 - \left(\frac{L}{2} + \Delta x\right)^2$$

or

$$y_c = t_w - \sqrt{(L_d)^2 - \left(\frac{L}{2} + \Delta x\right)^2} \qquad \text{(C-29)}$$

where $L_d$ is as given in Eq. C-22. For any further displacement, compressive forces will develop at the ends and center. The shortening in the half span at a deflection equal to the width is now reduced to

$$\delta = L_d - (L/2 + \Delta x) \qquad \text{(C-30)}$$

thereby reducing the average strain to

$$\epsilon_m = \frac{\delta}{L_d} = \frac{L_d - (L/2 + \Delta x)}{L_d} \quad . \qquad \text{(C-31)}$$

Again, for a purely elastic material, this results in a stress, $f_m = E_m \epsilon_m$. Since in most cases $f_m$ is greater than $f_m'$, it cannot exist. Assuming the shortening of the diagonals to be a linear function of the displacement results in the relationship

$$\frac{y_y - y_c}{t_w - y_c} = \frac{f_m'}{f_m} = \frac{f_m'}{E_m \epsilon_m}$$

or

$$y_y = \frac{(t_w - y_c)\, f_m'}{E_m \epsilon_m} + y_c \quad . \qquad \text{(C-32)}$$

The resisting moment at this point can again be determined from Eq. C-26 with the compressive force $P_y$ being given by

$$P_y = 1/2 \; f_m' (t_w - y_y) \quad . \qquad \text{(C-33)}$$

The moment and compressive force at any deflection between $y_c$ and $y_y$ may now be determined from

$$P_v = \frac{y - y_c}{y_y - y_c} P_y \qquad \text{(C-34)}$$

and

$$M = \frac{y - y_c}{y_y - y_c} M_y \quad . \qquad \text{(C-35)}$$

This situation of a pre-existing gap may be considered equivalent to that of the flexible support for a given vertical deflection if it is assumed that it makes no difference that the vertical deflection occurs as a result of a pre-existing gap or as a result of deflection of the supports under the compressive load P. This assumption should be fairly realistic provided short deflection intervals are used. The initial gap of magnitude $2\Delta x$ is equal to a deflection of $\Delta x$ at the supports, since each half wall deflects $\Delta x$ in both cases. The value of $\Delta x$ will be constantly changing as the compressive force $P_v$ changes. The procedure to be used is as follows:

1. Assume value of y
2. Assume value of $P_v$
3. Determine $\Delta x$ from Eq. C-28
4. Determine $y_c$, $\varepsilon_m$, $y_y$, and $P_y$ from Eqs. C-29, C-31, C-32, and C-33, respectively
5. Determine $P_v$ from Eq. C-34 and compare it with the assumed value in Step 2
    a. If within desired accuracy, calculate $M_y$ and M from Eqs. C-26 and C-35
    b. If not within desired accuracy, repeat Steps 3 to 5 using the new value of $P_v$

This procedure is fairly tedious, and a more direct method would be desirable. However, since such a method is not known to be available at this time, the above procedure was used.

## Appendix D

## COMPUTER PROGRAMS

## Appendix D

## COMPUTER PROGRAMS

The computer programs used in the dynamic analysis of the various wall types consist of several parts common to each program linked together with other segments pertaining only to each specific wall type. These parts are organized into the system of routines shown in the following flow chart (Figure D-1).

The input of data, integration of the equations of motion, applied force routine, and output of data are similar for all programs. The calculation of constants and the resistance-displacement subroutine are peculiar to each separate wall type. The resistance-displacement subroutines consist of the resistance functions determined in Section III, with the calculation of constants requiring determination of the various values associated with these resistance functions. The applied force subroutine consists of the loading cases discussed in Section II. The input data required are the wall properties and the values defining the specific loading. The equations of motion of the system are integrated using the Newmark $\beta$ Method (Ref. 8). Also required are transformation factors to reduce the distributed mass system to an equivalent single degree of freedom system (Ref. 7). A summary of this method follows.

### Newmark $\beta$ Method

The differential equation for a single degree-of-freedom system (with no damping) is:

$$ma + Q(y) = P(t)$$

where $a$ = acceleration of system

$v$ = velocity of system

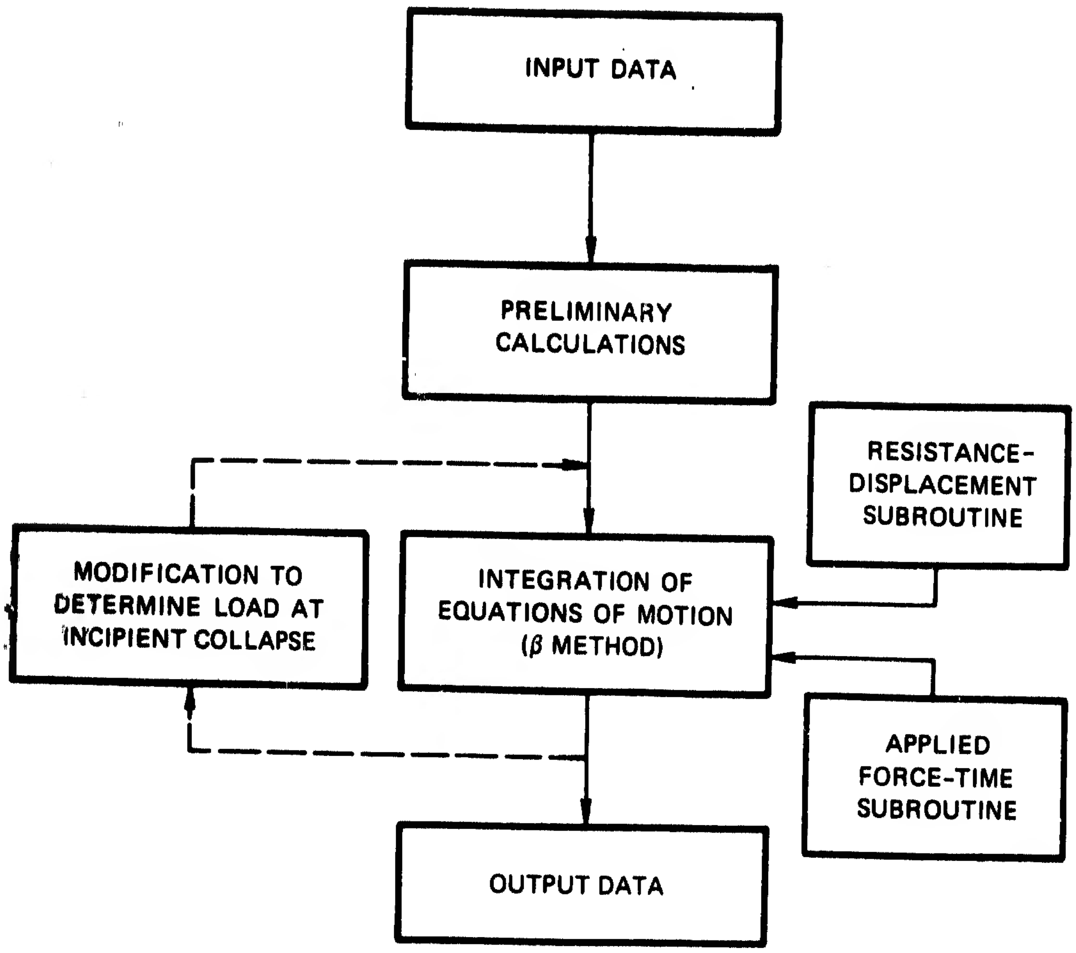


FIG. D-1 TYPICAL COMPUTER PROGRAM FLOW CHART

$y$ = displacement of system

$m$ = mass

$Q(y)$ = resistance force depending on the displacement

$P(t)$ = time-dependent forcing function

Solving for the acceleration, a, gives

$$a = \frac{1}{m}\left[P\ (t) - Q(y)\right] .$$

In many cases of practical interest, exact solutions to the differential equation are impossible to attain or too complex for practical use. Thus, numerical methods are often used to integrate the differential equation. One such numerical method is the Newmark β Method. In this method, the time coordinate is divided into short increments, $\Delta t$, and the differential equation is satisfied at the discrete points $t_1$, $t_2$, ... $t_i$, where $t_i = t_{i-1} + \Delta t$. The β Method expresses the velocity and displacement at the end of a time interval in terms of the acceleration, velocity, and displacement at the beginning of the interval and an assumed acceleration at the end of the interval. The factor β specifies the manner in which the acceleration is assumed to vary within the time interval $\Delta t$.

For $\beta = 1/6$, the acceleration is assumed to vary linearly within the time interval (thus also called the "linear acceleration method"). This variation and also the variation of the velocity and displacement (obtained by successive integration of the acceleration) is shown in the following figures. Also given are formulas for the velocity and displacement at the end of the interval.

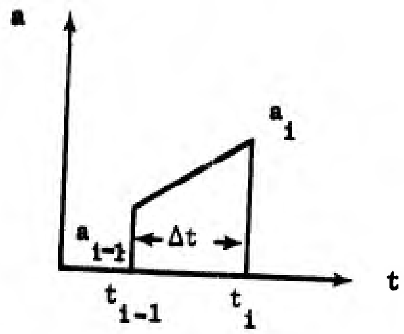


$\underline{\beta = 1/6 \quad \text{(Linear Acceleration)}}$

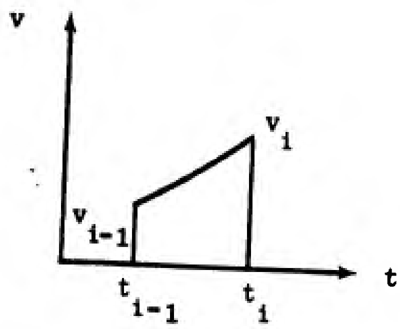


$$v_i = v_{i-1} + \Delta t \, a_{i-1} + \frac{\Delta t}{2} (a_i - a_{i-1})$$

$$\boxed{v_i = v_{i-1} + \frac{\Delta t}{2} (a_{i-1} + a_i)}$$

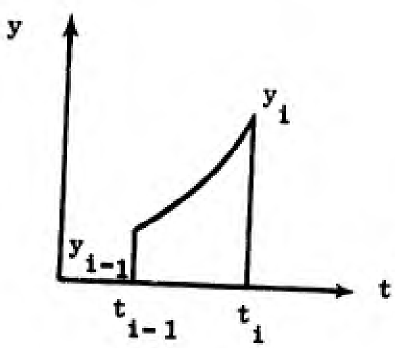


$$y_i = y_{i-1} + \Delta t \, v_{i-1} + \Delta t \frac{\Delta t}{2} a_{i-1} + \frac{\Delta t}{2} \frac{\Delta t}{2} (a_i - a_{i-1})$$

$$\boxed{y_i = y_{i-1} + \Delta t \, v_{i-1} + \frac{(\Delta t)^2}{6} (2a_{i-1} + a_i)}$$

In the general case, the expressions for $v_{i-1}$ and $y_{i-1}$ are

$$v_i = v_{i-1} + \frac{\Delta t}{2} (a_{i-1} + a_i)$$

$$y_i = y_{i-1} + \Delta t \, v_{i-1} + (\Delta t)^2 (1/2 - \beta) \, a_{i-1} + (\Delta t)^2 \beta \, a_i$$

where the assumed variation for $\beta = 1/4$ and $\beta = 1/8$ are as follows:

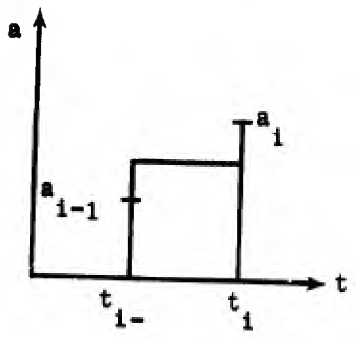


$\beta \; = \; 1/4$

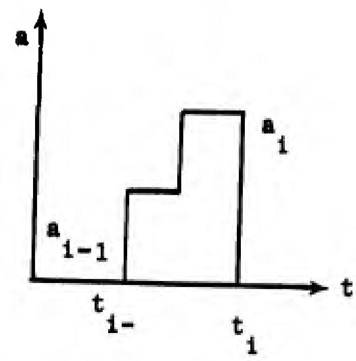


$\beta \; = \; 1/8$

The initial values of $v_o$ and $y_o$ at $t = 0$ must be known to being the process. They are usually assumed to be zero (system initially at rest). The initial acceleration is determined by

$$a_o = \frac{P(t = 0) - Q(y_o)}{m}.$$

The following step-by-step procedure is then used:

1. To initiate the process, a value of the acceleration at the end of the time interval is assumed. For the computer program, it was arbitrarily assumed to be equal to the beginning acceleration, i.e., $a_i = a_{i-1}$

2. Calculate $y_i$ from the equation

$$y_i = y_{i-1} + \Delta t \; v_{i-1} + \frac{(\Delta t)^2}{6} (2a_{i-1} + a_i) \; .$$

3. Determine $P(t_i)$

4. Determine $Q(y_i)$

5. The derived value of the acceleration at the end of the interval is given by

$$a_i' = \frac{P(t_i) - Q(y_i)}{m}$$

6. Calculate the difference between the assumed and derived values of the acceleration at the end of the interval. Thus

$$\Delta a = a_i' - a_i$$

7. Check whether the absolute value of $\Delta a$ is less than the allowable error desired.

   a. If $|\Delta a| \leq$ allowable error, go to Step 8

   b. If $|\Delta a| >$ allowable error, set $a_i = a_i'$ and repeat Steps 2 - 6

8. Calculate the velocity at the end of the interval from the equation

$$v_i = v_{i-1} + \frac{\Delta t}{2}(a_{i-1} + a_i)$$

9. Increase t by $\Delta t$ and repeat Steps 1 - 8.

This process is continued until the desired criteria are met (wall fails or maximum deflection is reached).

The length of the time interval, $\Delta t$, determines the stability and rate of convergence of the procedure. In general, with a time interval of 1/5 to 1/6 of the natural period of vibration, the rate of convergence will be rapid enough for practical purposes. If the natural period is not known or not calculated, the value of $\Delta t$ may be chosen so that the procedure converges to the correct acceleration within approximately three cycles. If more than three cycles are required, the time interval may be decreased. As the structure goes into the inelastic range, the time interval may be increased, since the period of vibration becomes longer. Consideration must also be given to the loading, with the time interval being short enough to describe the load-time function adequately.

## Modification to Determine Load at Incipient Failure

The program was modified slightly so that the load-causing incipient failure could be determined. This modification is shown in dashed lines in Figure D-1. This modification uses an interval-halving routine to search for the load-causing incipient failure. This consists of determining values of the load for which failure of the wall occurs and for which failure does not occur. The midpoint of this interval is then used to replace either the minimum or maximum value, depending on whether the wall fails. This procedure is continued until the size of the interval is within some predetermined value.

## Fxamples

Examples of computer runs for each of the three wall types are given in Figures D-2, D-3, and D-4.

```
INPUT WALL DATA (ZL,TW,E,FR,GAMMA,PVERT,LDTYPE)
?96,8,1000000,50,120,50,1

IS SPECIFIC LOAD, INCLUDING PRESSURE, TO BE GIVEN (INPUT 0),
OR IS INCIPIENT COLLAPSE PRESSURE TO BE FOUND (INPUT 1)?1

INPUT W,PO,CO,S?1000,14.7,1120,30

PROPERTIES OF UNREINFORCED MASONRY WALL BEING ANALYZED
   ZL =  96.0 INCHES     TW =  8.0 INCHES    E = 1000000.0 PSI
   FR = 50.00 PSI     GAMMA = 120.0 LB/CU.FT.     PVERT =  50.0 PSI

MAXIMUM STATIC BENDING RESISTANCE = 0.926 PSI
MAXIMUM ELASTIC DEFLECTION = 0.024 INCHES
MAXIMUM GEOMETRICAL RESISTANCE = 2.644 PSI

LOAD CAUSING INCIPIENT FAILURE IS AS FOLLOWS:
    LOAD TYPE NUMBER 1
          W =  1000.0 KT   PO = 14.70 PSI      CO =1120.0 FPS
          S =  30.0 FT      U = 1176.2 FPS     TO = 3.886 SEC
         PR =  3.710 PSI  PSO =  1.766 PSI    PDO =  0.074 PSI
         TC = 0.0765 SEC

WALL FAILED AT 0.288 SECONDS

IS TIME HISTORY OF WALL DESIRED (YES=1, NO=0)?1

THE TIME HISTORY OF THE WALL IS AS FOLLOWS:
```

| TIME | LOAD | ACCELERATION | VELOCITY | DISPLACEMENT | REACTION |
|---|---|---|---|---|---|
| 0. | 3.710 | 3305.7 | 0. | 0. | 38.11 |
| 0.001 | 3.685 | 3226.7 | 3.27 | 0.0016 | 40.24 |
| 0.002 | 3.660 | 3037.5 | 6.40 | 0.0065 | 47.03 |
| 0.003 | 3.634 | 2744.4 | 9.29 | 0.0144 | 58.23 |
| 0.004 | 3.609 | 2357.5 | 11.84 | 0.0250 | 73.39 |
| 0.005 | 3.583 | 1890.0 | 13.96 | 0.0379 | 91.96 |
| 0.006 | 3.558 | 1358.0 | 15.59 | 0.0527 | 113.28 |
| 0.007 | 3.533 | 779.5 | 16.66 | 0.0689 | 136.55 |
| 0.008 | 3.507 | 702.9 | 17.40 | 0.0859 | 144.31 |
| 0.018 | 3.253 | 513.2 | 23.48 | 0.2919 | 138.60 |
| 0.028 | 2.999 | 343.0 | 27.76 | 0.5495 | 132.22 |
| 0.038 | 2.745 | 185.8 | 30.40 | 0.8416 | 125.40 |
| 0.048 | 2.491 | 35.6 | 31.51 | 1.1524 | 118.34 |
| 0.058 | 2.237 | -113.2 | 31.12 | 1.4668 | 111.23 |
| 0.068 | 1.982 | -266.3 | 29.22 | 1.7698 | 104.26 |
| 0.078 | 1.765 | -391.0 | 25.94 | 2.0467 | 98.07 |
| 0.088 | 1.755 | -309.9 | 22.43 | 2.2879 | 94.84 |
| 0.098 | 1.746 | -240.5 | 19.68 | 2.4979 | 92.02 |
| 0.108 | 1.736 | -180.2 | 17.58 | 2.6837 | 89.50 |
| 0.118 | 1.727 | -126.8 | 16.04 | 2.8514 | 87.23 |
| 0.128 | 1.718 | -78.1 | 15.02 | 3.0063 | 85.11 |
| 0.138 | 1.708 | -32.4 | 14.47 | 3.1533 | 83.10 |
| 0.148 | 1.699 | 12.2 | 14.37 | 3.2971 | 81.13 |
| 0.158 | 1.690 | 57.3 | 14.71 | 3.4421 | 79.15 |
| 0.168 | 1.681 | 104.5 | 15.52 | 3.5929 | 77.09 |
| 0.178 | 1.671 | 155.8 | 16.82 | 3.7542 | 74.90 |
| 0.188 | 1.662 | 213.1 | 18.67 | 3.9312 | 72.50 |
| 0.198 | 1.653 | 278.5 | 21.13 | 4.1296 | 69.83 |
| 0.208 | 1.644 | 354.5 | 24.29 | 4.3561 | 66.80 |
| 0.218 | 1.635 | 444.1 | 28.29 | 4.6182 | 63.30 |
| 0.228 | 1.626 | 550.6 | 33.26 | 4.9251 | 59.23 |
| 0.238 | 1.617 | 678.0 | 39.40 | 5.2873 | 54.45 |
| 0.248 | 1.608 | 831.3 | 46.95 | 5.7178 | 48.78 |
| 0.258 | 1.600 | 1016.2 | 56.19 | 6.2319 | 42.03 |
| 0.268 | 1.591 | 1239.8 | 67.47 | 6.8483 | 33.96 |
| 0.278 | 1.582 | 1510.6 | 81.22 | 7.5895 | 24.29 |
| 0.288 | 1.573 | 1838.8 | 97.96 | 8.4827 | 12.64 |

FIG. D-2 SAMPLE COMPUTER OUTPUT FOR UNREINFORCED MASONRY WALL (WITHOUT ARCHING)

```
INPUT ZL,TW,FDC,FDY,EC,ES,P,PP,D DP,PVERT,ISUP,LDTYPE
?96,8,3750,42000,3E6,3E7,0.0025,0,7,0,0,1,1

IS SPECIFIC LOAD,INCLUDING PRESSURE, TO BE GIVEN (INPUT 0),
OR IS INCIPIENT COLLAPSE PRESSURE TO BE FOUND (INPUT 1)?1

INPUT W,PO,CO,S?1000,14.7,1120,30


PROPERTIES OF REINFORCED CONCRETE WALL BEING ANALYZED:
        ZL =   96.0 INCHES             TW =   8.0 INCHES
       FDC =  3750.0 PSI               EC =   3000000.0 PSI
       FDY = 42000.0 PSI               ES =  30000000.0 PSI
         P =   0.0025                   D =  7.00 INCHES
        PP =   0.                      DP =  0.     INCHES
     PVERT =       0.   LB.          ISUP =  1

LOAD-DEFLECTION CURVE -- SIMPLY SUPPORTED WALL

                 Q                 Y
               449.9             0.0392
               421.5             0.2035
               421.5             6.9653

LOAD CAUSING INCIPIENT FAILURE IS AS FOLLOWS:
    LOAD TYPE NUMBER 1
        W =   1000.0 KT     PO =  14.70 PSI        CO =1120.0 FPS
        S =   30.0 FT        U =1228.0 FPS         TO =  3.455 SEC
       PR =   7.615 PSI    PSO =    3.468 PSI     PDO =   0.283 PSI
       TC =  0.0733 SEC

WALL FAILED AT 0.144 SECONDS

IS TIME HISTORY OF WALL DESIRED (YES=1, NO=0)?1

THE TIME HISTORY OF THE WALL IS AS FOLLOWS:
```

| TIME | LOAD | ACCELERATION | VELOCITY | DISPLACEMENT | REACTION |
|---|---|---|---|---|---|
| 0. | 7.615 | 5614.7 | 0. | 0. | 78.22 |
| 0.001 | 7.560 | 2120.8 | 3.87 | 0.0022 | 254.36 |
| 0.002 | 7.505 | 2085.5 | 5.97 | 0.0071 | 253.52 |
| 0.003 | 7.450 | 2058.5 | 8.04 | 0.0142 | 252.57 |
| 0.004 | 7.395 | 2021.6 | 10.08 | 0.0232 | 251.51 |
| 0.005 | 7.340 | 1993.0 | 12.08 | 0.0343 | 250.33 |
| 0.006 | 7.285 | 1966.4 | 14.06 | 0.0474 | 249.05 |
| 0.007 | 7.230 | 1942.0 | 16.02 | 0.0624 | 247.66 |
| 0.008 | 7.175 | 1919.7 | 17.95 | 0.0794 | 246.16 |
| 0.009 | 7.120 | 1899.4 | 19.86 | 0.0983 | 244.56 |
| 0.010 | 7.065 | 1881.2 | 21.75 | 0.1191 | 242.85 |
| 0.011 | 7.010 | 1865.0 | 23.62 | 0.1418 | 241.04 |
| 0.012 | 6.955 | 1850.7 | 25.48 | 0.1664 | 239.13 |
| 0.013 | 6.900 | 1838.5 | 27.32 | 0.1928 | 237.11 |
| 0.014 | 6.845 | 1809.5 | 29.15 | 0.2210 | 240.20 |
| 0.024 | 6.294 | 1659.1 | 46.49 | 0.6004 | 233.59 |
| 0.034 | 5.744 | 1179.7 | 60.69 | 1.1403 | 226.99 |
| 0.044 | 5.194 | 700.3 | 70.09 | 1.7982 | 220.39 |
| 0.054 | 4.644 | 220.9 | 74.69 | 2.5261 | 213.79 |
| 0.064 | 4.094 | -256.5 | 74.50 | 3.2760 | 207.19 |
| 0.074 | 3.581 | -705.1 | 69.69 | 4.0007 | 201.04 |
| 0.084 | 3.559 | -724.7 | 62.54 | 4.6620 | 200.77 |
| 0.094 | 3.537 | -744.1 | 55.19 | 5.2508 | 200.50 |
| 0.104 | 3.514 | -763.5 | 47.65 | 5.7652 | 200.23 |
| 0.114 | 3.492 | -782.7 | 39.92 | 6.2032 | 199.97 |
| 0.124 | 3.470 | -801.8 | 32.00 | 6.5630 | 199.70 |
| 0.134 | 3.449 | -820.9 | 23.89 | 6.8426 | 199.44 |
| 0.144 | 3.427 | 2986.1 | 34.71 | 7.1039 | 41.12 |

FIG. D-3 SAMPLE COMPUTER OUTPUT FOR REINFORCED CONCRETE WALL

```
INPUT ZL,TW,EM,F'M,GSMMS,LDTYPE? 96,12,1000000,1000,120,1

IS SPECIFIC LØAD, INCLUDING PRESSURE, TØ BE GIVEN (INPUT 0),
ØR IS INCIPIENT CØLLAPSE PRESSURE TØ BE FØUND (INPUT 1)? 1

INPUT W,PØ,CØ,S? 1000,14.7,1120,30


PRØPERTIES ØF UNREINFØRCED MASØNRY WALL (ARCHING) BEING ANALYZED:
    ZL =  96.0 INCHES        TW = 12.0 INCHES    EM = 1000000.0 PSI
   F'M = 1000.0 PSI      GAMMA = 120 LB/CU.FT.

MAXIMUM STATIC RESISTANCE = 29.19 PSI
DEFLECTIØN AT MAX STATIC RESISTANCE = 0.4019 INCHES

LØAD CAUSING INCIPIENT FAILURE IS AS FØLLØWS:
    LØAD TYPE NUMBER 1
         W =  1000.0 KT     PØ =14.70 PSI       CØ = 1120.0 FPS
         S =   30.0 FT       U = 1436.0 FPS     TO = 2.313 SEC
        PR = 28.508 PSI  PSØ = 11.043 PSI   PDØ = 2.676 PSI
        TC = 0.0627 SEC

WALL FAILED AT  0.135 SEC (FINAL VELØCITY = 353.39 IN./SEC)

IS TIME HISTØRY ØF WALL DESIRED (YES=1, NØ=0)? 1


THE TIME HISTØRY ØF THE WALL IS AS FØLLØWS:
```

| TIME | LØAD | ACCELERATIØN | VELØCITY | DISPLACEMENT | REACTIØN |
|---|---|---|---|---|---|
| 0. | 28.508 | 19712.1 | 0. | 0. | 342.09 |
| 0.001 | 28.258 | 19050.0 | 19.38 | 0.0097 | 364.57 |
| 0.002 | 28.008 | 17439.1 | 37.63 | 0.0384 | 436.46 |
| 0.003 | 27.758 | 14959.6 | 53.82 | 0.0843 | 553.56 |
| 0.004 | 27.509 | 11735.1 | 67.17 | 0.1451 | 709.45 |
| 0.005 | 27.259 | 7926.0 | 77.00 | 0.2175 | 895.78 |
| 0.006 | 27.009 | 3722.2 | 82.83 | 0.2978 | 1102.65 |
| 0.007 | 26.759 | -667.4 | 84.35 | 0.3817 | 1319.20 |
| 0.008 | 26.510 | -1633.6 | 83.20 | 0.4656 | 1357.52 |
| 0.009 | 26.260 | -1522.0 | 81.63 | 0.5480 | 1339.72 |
| 0.010 | 26.010 | -1417.7 | 80.16 | 0.6289 | 1322.30 |
| 0.015 | 24.762 | -990.1 | 74.14 | 1.0137 | 1240.10 |
| 0.020 | 23.513 | -687.4 | 69.94 | 1.3733 | 1164.40 |
| 0.025 | 22.264 | -477.6 | 67.03 | 1.7153 | 1093.55 |
| 0.030 | 21.015 | -339.5 | 64.99 | 2.0450 | 1026.42 |
| 0.035 | 19.767 | -259.3 | 63.49 | 2.3660 | 962.30 |
| 0.040 | 18.518 | -228.7 | 62.27 | 2.6804 | 900.77 |
| 0.045 | 17.269 | -243.7 | 61.09 | 2.9888 | 841.62 |
| 0.050 | 16.021 | -303.7 | 59.72 | 3.2910 | 784.81 |
| 0.055 | 14.772 | -410.8 | 57.93 | 3.5853 | 730.44 |
| 0.065 | 12.824 | -392.4 | 53.92 | 4.1444 | 636.00 |
| 0.075 | 12.692 | 741.7 | 55.67 | 4.6829 | 570.58 |
| 0.085 | 12.560 | 1941.9 | 69.08 | 5.2966 | 501.78 |
| 0.095 | 12.430 | 3386.4 | 95.73 | 6.1086 | 420.31 |
| 0.105 | 12.300 | 5139.2 | 138.35 | 7.2644 | 322.86 |
| 0.115 | 12.172 | 7007.7 | 199.09 | 8.9361 | 219.43 |
| 0.125 | 12.046 | 8255.2 | 275.40 | 11.2981 | 148.40 |
| 0.135 | 11.920 | 7341.9 | 353.39 | 14.4497 | 189.91 |

FIG. D-4 SAMPLE COMPUTER OUTPUT FOR UNREINFORCED MASONRY WALL (WITH ARCHING)

## REFERENCES


1. Glasstone, S., ed., The Effects of Nuclear Weapons, Department of Defense and Atomic Energy Commission, Washington, D.C., February 1964.
2. Denton, D. R., Dynamic Ultimate Strength Study of Simply Supported Two-Way Reinforced Concrete Slabs, Technical Report No. 1-789, U.S. Army Engineer Waterways Experiment Station, (for the Office of Civil Defense), Vicksburg, Mississippi, July 1967.
3. Office of Civil Defense, A Computer Program to Analyze the Dynamic Response of High Rise Buildings to Nuclear Blast Loading, Review Draft PG 80-18-1 and 2, T. Y. Lin and Associates, Los Angeles, California, 1964.
4. Hill, E. L., A. A. Qadeer, and A. B. Nicholls, Structural Characteristics of NFSS Buildings, R-OR-237, Vols. I-V, Research Triangle Institute (for Office of Civil Defense), Research Triangle Park, North Carolina, June 1967.
5. Berg, G. V., and D. A. DaDeppo, The Response of Tier Buildings to Blast Loads, AFSWC-TR-57-45, University of Michigan, (for Air Force Special Weapons Center), Ann Arbor, Michigan, 1958.
6. Wiehle, C. K., and W. L. Durbin, Combined Effects of Nuclear Weapons on NFSS Type Structures, URS 685-3, URS Corporation (for the Office of Civil Defense), Burlingame, California, September 1966.
7. The Design of Structures to Resist the Effects of Atomic Weapons, EM 1110-345-414 to 421, Massachusetts Institute of Technology for the Office of Chief of Engineers, U.S. Army, Washington, D.C., 1957.
8. Newmark, N. M., "A Method of Computation for Structural Dynamics," ASCE Transactions, Paper No. 3384, Vol. 127, 1962, Part I.

9. Kaplan, K., and C. Wiehle, Air Blast Loading in the High Shock Strength Region (U). Part II - Prediction Methods and Examples (U), DASA 1460-1, URS Corporation (for Defense Atomic Support Agency), Burlingame, California, February 1965.
10. Newmark, N. M., and J. D. Haltiwanger, Air Force Design Manual - Principles and Practices for Design of Hardened Structures, AFSWC-TDR-62-138, University of Illinois (for Air Force Special Weapons Center), Urbana, Illinois, December 1962.
11. Willoughby, A. B., C. Wilton, and B. Gabrielsen, Development and Evaluation of a Shock Tunnel Facility for Conducting Full Scale Tests of Loading, Response, and Debris Characteristics of Structural Elements, URS 680-2, URS Corporation, (for Office of Civil Defense and Stanford Research Institute), Burlingame, California, December 1967.
12. Melin, J. W. and S. Sutcliffe, Development of Procedures for Rapid Computation of Dynamic Structural Response, SRS No. 171, University of Illinois (for U.S. Air Force), Urbana, Illinois, January 1959.
13. Winter, G., et al., Design of Concrete Structures, McGraw-Hill Book Co., New York, 1964.
14. Personal Communication with Professor M. A. Sozen, University of Illinois, Urbana, Illinois.
15. Personal Communication with Mr. A. B. Willoughby, URS Corporation, Burlingame, California.
16. Hedstrom, R. O., "Load Tests of Patterned Concrete Masonry Walls," J. American Concrete Institute, April 1961.
17. Large, G. E., Basic Reinforced Concrete Design: Elastic and Creep, The Roland Press Company, New York, 1957.
18. American Concrete Institute, Building Code Requirements for Reinforced Concrete, ACI 318-63, Detroit, Michigan, June 1963.
19. Allgood, J. R., S. K. Takahashi, and W. A. Shaw, Blast Loading of 15 ft R/C Beams, Technical Report TR-086, U.S. Naval Civil Engineering Laboratory, Port Hueneme, California, January 1961.

20. Roark, R. J., Formulas for Stress and Strain, McGraw-Hill Book Company, New York, 1965.

21. Anderson, F. E., Jr., et al., Design of Structures to Resist Nuclear Weapons Effects, American Society of Civil Engineers, Manual 42, New York, 1961.

22. Sevin, E., Tests on the Response of Wall and Roof Panels and the Transmission of Load to Supporting Structures, WT-724, Armed Forces Special Weapons Project, Sandia Base, Albuquerque, N. M., (for Air Material Command, Wright-Patterson A. F. Base), May 1955.

23. Whitney, C. S., B. G. Anderson, and E. Cohen, "Design of Blast Resistant Construction for Atomic Explosions," J. American Concrete Institute, Proceedings Vol. 51, March 1955.

24. Liber, T. and R. L. Barnett, An Experimental Investigation of Frangible Plate Fragmentation, IIT Research Institute, (for the Office of Civil Defense), Chicago, Illinois, October 1966.

25. Taylor, B. C., Blast Effects of Atomic Weapons Upon Curtain Walls and Partitions of Masonry and Other Materials, WT-741, Federal Defense Administration, Battle Creek, Michigan, August 1956.

26. Allgood, J. R., and W. A. Shaw, Elasto-Plastic Response of Beams to Dynamic Loads, Technical Memorandum M-130, U.S. Naval Civil Engineering Laboratory, Port Hueneme, California, March 1958.

27. American Society of Civil Engineers, "Report of ASCE-ACI Joint Committee on Ultimate Strength Design," J. Structural Div., Vol. 81, October 1955.

28. Hognestad, E., N. W. Hanson, and D. McHenry, "Concrete Stress Distribution in Ultimate Strength Design," J. American Concrete Institute, December 1955.

29. Hognestad, E., A Study of Combined Bending and Axial Load in Reinforced Concrete Members, No. 399, University of Illinois Experiment Station, Urbana, Illinois, November 1951.

30. Pfrang, E. O., C. P. Siess, and M. A. Sozen, "Load-Moment-Curvature Characteristics of Reinforced Concrete Cross Sections," J. American Concrete Institute Proceedings Vol. 61, No. 7, July 1964.

31 McDowell, E. L., K. E. McKee, and E. Sevin, "Arching Action Theory of Masonry Walls," ASCE Journal of the Structural Division, Proceedings Paper 915, March 1958.

32. McKee, Keith E. and Eugene Sevin, "Design of Masonry Walls for Blast Loading," ASCE Transactions, Paper No. 2988, Volume 124, 1959.

33. Berg, Glen V., Donald A. DaDeppo, and Bruce G. Johnston, The Response of Tier Buildings to Blast Loads, Engineering Research Institute, University of Michigan, March 1956.

34. Abrahamsson, Eddy, Dome Action in Slabs, Stockholm, 1967.

35. Brotchie, John F., Amnon Jacobson, and Sudaji Okubo, Effect of Membrane Action on Slab Behavior, Massachusetts Institute of Technology, August 1965.

36. Gurfinkel, German and Chester P. Siess, "Longitudinally Restrained Reinforced Concrete Beams," ASCE Journal of the Structural Division, Proceedings Paper 5859, March 1968.

## NOMENCLATURE

| | |
|---|---|
| $a$ | Width of equivalent rectangular stress block, in.<br>Acceleration, in./sec$^2$ |
| $A$ | Cross sectional area, sq. in. |
| $A_s$ | Area of tension steel in a reinforced concrete member, sq. in. |
| $A_s'$ | Area of compression steel in a reinforced concrete member, sq. in. |
| $b$ | Width of cross section, in. |
| $B$ | Width of wall, in. |
| $\Delta B$ | Elemental width of wall |
| $c$ | Distance from neutral axis to extreme fiber, in.<br>Distance from centerline to inner edge of stress block in arching, in. |
| $c_o$ | Ambient sound velocity ahead of shock, fps |
| $C$ | Compressive force in concrete, lb |
| $C'$ | Compressive force in compression steel, lb |
| $C_{df}$ | Pressure coefficient, front face |
| $C_m$ | Maximum potential compressive force available for a concrete stress block with the neutral axis located at the centerline of the compression steel, lb |
| $d$ | Distance from the compression face to the centroid of the tension steel, in. |
| $d'$ | Distance from the compression face to the centroid of the compression steel, in. |
| $e$ | Eccentricity of axial load, measured from the centroid of tension steel, in. |
| $E$ | Modulus of elasticity, psi |
| $E_c$ | Modulus of elasticity of concrete, psi |
| $E_m$ | Modulus of elasticity of masonry, psi |
| $E_s$ | Modulus of elasticity of steel, psi |
| $f$ | Unit stress, psi |
| $f_c$ | Compressive stress in concrete, psi |
| $f_c'$ | Compressive strength of 6- by 12-in. concrete cylinders, psi |

| | |
|---|---|
| $f''_c$ | Compressive strength of concrete in flexure, psi |
| $f'_{dc}$ | Dynamic compressive strength in concrete, psi |
| $f_{dy}$ | Dynamic yield strength of reinforcing steel, psi |
| $f_m$ | Elastic compressive stress in masonry corresponding to the strain $\epsilon_m$, psi |
| $f'_m$ | Ultimate compressive strength of masonry unit wall, psi |
| $f_r$ | Modulus of rupture of concrete, psi |
| $f'_s$ | Stress in compression steel, psi |
| $f_u$ | Ultimate strength of reinforcing steel, psi |
| I | Moment of inertia of a section, $in.^4$<br>Inertial force per unit width, lb/in. |
| $I_c$ | Moment of inertia of a reinforced concrete cracked section, $in.^4$ |
| $I_g$ | Moment of inertia of a reinforced concrete uncracked section, $in.^4$ |
| $k_s$ | Stiffness of support, lb/in. |
| $k_u$ | Coefficient indicating position of neutral axis of reinforced concrete member at ultimate strength |
| $k_1$ | Coefficient relating the average concrete compressive stress to the maximum compressive strength of concrete in flexure |
| $k_2$ | Coefficient relating the location of the total concrete compressive force to the distance from the compressive face to the neutral axis |
| $k_3$ | Coefficient relating the maximum compressive strength in concrete in flexure to the compressive strength of 6- by 12-in. cylinders |
| $\ell$ | Length required to develop the ultimate tensile strength of the reinforcing steel in bond to the concrete, in. |
| L | Span length, or height, of wall, in. |
| $L_d$ | Diagonal length of half-span of wall, in. |
| $L_e$ | Equivalent one-way action span length for two-way action wall, in. |
| $L_L$ | Length of long span for two-way action wall, in. |
| $L_S$ | Length of short span for two-way action wall, in. |
| M | Bending moment per unit width, in.-lb/in. |
| $\Delta M$ | Additional moment resistance developed during elasto-plastic phase of fixed end and propped cantilever reinforced concrete walls per unit width, in.-lb/in. |

| | |
|---|---|
| $M_c$ | Bending moment per unit width at center of span, in.-lb/in. |
| $M_{ca}$ | Bending moment per unit width at center of span at the end of the elastic phase for fixed and propped cantilever walls, in.-lb/in. |
| $M_e$ | Bending moment per unit width at end of span, in.-lb/in. |
| $M_{mc}$ | Ultimate moment capacity per unit width of uncracked center section, in.-lb/in. |
| $M_{me}$ | Ultimate moment capacity per unit width of uncracked end section, in.-lb/in. |
| $M_r$ | Bending moment per unit width at center of span during rigid body rotational mode, in.-lb/in. |
| $M_u$ | Ultimate moment capacity per unit width of a section, in.-lb/in. |
| $M_{uc}$ | Ultimate moment capacity per unit width of cracked center section for reinforced concrete walls, in.-lb/in. |
| $M_{ue}$ | Ultimate moment capacity per unit width of cracked end section for reinforced concrete walls, in.-lb/in. |
| $M_y$ | Arching moment per unit width corresponding to yielding of masonry, in.-lb/in. |
| $p$ | Steel ratio, tension steel, $A_s/bd$ |
| $p'$ | Steel ratio, compression steel, $A_s'/bd$ |
| $p(t)$ | Unit pressure exerted against any surface varying with time, psi |
| $p_c$ | Pressure exerted at time $t_c$, psi |
| $p_d$ | Dynamic pressure varying with time, psi |
| $p_{do}$ | Peak dynamic pressure, psi |
| $p_m$ | Peak pressure exerted against any surface, psi |
| $p_r$ | Reflected overpressure, psi |
| $p_s$ | Incident, or side-on, overpressure varying with time, psi |
| $p_{so}$ | Peak incident, or side-on, overpressure, psi |
| $P$ | Total lateral load per unit width, lb/in. |
| $P_v$ | Total vertical force per unit width, lb/in. |
| $p_o$ | Ambient atmospheric pressure, psi |
| $P_y$ | Vertical force per unit width corresponding to yield of masonry during arching, lb/in. |
| $q$ | Unit resistance for uniformly loaded wall, psi |

| | |
|---|---|
| $Q$ | Total resistance per unit width for uniformly loaded wall, lb/in. |
| $\Delta Q$ | Additional resistance per unit width developed during elasto-plastic phase of fixed end and propped cantilever reinforced concrete walls, lb/in. |
| $Q_u$ | Ultimate resistance per unit width for uniformly loaded wall, lb/in. |
| $Q_y$ | Total resistance per unit width corresponding to yield of masonry during arching, lb/in. |
| $Q_1$ | Maximum resistance per unit width for uncracked portion of elastic phase, lb/in. |
| $Q_2$ | Maximum resistance per unit width for cracked portion of elastic phase for reinforced concrete walls, lb/in. Maximum resistance per unit width for decaying phase of unreinforced masonry walls without arching, lb/in. |
| $r$ | Moment arm of resisting moment developed by arching forces, in. |
| $R$ | Nondimensional variable defined by Equation C-11 |
| $R_t$ | Total area under reaction-time curve per unit width, lb-sec/in. |
| $S$ | Clearing distance, height or half width, whichever is smaller, ft |
| $t$ | Time, sec |
| $\Delta t$ | Time increment, sec |
| $t_c$ | Clearing time, front face, sec |
| $t_{cr}$ | Time to initial cracking of wall, sec |
| $t_o$ | Duration of positive overpressure phase, sec |
| $t_r$ | Rise time of blast wave, sec |
| $t_u$ | Duration of positive dynamic pressure phase, sec |
| $t_w$ | Thickness of wall, in. |
| $T$ | Tensile force in tension steel at yield per unit width, lb/in. |
| $T'$ | Tensile force in compression steel for the case where the neutral axis is less than the distance $d'$ from the compression face of the concrete per unit width, lb/in. |
| $T_p$ | Sum of tensile force in tension steel and total vertical force per unit width, lb/in. |
| $u$ | Nondimensional lateral deflection at center of wall equal to $y/t_w$ |
| $U$ | Shock front velocity, fps |
| $U_u'$ | Ultimate average bond force per in. of length of reinforcing bar, lb/in. |

| | |
|---|---|
| $v$ | Velocity, in./sec |
| $V$ | Reaction, or shear at end of wall span, per unit width, lb/in. |
| $V_1$ | Reaction per unit width at simply supported end of propped cantilever wall, lb/in. |
| $V_2$ | Reaction per unit width at fixed end of propped cantilever wall, lb/in. |
| $W$ | Weapon yield, kt<br>Weight of wall per unit width, lb/in. |
| $x$ | Vertical distance along wall, in. |
| $\Delta x$ | Vertical deflection of half wall, in. |
| $\bar{x}$ | Distance from end to center of gravity of the inertia forces on half-span of the wall, in. |
| $y$ | Lateral deflection at center of wall, in. |
| $\Delta y$ | Additional deflection at center of wall during elasto-plastic phase of fixed end and propped cantilever reinforced concrete walls, in. |
| $y_c$ | Lateral deflection of wall defined by Eq. C-29, in. |
| $y_f$ | Lateral deflection at failure, or collapse, of wall, in. |
| $y_y$ | Lateral deflection corresponding to yielding of masonry during arching, in. |
| $y_1$ | Maximum deflection for uncracked portion of elastic phase, in. |
| $y_2$ | Maximum deflection for cracked portion of elastic phase, in. |
| $z$ | Distance from centerline of wall to inner edge of contact surface during arching, in. |
| $\alpha t_w$ | Width of contact surface during arching, in. |
| $\beta$ | Coefficient used in the $\beta$ Method |
| $\gamma$ | Unit weight, pcf |
| $\delta$ | Shortening of a vertical fiber of the wall a distance $\xi$ from the edge, in. |
| $\epsilon$ | Unit strain, in./in. |
| $\epsilon_{avg}$ | Average strain along a vertical fiber of the wall a distance $\xi$ from the edge, in./in. |
| $\epsilon_c$ | Strain in the concrete, in./in. |

| | |
|---|---|
| $\epsilon_m$ | Strain in the masonry wall, in./in. |
| $\epsilon_o$ | Compressive strain in concrete corresponding to the maximum stress, in./in. |
| $\epsilon_s$ | Strain in tension steel, in./in. |
| $\epsilon_{su}$ | Ultimate strain in tension steel, in./in. |
| $\epsilon_s'$ | Strain in compression steel, in./in. |
| $\epsilon_u$ | Ultimate concrete strain in flexure, in./in. |
| $\epsilon_y$ | Compressive strain in masonry corresponding to ultimate stress, in./in. |
| $\theta$ | Angle of rotation of half wall considered as a rigid body, radians |
| $\lambda$ | Distance from the centerline of the wall to the inner edge of the rectangular stress block, in. |
| $\mu$ | Ductility factor, ratio of maximum deflection to deflection at yield |
| $\xi$ | Distance along cross section of the wall, measured from the edge, in. |
| $\xi'$ | Distance along the contact surface of the wall from the edge to the centroid of the stress distribution, in. |
| $\phi$ | Curvature of reinforced concrete cross section, radians |
| $\phi_u$ | Curvature corresponding to the ultimate concrete strain in flexure, radians |

UNCLASSIFIED
Security Classification

## DOCUMENT CONTROL DATA - R & D

(Security classification of title, body of abstract and indexing annotation must be entered when the overall report is classified)

| | |
|---|---|
| 1. ORIGINATING ACTIVITY (Corporate author) STANFORD RESEARCH INSTITUTE Menlo Park, California 94025 | 2a. REPORT SECURITY CLASSIFICATION Unclassified |
| | 2b. GROUP Not Applicable |

3. REPORT TITLE

EXISTING STRUCTURES EVALUATION - PART I: WALLS

4. DESCRIPTIVE NOTES (Type of report and inclusive dates)
Technical Report

5. AUTHOR(S) (First name, middle initial, last name)
Carl K. Wiehle
James L. Bockholt

| | | |
|---|---|---|
| 6. REPORT DATE November, 1968 | 7a. TOTAL NO. OF PAGES 236 | 7b. NO. OF REFS 36 |
| 8a. CONTRACT OR GRANT NO. OCD-DAHC20-67-C-0136 | 9a. ORIGINATOR'S REPORT NUMBER(S) None | |
| b. PROJECT NO. Work Unit No. 1126C | | |
| c. | 9b. OTHER REPORT NO(S) (Any other numbers that may be assigned this report) | |
| d. | | |

10. DISTRIBUTION STATEMENT

This document has been approved for public release and sale; its distribution is unlimited.

| | |
|---|---|
| 11. SUPPLEMENTARY NOTES | 12. SPONSORING MILITARY ACTIVITY Office of Civil Defense Office of the Secretary of the Army Washington, D.C. 20310 |

13. ABSTRACT

The objective of this investigation was to develop an evaluation procedure applicable to existing NFSS-type structures for determining the blast protection afforded and the cost of structure modifications to improve the blast protection. The approach adopted was to formulate a procedure that would permit examining the response of a structure over a range of incident overpressure levels to determine the pressure at which failure of the various elements occurs. Because of the scope of the overall evaluation program, the initial phase was primarily concerned with the response of the exterior walls.

The initial effort included the development of analytical procedures and computer programs to predict the collapse of three types of blast loaded exterior wall elements. The wall types considered were unreinforced concrete or masonry unit walls without arching, reinforced concrete walls, and unreinforced concrete or masonry unit walls with arching. To determine the sensitivity of the collapse pressure of exterior walls to various factors, a parametric study was conducted of the response of selected wall elements subjected to arbitrary dynamic loads. In addition, the analytical predictions were compared with the limited laboratory and nuclear field test data.

DD FORM 1 NOV 65 1473 REPLACES DD FORM 1473, 1 JAN 64, WHICH IS OBSOLETE FOR ARMY USE.

UNCLASSIFIED
Security Classification

Unclassified

Security Classification

| 14. KEY WORDS | LINK A | | LINK B | | LINK C | |
|---|---|---|---|---|---|---|
| | ROLE | WT | ROLE | WT | ROLE | WT |
| Blast protection | | | | | | |
| Structure evaluation procedure | | | | | | |
| Wall response | | | | | | |
| Dynamic analysis | | | | | | |
| Arching in walls | | | | | | |
| Reinforced concrete walls | | | | | | |
| Masonry Unit walls | | | | | | |

UNCLASSIFIED

Security Classification